5-22-2019

Stalking Flu: Development and Characterization of a Broadly Neutralizing Monoclonal Antibody Targeting the Influenza Hemagglutinin Stem

Elizabeth Newman

STALKING FLU:

DEVELOPMENT AND CHARACTERIZATION OF A BROADLY NEUTRALIZING MONOCLONAL ANTIBODY TARGETING THE INFLUENZA HEMAGGLUTININ STEM

Elizabeth P. Newman

A Doctoral Dissertation in the Program in Microbiology and Immunology
Submitted to the Faculty of the Graduate School of Basic Medical Sciences in
Partial Fulfillment of the Requirements for the Degree of Doctor of Philosophy
at New York Medical College

2019

STALKING FLU:
DEVELOPMENT AND CHARACTERIZATION OF A BROADLY NEUTRALIZING MONOCLONAL ANTIBODY TARGETING THE INFLUENZA HEMAGGLUTININ STEM

Elizabeth P. Newman

Dr. Doris Bucher, Sponsor

Dr. Shekhar Bakshi

Dr. Jose Galarza

Dr. Mary Petzke

Dr. Petra Rocic

Dr. Penghua Wang

Date of Approval

ACKNOWLEDGEMENTS

I would like to acknowledge my mentor Dr. Doris J Bucher as well as my colleagues in the lab, especially Dr. Yu He, Dr. Jianhua Le, Jean Marie Silverman, Rene Devis, and Barbara Pokorny. I will never forget their encouragement and support both professionally and personally. I would also like to thank my friends at New York Medical College, especially the graduate students and faculty in the Department of Microbiology and Immunology. Lastly I want to thank my committee for their time, effort, and guidance.

"For small creatures such as we, the vastness is bearable only through love"

- Carl Sagan

I wish to dedicate this thesis to my parents Amber and Paul Newman and my partner Dr. Gregory Joseph. I can only say thank you.

TABLE OF CONTENTS

SIGNATURE PAGE **ii**

AKNOWLEDGEMENTS **iv**

LIST OF FIGURES **vi**

LIST OF TABLES **viii**

LIST OF ABBREVIATIONS **ix**

ABSTRACT **x**

INTRODUCTION **1**
- Influenza Virus Structure 3
- Influenza Virus Life Cycle 4
- Hemagglutinin and Neuraminidase 7
- Genetic Drift and Shift 12
- Vaccination Strategy and Antivirals 13
- HA Antibodies and Hybridoma Technology 19

SPECIFIC AIMS **32**

MATERIALS AND METHODS **34**

EXPERIMENTAL RESULTS **40**
- Aim 1. Develop and purify anti-Flu Monoclonal Antibodies (mAbs) 40
- Aim 2. Characterize binding profile and epitope of candidate mAbs 54
- Aim 3. Evaluate candidate mAbs efficacy *in vitro* and *in ovo* 85

CONCLUSIONS **106**

DISCUSSION **108**
- Therapeutic Antibodies 110
- Influenza Monoclonal Antibodies 115
- Future Directions 119

APPENDIX **127**
1. Table of Viruses 127
2. Peptide Map 128

CITATIONS **141**

LIST OF FIGURES

Figure 1: CDC estimates for number of cases, hospitalizations, and deaths as a result of seasonal influenza infection each year in the United States (17) 23
Figure 2: Influenza viral structure shown with spherical morphology (24) 24
Figure 3: Influenza A virus life cycle 25
Figure 4: A complete influenza A HA monomer and HA phylogenetic tree (115) 26
Figure 5: Ribbon diagram of engaged trimeric influenza A HA (42) 27
Figure 6: Phylogenetic tree of all NA subtypes and ribbon diagram of influenza A N1 (99) 28
Figure 7: Antigenic drift and shift in influenza A and B viruses 29
Figure 8: Hybridoma cell generation 31
Figure 9: Immunization Protocol Alpha 46
Figure 10: Immunization Protocol Beta 47
Figure 11: NA activity of sera collected from animals enrolled in Immunization Protocol Beta 48
Figure 12: NA inhibition activity of seven antibody candidates developed from Immunization Protocol Alpha 49
Figure 13: Relative NA inhibition activity following incubation of virus and purified antibody 51
Figure 14: NA inhibition following incubation of Trition X-100 treated virus and antibody containing hybridoma supernatant 52
Figure 15: Representative hemagglutination inhibition assay plate 53
Figure 16: Non-reducing Western blot of recombinant A/Puerto Rico/8/1934 HA, NYMC X-162 and native PR8 in allantoic fluid 68
Figure 17: Reducing Western blot of recombinant A/Puerto Rico/8/1934 HA, NYMC X-162 and native PR8 in allantoic fluid 69
Figure 18: Western blot of A/California/07/09, A/Wisconsin/67/05, and A/Puerto Rico/8/1934 70
Figure 19: Western blot of two H3N2, two H1N1, and two influenza B viruses in allantoic fluid 71
Figure 20: Western blot A/Puerto Rico/8/1934, A/California/07/2009, and A/Wisconsin/67/2005 treated with PNGase F 72
Figure 21: Western blot of high concentration purified A/Puerto Rico/8/1934 HANA, NYMC X-187, and NYMC X-179A HANA 73
Figure 22: Western blot of low concentration purified A/Puerto Rico/8/1934 HANA, NYMC X-187, and NYMC X-179A HANA 74
Figure 23: Western blot of low concentration purified A/Puerto Rico/8/1934 HANA, NYMC X-187, and NYMC X-179A HANA using PR8 specific anti-HA 2A6 75
Figure 24: Reducing Western blot of purified A/Puerto Rico/8/1934 HANA, NYMC X-187, and NYMC X-179A HANA following treatment with trypsin 76
Figure 25: Western blot using recombinant HA proteins from A/Puerto Rico/8/1934 (PR8, H1), A/Perth/16/2009 (H3) and A/Vietnam/1194/2004 (H5). 77
Figure 26: Western blot using sucrose gradient purified antigen from Sendai and Respiratory Syncytial Virus as well as an uninfected allantoic fluid control. 78
Figure 27: Summary of Western blot results 79
Figure 28: Sequence alignment of the HA segments of PR8, A/Victoria/201/2008, and A/California/07/2009 80
Figure 29: Fluorescent intensity on PEPperMap linear peptide array 81

Figure 30: HA amino acid sequence of A/Puerto Rico/8/1934 with pitope sequences of known HA stem antibodies 82
Figure 31: 3D visualization of A/Puerto Rico/8/1934 HA with predicted 1G3 epitope 83
Figure 32: HA amino acid sequence of A/Hong Kong/4801/2014 and B/Brisbane/60/2008 84
Figure 33: Percent plaque reduction relative to NYMC X-162 of seven hybridoma supernatants prior to treatment with receptor destroying enzyme 93
Figure 34: Percent plaque reduction relative to NYMC X-162 of seven receptor destroying enzyme treated hybridoma supernatants 94
Figure 35: Percent plaque reduction relative to A/Puerto Rico/8/1934, A/California/07/2009, A/Hong Kong/50/2016 and NYMC X-162 of seven receptor destroying enzyme treated hybridoma supernatants 95
Figure 36: Plaque size reduction mediated by mAb 1G3 vs NYMC X-162 96
Figure 37: Average plaque size following infection with A/Puerto Rico/8/1934, A/California/07/2009, and NYMC X-162 97
Figure 38: Plaque Reduction and Neutralization Test completed with purified mAb 1G3 98
Figure 39: Average plaque number following infection with B/Brisbane/60/2008 99
Figure 40: Representative images of plaque morphology of infuenza A and B viruses 100
Figure 41: Indirect fluorescent staining of A/Puerto Rico/8/1934 HA in infected MDCK cells 101
Figure 42: Quantification of infected cells from indirect fluorescent staining 102
Figure 43: A/Puerto Rico/8/1934 viral growth *in ovo* 103
Figure 44: NYMC X-163 viral growth *in ovo* 104
Figure 45: BX-31B viral growth *in ovo* 105
Figure 46: Influenza HA targeted broadly neutralizing monoclonal antibodies (32) 124
Figure 47: Influenza targeted monoclonal antibodies currently in development 125
Figure 48: Mechanisms of HA antibody inhibition of influenza virus infection (11) 126

LIST OF TABLES

Table 1: Licensed flu vaccines in the United States for the 2017-2018 influenza season. (17) 30
Table 2: Candidate monoclonal antibodies identified following Immunization Protocol Alpha 50

LIST OF ABBREVIATIONS

IAV: Influenza A Virus

HA: Hemagglutinin

NA: Neuraminidase

mAb: Monoclonal Antibody

NI: Neuraminidase Inhibition

HAI: Hemagglutinin Inhibition

MDCK: Madin Darby Canine Kidney

PRNT: Plaque Reduction and Neutralization Test

HPAI: Highly Pathogenic Avian Influenza

HYR: High Yield Reassortant

ORF: Open Reading Frame

NP: Nucleoprotein

vRNP: Viral Ribonucleotide Protein

M1: Matrix Protein

PB: Polymerase Basic Protein

PA: Polymerase Acidic Protein

NS: Nonstructural Protein

NEP: Nuclear Export Protein

NLS: Nuclear Localization Signal

TLR: Toll Like Receptor

LIAV: Live Inactivated Influenza Vaccine

ELISA: Enzyme Linked Immunosorbent Assay

IFA: Indirect Immunofluorescence

RDE: Receptor Destroying Enzyme

SPF: Specific Pathogen Free

BSL: Biosafety Level

MOI: Multiplicity of Infection

ABSTRACT

Seasonal epidemics caused by influenza A viruses (IAV) result in an estimated 290,000- 650,000 deaths worldwide each year (17). While antivirals targeted to influenza exist, resistance to these drugs is increasing and regular vaccination remains the most effective way to prevent infection (26, 73, 99). However due to the persistence of antigenic drift and shift, influenza vaccines must be updated each season and antigenic mismatches can reduce efficacy (24, 118).

Immunity to influenza either from vaccination or infection is principally mediated by antibodies generated to one of its major surface proteins, Hemagglutinin (HA). HA is a homotrimer, each monomer HA0 is composed of a globular head and stem (100, 111). Proteases present in the host cleave native HA0 into two subunits, HA1 and HA2. Residues in HA1 form the receptor binding pocket within the head and facilitate interaction with the host cell. The stem is encoded by both HA1 and HA2 and contains the fusion peptide required for cytosolic release (10, 112). Most antibodies isolated from patients following infection or vaccination are targeted to the receptor binding domain of the HA head. These antibodies are efficient neutralizers but highly strain specific, recognizing only antigenically similar strains of the same IAV group and consequently lose relevance rapidly as viruses undergo drift (68, 141). However, patients immunized with heterosubtypic HA can also develop antibodies that target the HA stem domain. These antibodies are often effective against multiple HA subtypes, reflecting strong structural constraints imposed on the HA stem epitope, and are referred to as “broadly neutralizing”. It is because of this strong conservation that there has been an interest in characterizing HA stem antibodies in the development of a universal flu vaccine (22, 115, 123). Since their discovery in 1991, dozens

of broadly neutralizing stem antibodies have been isolated in humans and even more have been derived using targeted technologies, including hybridoma cell generation (69).

We used two immunization protocols that each featured successive injection of influenza with antigenically distinct HA components, H1 then H3, followed by hybridoma cell development to generate candidate monoclonal antibodies (mAbs) targeted to the IAV surface glycoproteins. We screened antibody containing hybridoma supernatant for activity against influenza proteins using ELISA, Neuraminidase Inhibition (NI), and Hemagglutinin Inhibition (HAI) assays. Those antibodies which showed appreciable activity against the immunizing viruses from hybridoma generation were purified for further study. Of 114 antibodies, mAb 1G3 (IgG1) was found by Western blotting to successfully bind the HA protein of H1, H1pdm, and H3 influenza A viruses as well as influenza B viruses of both major lineages (Yamagata and Victoria). Significantly, mAb 1G3 was able to successfully neutralize both influenza A and B viruses *in vitro* as shown by plaque assay and indirect immunofluorescence of infected cells. 1G3 was also shown to be effective against H1, H3, and an influenza B virus *in ovo*, delaying onset of positive viral titer and preventing viral expansion overall.

Although we believe mAb 1G3 to have a conformational epitope, linear epitope mapping revealed that 1G3 likely binds in the stalk domain near to the fusion peptide and across the C terminus of HA1 and N terminus of HA2. We found this locus to be strongly conserved among heterosubtypic influenza strains, including influenza B. Importantly, only one other antibody known as CR9114 has been identified that can neutralize both influenza A and B viruses *in vivo* (32). CR9114's epitope appears to have significant overlap with the proposed epitope of our mAb 1G3, although they are not identical. Where CR9114

displayed no activity against B viruses *in vitro*, 1G3 is the only antibody to date that inhibits both A and B viruses in cells. This previously unseen neutralization profile may suggest the possible presence of an additional inhibition mechanism or mechanisms active in cell culture. While CR9114 prevents the fusogenic conformational change of HA within the host endosome and incites Antibody Dependent Cellular Cytotoxicity (ADCC) *in vivo*, we have demonstrated through Western blotting and neuraminidase inhibition that our mAb 1G3 likely also prevents extracellular HA cleavage and interferes with virion budding (11, 29, 122).

Therefore, mAb 1G3 is a unique and previously uncharacterized antibody that is broadly neutralizing against Group 1 and Group 2 influenza A as well as both lineages of influenza B.

INTRODUCTION

The Centers for Disease Control (CDC) estimates that seasonal influenza epidemics in the United States have been responsible for between 10 and 35 million cases of illness, between 200,000 and 750,000 hospitalizations, and 12,000 to 60,000 deaths annually since 2010 **(Figure 1)**. The total economic burden of each epidemic is projected to be about 87.1 billion dollars annually (17, 41). The 2017-2018 flu season was characterized as "severe" in the United States across all age groups. At its peak, 7.5% of all outpatient visits were as a result of influenza or influenza like illness, the highest levels seen since the 2009 swine flu pandemic. Morbidity was above the national baseline for 19 weeks, making the 2017 flu season one of the longest in recent years. 183 pediatric deaths from influenza were reported to the CDC, the highest number for a seasonal epidemic since pediatric influenza motility became a reportable condition in 2004 (17). While flu can be underestimated by the general population, it is clearly a substantial public health concern.

Commonly known as the flu, influenza is a respiratory illness caused by influenza viruses. Symptoms are non-specific and generally have a rapid onset which may include: fever, cough, muscle aches, headaches, and malaise (17). Influenza infection can also present with vomiting and gastrointestinal distress in young children and more rarely in adults and seniors. Commonly spread in droplets, influenza virus is easily communicable through coughing, sneezing, talking, and to a lesser extent, following contact with contaminated fomites. Most people are contagious in the first 72 - 96 hours of illness and may be able to transmit the virus up to 24 hours before symptoms begin. Immunocompromised people as well as children may continue to shed virus and spread disease for well over a week after symptom resolution (53).

Healthy adults can generally recover from an influenza infection with help from over the counter treatment. However, some populations are at risk for serious complications. Immunocompromised persons including the elderly and transplant recipients are especially susceptible to severe disease and even death (17). The most common causes of death related to influenza infection are secondary bacterial pneumonia and primary viral pneumonia, both of which induce lung damage and pathology via the generation of immune infiltrates, free radicals, and excess mucus (53). Influenza can also be particularly dangerous for pregnant women and fetuses. The risk of stillbirth among vaccinated mothers is 51% lower than their unvaccinated counterparts. Although the exact mechanisms remain unknown, it is believed that fever and placental inflammation associated with influenza infection is correlated with an increased risk of miscarriage and various birth defects including low birth weight and even personality disorders like schizophrenia (46). It is recommended that all women who become pregnant during the regular flu season receive the influenza vaccine, regardless of their current trimester or gestational status (131). Another possible complication seen in some populations is hemorrhaging from mucus membranes as a result of immune mediated destruction of infected epithelial cells (3).

A subset of influenza strains possess a mutation which allows for growth outside of the respiratory tract - causing a very high mortality rate of upwards of 80% (3). Known as Highly Pathogenic Avian Influenza (HPAI), these viruses can be transmitted to multiple critical organs, including the brain via the olfactory mucosa and then olfactory nerves where the virus activates local glial cells (99). The resulting cytokine storm as well as TNF-induced mitochondrial mediated apoptosis causes extensive cellular damage and ultimately a disruption of the blood brain barrier followed by rapid death (75). Fortunately, these viruses

are not easily communicable between people and are therefore not incorporated into the seasonal vaccine.

In addition to seasonal epidemics, some influenza viruses can cause pandemics when introduced to a novel human population. The H1N1 "Spanish Flu" of 1918 is estimated to have killed between 50 and 100 million people worldwide – about 5% of the global population at the time (89, 117). Other pandemic influenza events include "Asian" flu in 1957, the "Hong Kong" flu in 1968, and most recently the "Swine" flu pandemic of 2009. The CDC estimates that there were almost 60 million cases of the "swine" flu in the United States in 2009 alone (120).

Influenza Virus Structure

Influenza viruses are a group of respiratory pathogens belonging to the family *Orthomyxoviridae* that are further divided into four genera: *Influenzavirus* A, B, C and the most recently described D (33). Influenza viruses are characterized as having a single stranded, negative sense RNA genome which is uniquely segmented. Influenza A and B each contain eight viral segments while influenza C and D only contain seven. These segments in turn encode viral proteins; with types A and B each producing at least 11 *in vivo* as a result of alternative splicing and open reading frames (ORFs) (96, 100). Each RNA segment is coated with nucleoprotein (NP) to form what is known as the viral Ribonucleotide Nucleoprotein (vRNP) complex. vRNP complexes are assembled and housed in many repeated matrix (M1) proteins. This viral core surrounded by a host derived lipid bilayer acquired during budding from an infected cell (100). The virion surface features two glycoproteins and one integral membrane protein, M2. All known naturally occurring immunity is in response to the primary surface antigens, Hemagglutinin (HA) and

Neuraminidase (NA) (132). Also present within an infectious virion are polymerase basic proteins 1 and 2 (PB1 and PB2), which taken together with polymerase acidic protein (PA) form the viral RNA dependent RNA polymerase (20). Additionally synthesized are nonstructural protein 1 (NS1) which is critical for viral immune evasion, as well as nuclear export protein/nonstructural protein 2 (NS2 or NEP). Virions are known to display a variety of shapes, with the most well-known and abundant *in vivo* being roughly spherical **(Figure 2)** (42).

Influenza Virus Life Cycle

The influenza virus life cycle can be divided into the following stages: binding and entry into the host cell, transport of genetic information into the nucleus, transcription of viral proteins, export and translation, and finally assembly and budding at the host membrane **(Figure 3)** (53).

Entry is facilitated by the binding of HA to sialic acid receptors on the host cell. Different HA subtypes have varying affinity for each of the two major types of sialic acid linkages found in nature. Neu5Ac α(*2,3*)-Gal is generally found within the gastrointestinal tract of aquatic birds and deep in the human respiratory tract. Neu5Ac α(*2,6*)-Gal is found throughout the length of the human respiratory system but is primarily concentrated in the upper limits (84). Both types of sialic acid linkages are readily available in swine species (94). Avian IAV strains generally have higher affinity for 2,3 linkages and circulating human viruses for 2,6 linkages (43, 105). Following HA binding of either sialic acid isoform, the virion enters the host cell in an endosome via receptor mediated endocytosis (109). The low pH in the endosome provides the necessary acidic environment for both a conformational change in HA and the activation of the M2 ion channel. HA subunits HA1

and HA2 disassociate at an acidic pH. This exposes the fusion peptide on HA2 that mediates the fusion of the viral and host endosomal membranes, allowing viral contents to empty into the cytoplasm (133). Opening of M2 ion channels causes further acidification within the viral core, necessary for the release of vRNP complexes from the M1 matrix (42).

Because the influenza virus genome is composed of negative sense RNA, it must first be converted to the positive sense before transcription can proceed. The virus carries with it a viral RNA dependent RNA polymerase (vRNP) which initiates replication (6). This polymerase is composed of 4 proteins: NP (Nucleoprotein), PA (Polymerase Acidic), PB1 (Polymerase Basic 1), and PB2 (Polymerase Basic 2). None of these proteins have been found to have proofreading ability, therefore the influenza polymerase is considered error prone (139). Unlike other RNA viruses, influenza virus replicates within the host nucleus. All protein components of the vRNP contain Nuclear Localization Signals (NLSs). These viral proteins can use their NLSs as well as co-opt host nuclear import machinery to gain passage along microtubules and eventually through nuclear pores (14). It is unknown whether NLSs must be present on each individual protein or if some components of the vRNP contribute to nuclear import more than others (11).

The PA component of the polymerase has endonuclease activity and participates in a process called “cap snatching”, whereby the 5’ prime methylated caps of mature cellular mRNAs are cleaved and used by the cellular RNA polymerase to prime viral transcription (20). Cap snatching may also serve to protect viral mRNAs from being recognized by innate host immunity, especially Toll Like Receptors (TLRs) and the RIG-1 system (133, 142).

Several segments of the IAV genome encode for multiple proteins products due to alternative splicing and ORFs. Segment 8 encodes both M1 (Matrix 1) and M2 (Matrix 2)

proteins while segment 7 is known to encode NS1 (Non-structural protein 1) and NEP (Nuclear Export Protein) (6). As M2 and NEP are the secondary splice products, they are generally found in much lower abundance than their counterparts M1 and NS1, respectively (134). An important function of NS1 is to bind to components of the host spliceosome, especially U6 small nuclear RNAs, and relocate them to the nucleus in order to sequester splicing capabilities to local viral mRNAs (79). In addition to the 11 canonical IAV proteins, other products have been recently described. In 2001 PB-F2 was identified as the result of an ORF in the PB1 gene segment and appears to be implicated in *in vivo* infections, especially in modulating host immunity and the apoptotic response (79, 100). PB1-N40, also known as N40, is a third protein product from the PB1 gene. Recombinant viruses that lack N40 display slower growth kinetics *in vitro*, but the exact mechanism and function or functions of N40 are unknown (20, 79). The most recently discovered influenza protein has been named PA-X, as it is a protein product from the PA gene segment. Infection studies of viruses lacking PA-X have shown that it functions heavily in mediating the viral shut off of host protein synthesis through cellular mRNA decay and is therefore a major virulence determinant. Experiments are ongoing (50, 70)

Export of negatively sensed viral mRNAs from the nucleus through pores occurs through the interaction of viral NP with host CRM1 dependent pathways. There also appears to be a role for the M1 protein in the process, as viruses without M1 are deficient in protein synthesis, although the mechanism remains to be elucidated (14, 18). Live imaging studies have shown that NP proteins localize to the apical side of infected nuclei, implying an as of yet unidentified mechanism of polarized exit from the host nucleus (68).

Once translated by the host ribosomes, all viral components must assemble in the cytosol and bud from the host cell's plasma membrane. Influenza viruses use the host cell membrane for the formation of the envelope and also as an aggregation point for proteins needed for the progeny virions (98, 101). Two models have been proposed regarding packaging of viral genomic segments into progeny virions. One model predicts that segments are randomly packaged, and complete virions are the result of random probability. Evidence cited by proponents of this model includes the well documented existence of incomplete virions in cellular and *in vivo* infections (6). Noninfectious particles lacking a complete complement of viral genes can and do form, but only virions with HA, NA, and M2 can successfully bud from the host membrane (69). The other model is known as the specific packaging model and hypothesizes there is an intrinsic system to encourage the correct assembly of all necessary eight genomic segments and incomplete virions are as a result of a failure of this system. This model is comparatively newer, but is thus far supported by the discovery of packaging signals on the 5' and 3' ends of some viral segments that appears to interact directly with lipid rafts (126).

Of critical importance during budding is the cleavage of sialic acid residues on the infected host cell mediated by the Neuraminidase (NA) enzyme. Without productive NA, progeny virions crowd at the cellular surface as a result of interaction between its HA and intact sialic acid on the host surface. Trapped virions cannot move between cells and therefore cannot propagate further infection (87).

Hemagglutinin (HA) and Neuraminidase (NA)

Because of their roles in the viral lifecycle and in mediating immunity, HA and NA are the two most well studied influenza proteins and are used to classify different subtypes

influenza A viruses. To date, there are 18 subtypes of HA and 11 of NA, although not all of these are able to readily infect humans (104).

Functional HA is a homotrimer with each monomer (HA0) composed of a globular head and stalk anchored into the membrane at its C terminus (**Figure 4**). Synthesized as a single polypeptide chain, HA0 undergoes significant post translational modification, including glycosylation, palmitoylation, and eventually cleavage into its active subunits (42, 115, 132). HA is phylogenetically divided into 2 groups based on structural aspects of the stalk, with H1 stalk structure defining group 1 and H3 defining group 2. The globular head is the most variable domain of HA while the stem and membrane proximal domains feature a conservation of sequence among IAVs ranging from 75-99% between HA groups 1 and 2. HA from influenza B viruses has <75% sequence identity with any HA from IAV, although the structure is highly conserved (42, 49).

Trypsin-like proteases present in the host cleave native HA0 into its subunits HA1 and HA2 at a single invariant arginine residue present on all HA subtypes except HA14 (109, 112). The N terminus of the newly formed HA2 relocates to the trimer interior, however the subunits stay associated via disulphide bonds at amino acids 52 and 277 despite cleavage (15, 107). During entry, HA1 binds to sialic acid on the surface of the host cell and triggers endocytosis (22). The low pH of the resulting endosome causes a conformational change in HA0 that exposes the fusion peptide present chiefly on HA2 (**Figure 5**). HA2 mediates a close association and eventual fusion between the viral membrane and that of the late host endosome, allowing for the genetic content of the virion to enter the cytoplasm and then the nucleus where replication can proceed (42, 117). Without cleavage of HA0 by cellular proteases prior to endocytosis, the fusion peptide remains unavailable and the fusion

of the viral and endocytic membranes cannot occur. In humans, this limits most influenza viruses to the respiratory tract where the necessary trypsin-like proteases are produced; including TMPRSS-2, Human Airway Trypsin 1, and possibly others which are still being identified (11, 32).

The HA proteins of HPAI H5 and H7 viruses have additional basic residues at their cleavage sites upstream of the invariant arginine (123). This allows for a larger number of enzymes present in the avian and human host to cleave and activate the HA, including ubiquitous proteases present in the liver, kidneys, and brain. This may explain why H5 and H7 viruses have been demonstrated to grow in cell culture without supplemental trypsin as well as outside of the human airway epithelium *in vivo,* causing severe and disseminated disease (99). HPAI viruses have a mortality rate of roughly 60-80% in humans and between 90-100% in birds (3).

HA has two well described functions in the influenza viral life cycle. The head serves to bind sialic acid on host cell membranes and facilitates viral entry. The stem and fusion peptide associate the viral and host endosomal membranes to allow for uncoating. Both roles are necessary; if HA1, HA2, or the HA0 monomer are compromised, infection cannot proceed and either the virus will not enter the cell or the virus will be restricted to the endosomal compartment (105, 117). Notably, there is also some data supporting an additional HA function during packaging of progeny viruses, namely that the highly conserved HA0 cytoplasmic tail directly impacts the ability of vRNPs to interact with lipid rafts during virion assembly (132). The degree to which HA contributes to packaging is unknown.

Historically, influenza research has focused on HA because of its antigenic and immunologic dominance in both natural and experimental infections. Recently however, NA has gained attention both as a protein and as an antigen because of the advent of NA targeted influenza inhibitors. NA is an exosialidase that cleaves α-ketosidic linkages between a sugar and an adjacent N-acetyl-neuramic (sialic) acid. There are four main steps that comprise the catalytic pathway of NA, beginning with binding followed by the donation of protons from the solvent and the formation of a cation transition state intermediate. The final steps are the formation and release of N-acetyl-neuramic acid (47). There are 11 NA subtypes among influenza A viruses, those which can infect humans are divided into two groups based on sequence phylogeny. The first group consists of N1, N4, N5, and N8 while the second group includes N2, N3, N6, and N9 (2, 129).

Functional NA on a virion surface is a homotetramer of "boat propeller" or "mushroom" shape. Each monomer is composed of 470 amino acid residues and has 4 domains: the cytoplasmic tail which anchors the protein at its C terminus, the transmembrane domain, the enzymatically active head, and a thin stem (2) (**Figure 6**). While NA from influenza A and B viruses only have roughly a 30% sequence homology, their 3D structures are identical (103, 135).

The head is the most well studied NA domain. as it contains both the active site and the calcium binding site which is indispensable as it stabilizes the conformation of the entire tetramer. Residues which comprise the active site (Arg 118, Asp 151, Arg 152, Arg 224, Glu 276, Arg 292, Arg 371, Tyr 406) are highly conserved and found in all subtypes of influenza A and B (104). The NA head also features major glycosylation sites which have been shown to impact virus stability, enzymatic activity, as well as tissue targeting. Interestingly, a lack

of glycosylation at Asn 146 has been demonstrated to be one of the major determinants of the unique tropism of A/WSN/1933 (H1N1), a well-documented uniquely neuropathic influenza (99). The characteristic fourfold symmetry of the NA tetramer is maintained by an inward facing carbohydrate side chain on each monomer as well as bound metal ions. It has been suggested that calcium binding may have physiological import in addition to structural relevance in the context of a natural infection as a component of positive modulation of viral activity within a host cell (47).

Data supports two main functions for NA during the influenza virus life cycle. The most well studied role is in the final stages of budding as NA cleaves sialic acid found on the virion to prevent aggregation of progeny at the host cell membrane (2). This was first described by George Hirst in 1942 when he found that red blood cells were not susceptible to re-hemagglutination by influenza virus following pretreatment with the same virus (54). This was later solidified by a series of papers published by Peter Palese's group in the 1970's showing that virions with defective NA collect at the surface of infected cells (87).

A second less well explored role for NA is to allow penetration to the respiratory epithelium by cleaving sialic acid from local mucins thus minimizing binding to irrelevant receptors (47). Additional functions have also been suggested but remain poorly understood. Some data suggests that NA may play a role in the synergistic relationship between influenza virus and *Streptococcus pneumoniae,* as NA can serve to increase bacterial adherence in the respiratory epithelium and may underlie the high incidence of secondary bacterial pneumonia refractory to influenza infection in some patient populations (90). Purified NA has also been shown to elicit a pro inflammatory cytokine response from

alveolar macrophages, especially TGF-β, that may contribute to lung damage and overall pathogenesis of influenza (53).

One of the most interesting things about influenza viruses is the presence of two surface proteins which both recognize terminal neuraminic acid residues, but have contradictory functions. Studies done in viruses that lack NA or HA activity or done with artificial viruses obtained by reverse genetics show that these proteins act in concert, and their ratios to one another are tightly regulated at the virion surface (129). Moreover, phylogenetic analyses have demonstrated that these two proteins not only function together but have evolved and continue to evolve in an interdependent manner (105). HA and NA must function in a delicate balance to prevent the HA studding the surface of newly made progeny from attaching to the surface of their parental host cell instead of moving away to infect neighboring host cells. It is NA that affords freedom from the cell and the propagation of infection by HA (43, 68).

Genetic Drift and Shift

All influenza viruses undergo continued change in response to host immunity, a process of mutation known as antigenic drift (49). These minor changes that occur over time because of point mutations in HA or NA are driven by positive selection of random mutations enabling virus to subvert host antibodies; likely as a direct result of the error prone viral RNA polymerase. Seasonal epidemics are generally due to drift away from the previous season's circulating virus (118). This process has also been documented in NA as a result of anti-influenza antivirals that specifically target NA (133, 142).

While both influenza A and B viruses can undergo antigenic drift, only influenza A viruses can participate in antigenic shift (49, 118). Where drift is described as a slow change

over time, shift is when a novel HA or NA is introduced into a human population from an animal reservoir and can result in a new, pandemic virus (**Figure 7**). Antigenic shift is usually caused by of a reassortment of genes, where the shuffling of independent gene segments from at least two different virus occurs as a result of infection in the same host cell (80). The three most recent human influenza pandemics were each caused by reassortment within influenza A viruses. The "Asian Influenza" in 1957 and the "Hong Kong Influenza" in 1968 were caused by reassortment events between human and avian viruses (9, 126). The 2009 "Swine Flu" pandemic strain was a triple reassortant of human, avian, and swine influenza viruses (120). Swine are an important animal host for influenza and are often referred to as a "perfect mixing vessel" because they express both types of glycosidic linkages found in aquatic birds and the human upper respiratory tract. This availability of both 2,3 and 2,6 glycosidic linkages encourages recombination between avian and human viruses (94, 120). The ability to undergo both drift and shift is an incredible evolutionary advantage for influenza virus which underlies the necessity behind a consistently updating seasonal vaccine as well as highlights the challenges of developing universally applicable control strategies.

Vaccination Strategy and Antivirals

The first drugs developed to control influenza infections were M2 ion channel inhibitors (5). The M2 ion channel is a proton pump active following endocytosis of the virion into the host cell. Without a properly functioning M2 channel, the genome is not be able to uncoat from the M1 matrix and the replication cycle is arrested (5, 114). Amantadine was developed in the late 1960's as prophylaxis in response to the 1968 Hong Kong Flu pandemic followed quickly by Rimantadine. Mechanistically, both appear to bind the inward

facing lipid pocket and block proton translocation although there is some degree of debate about a second drug interaction site (91). The official CDC guidelines now suggest a total moratorium on the use of M2 ion channel inhibitors as widespread resistance developed while resistant viruses have maintained identical infectious and pathogenic properties. A survey from 2009 showed 100% of wild type H3N2 viruses as well as 100% of non pandemic H1N1 viruses were resistant (114, 124).

Drugs that targeted the viral NA were also first discovered in the 1960s. The first anti-NA drug was a transition state analogue known as DANA. While effective *in vitro*, DANA failed to perform well *in vivo* as it could not readily cross cellular membranes and was very quickly metabolized (40). Following the successful crystallization of N2, it was theorized that the addition of a 4-guanidino group would improve binding to the catalytic site and led to the creation of Zanamivir (Relenza^{TM}). The same crystal structure was used by competing scientists to design Oseltamivir (Tamiflu^{TM}) with the promise of easier of synthesis and greater bioavailability, as well as the option of oral administration (129). Wild type influenza viruses with resistance to both types of available NA inhibitors have been isolated, but unlike what has been observed with M2 inhibitors, resistance is often associated with a decrease in viral fitness (52, 138). However in 2008, an H1N1 virus with a substitution in NA at position 275 and a compensating mutation in HA was found to be resistant to inhibitors while maintaining infectivity. This clade of virus was quickly replaced in the population by the 2009 "Swine Flu" H1N1 virus (H1N1pdm09), but this emergence remains one of many troubling facts that undermines confidence in our current reliance on NA inhibitors in clinical settings (120).

In addition to the ever-looming threat of resistance mutations, NA inhibitors have their own set of clinical limitations. Because NA functions at the end of the viral life cycle, patients must begin their course of NA inhibitors very early in symptomatic onset. Its recommended that patients begin Oseltamivir or Zanamivir within 48 hours of falling ill, which presents a challenge as many patients do not seek medical intervention so early in clinical disease course (47, 91). Additionally, several large-scale retrospective studies have called into question whether NA inhibitors work at all in most clinical settings, with the general consensus being that drug intervention results in only a one day reduction in illness. In fact, some medical professionals report having serious doubts about the efficacy of NA inhibitors and often only prescribe them to patients who make a request (39, 59). This coupled with widely reported side effects that include gastrointestinal distress make NA inhibitors far from an ideal treatment for influenza infection.

The newest drug developed for influenza infection is S-033188 or Baloxavir marboxil, marketed as Xofluxa^{TM}. Developed by Shionogi Co in Japan and recently acquired by Roche, Baloxavir is a small molecular inhibitor of the cap dependent endonuclease (51). This endonuclease is found on the N terminal domain of the PA subunit of the influenza RNA dependent RNA polymerase and mediates a process known as “cap snatching” (27). Translation of mRNA in human cells requires that transcripts are capped at the 5’ end. The viral endonuclease cleaves caps from host mRNA allowing them to serve as primers for viral mRNA. Mutations in the endonuclease domain of PA are rare and often result in a decrease in viral fitness, making this location an ideal target for inhibitor therapy (27, 139). Studies have shown that a single dose of Baloxavir was superior to both placebo and Oseltamivir in relieving influenza symptoms and decreasing viral titers. Unlike

Oseltamivir, Baloxavir showed efficacy up to five days post symptomatic onset and has a more favorable safety profile as Oseltamivir often presents with gastrointestinal distress (51, 92). Already approved in Japan, Baloxavir was given a "Priority Review" status by the Federal Drug Agency and approved in October of 2018. It became available to American patients and prescribers before the end of 2018 and costs roughly $150 USD without health insurance, the same as a course of Tamiflu™ despite being a single dose pill (51).

While drugs for mild infection are very limited, there is no drug currently licensed for those who are hospitalized with influenza, although NA inhibitors have been used off label for this purpose to mixed success (129). Therefore, regular seasonal vaccination remains the best option to both prevent illness and combat potential pandemics (**Table 1**). While the intranasal live attenuated vaccine (LAIV) has been recently re-added to the CDC recommendations, the current standard of care for all people between 6 months and 65 years of age is the quadrivalent inactivated vaccine (QIV). Other formulations are available, including a high dose vaccine designed for those over 65 years old who may be generally weak responders to vaccination (17).

The QIV is composed of two inactivated influenza A strains and two inactivated influenza B strains. Each of the four strain components are determined to be biologically relevant for the coming flu season by the CDC pursuant to global recommendations from the World Health Organization (131). While the flu season may start in the fall, strain recommendations are generally made for the Northern Hemisphere vaccine in February. This allows manufacturers time to prepare reagents and viral components, which must be specific to the viruses in that year's vaccine, for some 160 million doses. Pharmaceutical companies typically start manufacturing vaccine ahead of official recommendation

announcements in order to have the vaccine ready for distribution as soon as possible; although this puts them at significant financial risk if recommendations change. Vaccine strain selection is a multi-factorial process that requires input from scientists and influenza experts from around the world in addition to epidemiological algorithms that predict the upcoming season based on data from the opposite hemisphere as well as epidemics from the previous year (17, 131). Despite the incredible amount of effort and data analysis that goes into vaccine strain selection, there is the opportunity for error when chasing an ever-moving target. Vaccine mismatches can happen that would leave even healthy, vaccinated, individuals vulnerable to infection (24). It also possible that any one or a combination of the circulating viruses chosen will make significant antigenically relevant changes between strain selection in February and vaccine delivery to points of care in the early fall (120).

Despite many obstacles, vaccine efficacy is generally between 30 and 70% (16, 48, 118). The quadrivalent inactivated vaccine for the 2017-2018 season had an overall efficacy of 40% against all four strains, meaning a vaccinated individual was 40% less likely to seek medical care for flu. H3N2 viruses generally dominated the season, and strain specific efficacy of the vaccine against the H3N2 virus was 25%. There were 184 pediatric deaths; between 80 and 90% of deceased children were unvaccinated (17). While the 2018-2019 season is ongoing, interim estimates from the CDC show a H1N1pdm dominant season with a slightly higher vaccine efficacy of nearly 50%. As of February 2019 seasonal influenza may have caused as many of 17.8 million cases of illness and 19,000 deaths in the United States (17). Even when vaccine efficacy is low or in seasons with a considerable mismatch, studies have shown that vaccination still reduces the need for hospitalization (81, 86, 119).

In the 1960's, Dr. Edward Kilbourne invented a technique of exploiting viral antigenic shift in a controlled laboratory setting to introduce desired characteristics for vaccine production into wild type viruses (62). This process, known as classical reassortment, was first used in vaccine production in 1971 and is still used by our laboratory and others in the United States and around the world. Using classical reassortment, candidate vaccine viruses are selected to express the circulating HA and NA proteins of those viruses recommended by the CDC but contain the internal genes of a high growing donor virus, A/Puerto Rico/8/1934 (PR8). The resulting reassortant viruses are designated high yield reassortants (HYRs), as the inclusion of PR8 internal genes often results in an upregulation of viral growth when injected into embryonated chicken eggs (63). An increase in protein/antigen output is highly desirable to manufacturers as it makes producing the vaccine less costly and more efficient.

Because of influenza virus' segmented genome, co-infection of a single egg with two viruses results in a possible 256 distinct viral progeny. Selection of candidate reassortment viruses from the viral population present within an egg is accomplished by applying polyclonal antibodies to PR8 HA and NA. This inhibits the growth of those viruses expressing PR8 donor glycoproteins on the surface and encourages expansion of the wild type HA and NA bearing viruses. Candidate HYR seed viruses are then cloned by limiting dilution and fully characterized in sequence and antigenicity in house and by government regulatory agencies before being sent to manufacturers for large scale production in eggs. The process of generating seed viruses is a rate limiting step in vaccine production and can vary in time depending on properties of the wild type target, taking on average about four weeks (41, 96).

HA Antibodies and Hybridoma Technology

One of the newest approaches to combating influenza is the use of antibodies (Abs). It has long been known that there is therapeutic benefit to treating serious influenza infections with convalescent plasma, especially in cases of HPAI infection (22). The vast majority of antibodies isolated from people either after a naturally occurring infection or vaccination are targeted to the immunodominant HA. Of these, the highest percentage are targeted to the variable loops surrounding the receptor binding site within the HA head domain. These antibodies function to neutralize virus by preventing viral entry via inhibition of interactions with sialic acid (11). These antibodies are effective but highly strain specific, recognizing only antigenically similar strains of the same group and therefore lose relevance rapidly over time as viruses undergo shift and drift (40, 115).

Rarely, a patient may develop an antibody that instead of targeting the HA head targets the membrane proximal or HA stem domain. These antibodies are often broadly neutralizing and able to inhibit many viruses even across IAV group. The unique cross reactivity of stem antibodies reflects the strong structural constraints imposed on the HA stem epitope as a result of the necessity of its function (121). The stem itself is composed of the N and C terminal domains of HA1 (1-52, and 277-345 H3 numbering) as well as the entirety of the N terminal region of HA2 (109). The accepted demarcation between the HA stalk and head is a disulfide bond between two cysteine residues at amino acids 55 and 277 (69). Because of its conservation, there has been a growing interest in characterizing HA stem antibodies as the basis of a universal vaccine – a vaccine that may one day be able to prevent infection by all influenza A and B subtypes. Since their discovery in 1991, well over a dozen stem antibodies have been isolated in humans in response to heterosubtypic HA

vaccination and more have been derived using targeted technology, including hybridomas and single B cell isolation (65, 80).

Most patient derived HA stem antibodies thus far characterized share common features that may elucidate possible *in vitro* and *in vivo* protection mechanisms. While their exact epitopes differ, generally it lies around or across the HA1/HA2 cleavage site, meaning mAb binding depends on residues found on both HA1 and HA2 subunits (24, 80). Unlike HA head antibodies which inhibit receptor binding, these antibodies target influenza in a multitude of ways both intracellularly and extracellularly and can work at many steps in the viral life cycle. Stem antibodies have been shown to be able to be internalized as a complex with viral particles during receptor mediated endocytosis, and therefore act between entry and exit in the viral life cycle within the host cell (11). Here, binding to the stalk of an incoming HA may inhibit pH induced conformational changes that would normally expose the HA fusion domain, preventing viral and endosomal membrane fusion (115, 133). Another proposed mechanism involves averting the extracellular cleavage of HA0 into HA1 and HA2 by local cellular trypsin-like proteases via site occlusion. This is supported by data suggesting that some stem targeting antibodies with footprints overlapping the protease recognition site are not capable of neutralizing HPAI viruses. These viruses have a multibasic site mutation and are cleaved intracellularly instead of extracellularly unlike most other influenza viruses and are therefore precluded from antibody recognition if internalized unbound (42). While HA stem antibodies do not directly bind NA, they have also been shown to inhibit NA activity *in vitro* through steric hindrance because of the close physical proximity of HA and NA on the virion membrane (68). *In vivo* protection is likely modulated by these mechanisms in addition to others, including ADCC as well as activity

through FCγ receptors on immune cells (28). It is likely a combination of these means and others yet undiscovered coupled with the unique conservation of the HA stem that make stem antibodies so effective at limiting influenza replication *in vitro* and *in vivo* and a very attractive target for vaccine design and therapeutics.

HA stem directed antibodies have been found in human plasma in response to vaccination with more than one HA subtype, but there has also been a concentrated effort to design antibodies targeted to the HA stem. While polyclonal antibodies represent the entire B cell repertoire to an antigen, a monoclonal antibody (mAb) is the result of a single B cell producing one antibody to a specific epitope of that antigen. MAbs are therefore more specific and consistent in a translational context and can be easily modified to be appropriate for administration to humans (106). MAbs can be created using a variety of techniques, including hybridoma technology (**Figure 8**). Using this method, splenic B cells from a mouse immunized against the desired target antigen are fused with myeloma cells to produce hybridoma cells. Hybridoma cells produce antibody like the parental B cell as well as have the ability to divide indefinitely like the parental myeloma cell (56). Successfully fused cells are selected using specialty HAT media which contains hypoxanthine, aminopterin, and thymidine. This blocks the *de novo* nucleic acid synthesis pathway and forces cells to rely on salvage synthesis for DNA and RNA. Unfused splenic cells die quickly due to their short life span and limited doubling capacity. Unfused myeloma cells lack hypoxanthine guanine phosphoribosyl transferase (HGPRT) and are unable to participate in salvage synthesis and therefore also die. The only cells capable of survival in these conditions are successfully fused hybridoma cells. These cells are selected, screened by the method of investigator choice, and finally cloned by limiting dilution so identical

mAbs can be continuously and reliably be produced in cell culture (45).

Through the screening of hybridoma cell lines developed in response to heterosubtypic influenza vaccination of mice, we believe we have generated a novel monoclonal antibody 1G3 (IgG1) targeted to the stem of the influenza HA that may provide insight into shared influenza epitopes and eventually new vaccination and treatment modalities.

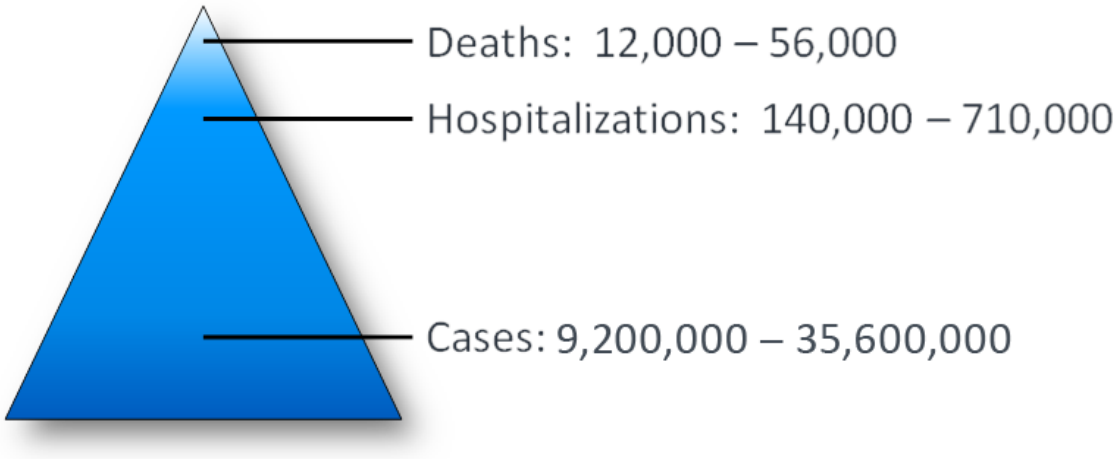

Figure 1*: CDC estimates for number of cases, hospitalizations, and deaths as a result of seasonal influenza infection each year in the United States. Precise calculations are made difficult as many patients will not seek care for mild illness.* (17)

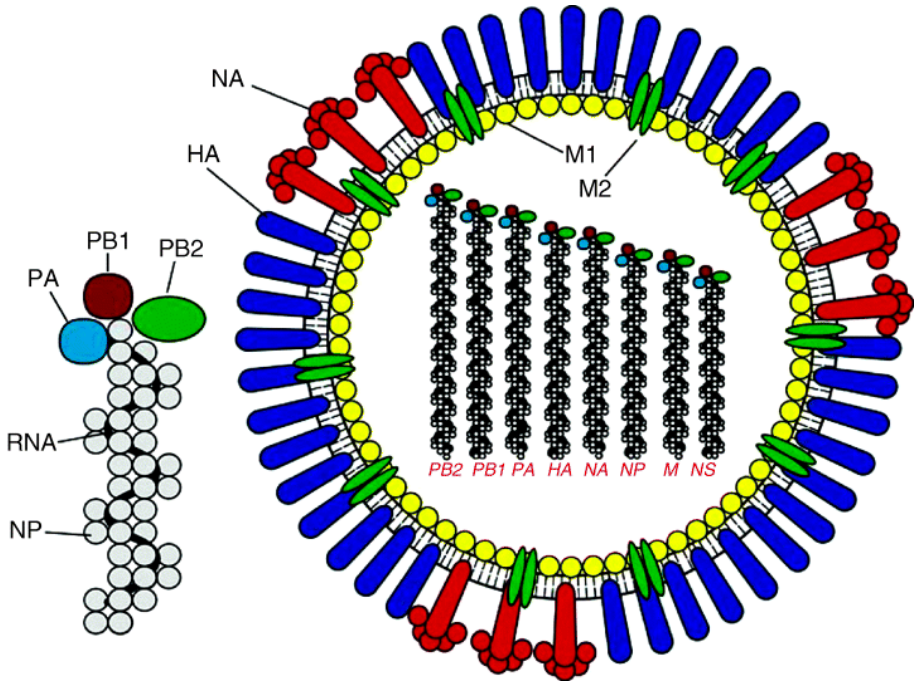

***Figure 2**: Influenza viral structure (on right), shown with spherical morphology. Eight segmented genome segments are shown on the interior of the virion according to descending size. Major surface glycoprotein Neuraminidase (NA) is in red, Hemagglutinin (HA) is shown in blue, while the M2 ion channel embedded within the viral envelope is depicted in green. An individual viral ribonucleoprotein (vRNP) complex is visible to the left of the virion. The viral RNA dependent RNA polymerase is composed of PA, PB1, and PB2.* (24)

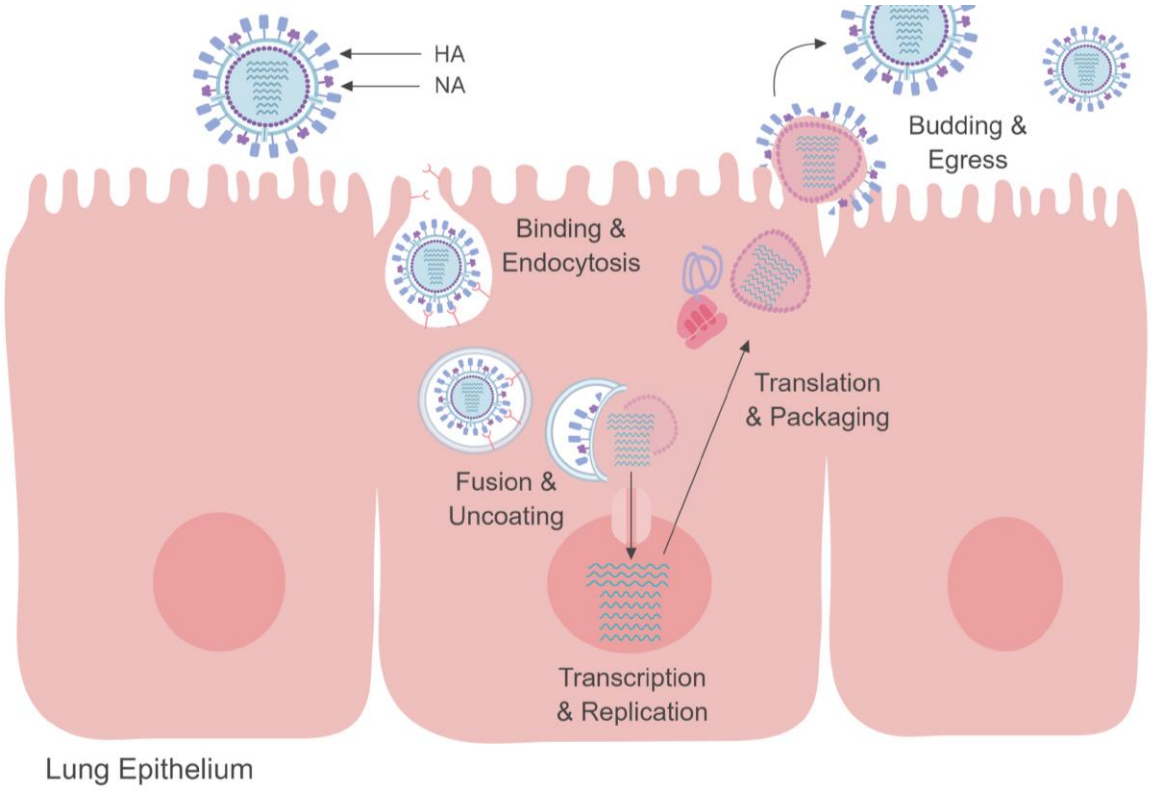

Figure 3*: Influenza A virus life cycle shown with steps labeled from left to right across the infected host lung epithelial cell. This include binding, receptor mediated endocytosis of the virus, fusion of the viral and host endosomal membrane and uncoating of the genome from the viral core. This is followed by replication and transcription in the host cell nucleus, translation and assembly in the cytoplasm, and release as the host cell surface. Image created with BioRender©*

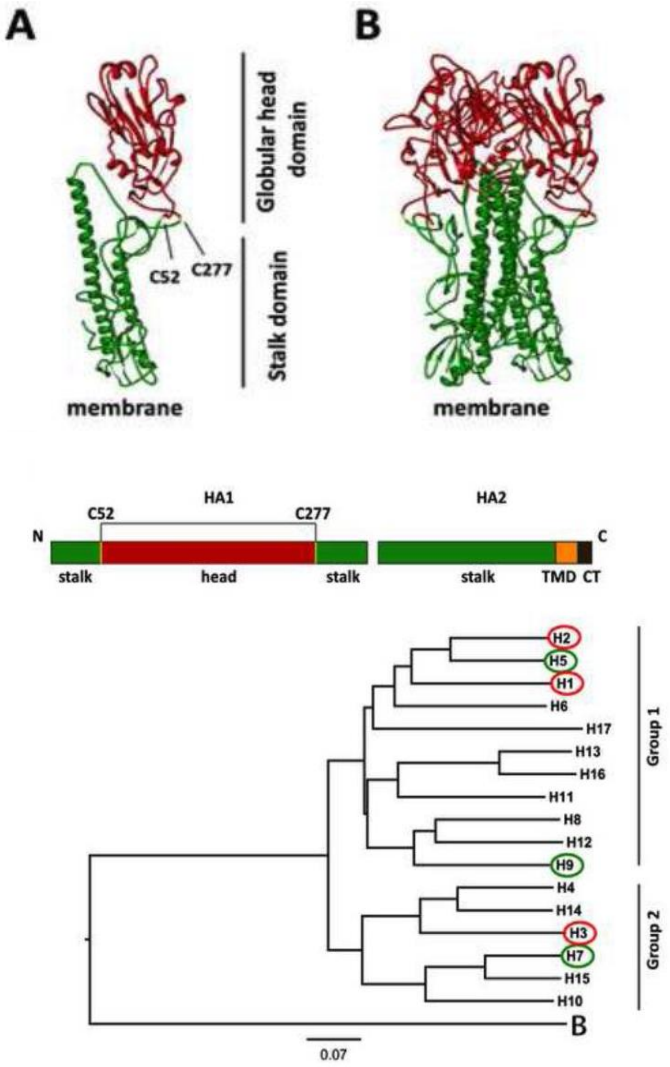

Figure 4*: A) A complete influenza A HA monomer, known as HA0, with subunits HA1 in red and HA2 in green. The globular head and stem domains are technically distinguished by a disulphide bond noted at C52 and C277. B) A native HA homotrimer as it would sit in the membrane of the virus or a host cell with the head facing externally. The basic subunits and domains of HA protein include HA1 and HA2. The HA head is primarily encoded by HA1, while the stalk is composed of the N and C terminal ends of HAI as well as the majority of HA2. HA phylogenetic tree demonstrating the separation of HA into two groups based on stalk sequence. The HA subtypes circled in red circulate as seasonal pandemics while those in green are associated with Highly Pathogenic Avian Influenza (HPAI). (115)*

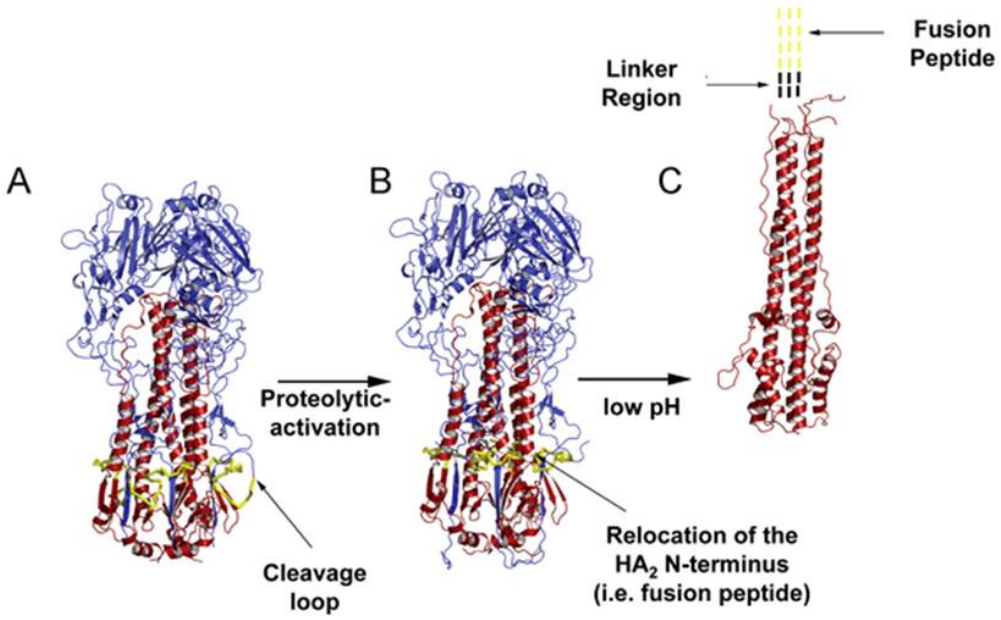

Figure 5*: Ribbon diagram of engaged trimeric influenza A HA. Proteolytic activation by trypsin-like proteases occurs extracellularly for seasonal viruses at the cleavage loop (yellow) yielding distinct HA subunits HA1 (blue) and HA2 (red). HA1 and HA2 stay associated via disulphide bonds throughout binding and endocytosis until low pH present in the host endosome facilitates rearrangement to expose the fusion peptide. The fusion peptide is then free to embed itself in the host endosomal membrane and facilitate the merging of the host and viral membrane. (42)*

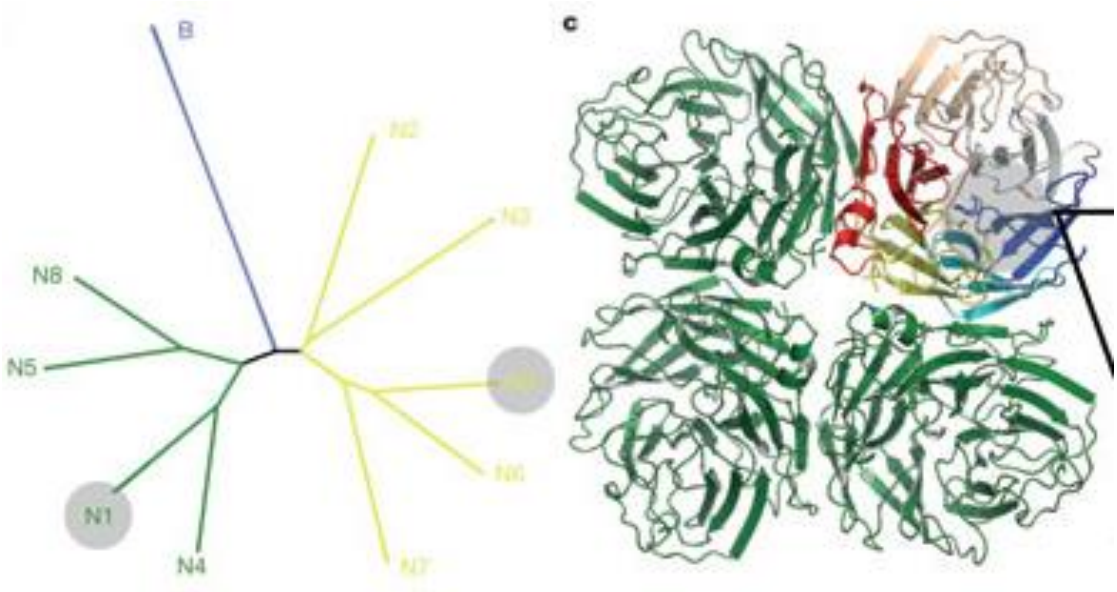

Figure 6*: Left) The phylogenetic tree of all known neuraminidase (NA) subtypes within influenza A and B viruses. Green denotes influenza A Group 1 with is typified by the N1 protein common in seasonal as well as some HPAI viruses. The yellow lines represent influenza A Group 2, this includes N2 which is also common in seasonally circulating viruses. Shown in blue are the NA proteins from influenza B viruses, which share about half of their sequence with those from influenza A viruses. Right) Top down ribbon diagram of influenza A N1 based on X-ray crystallography. Its characteristic "boat propeller" formation is highly conserved between influenza A and B viruses despite considerable sequence variation.(99)*

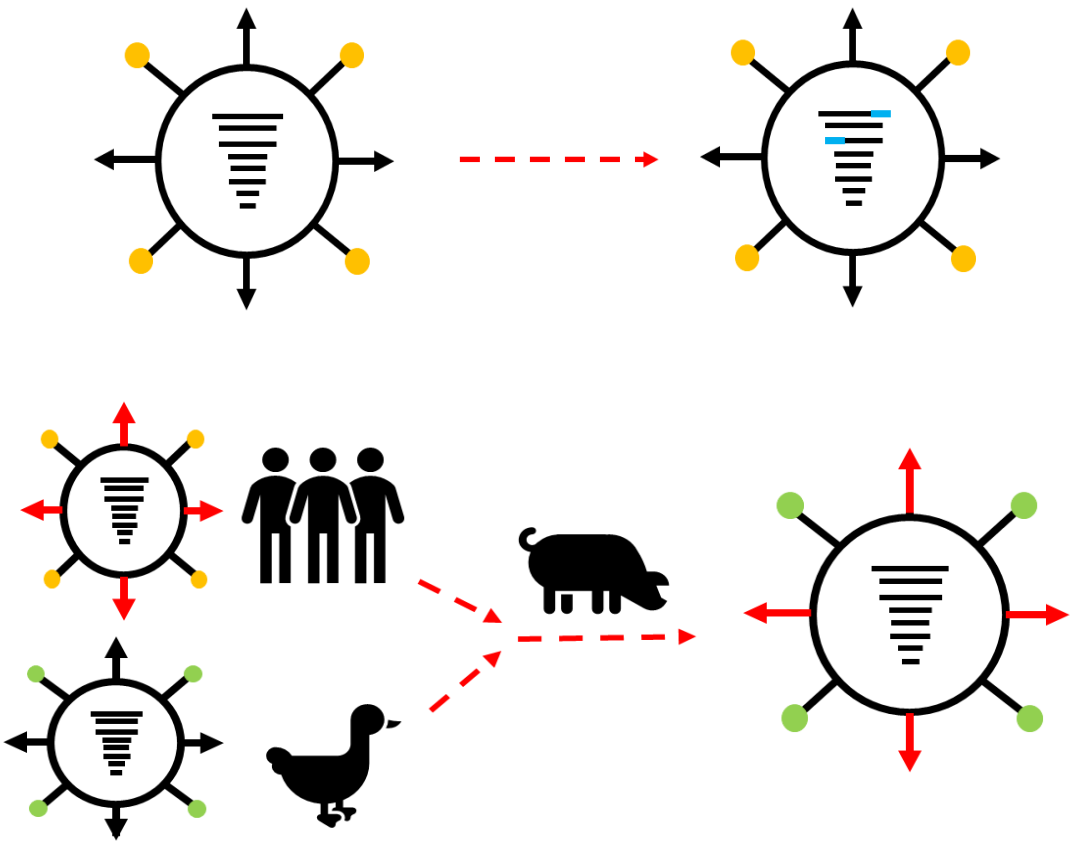

***Figure 7**: Top) Antigenic drift in both influenza A and B viruses is caused by small mutational changes introduced by the error prone viral polymerase. These changes may select for viruses which drift away from neutralizing epitopes and prevent immune recognition - resulting in regular seasonal epidemics. Bottom) Antigenic shift is the introduction of novel proteins into a naïve population. Shift of influenza A viruses can result in pandemic strains. Shift is illustrated here as a triple reassortment in a swine intermediate host resulting in an HA protein not previously seen in humans - as was the case in the 2009 "Swine Flu". Influenzas B and C are not known to participate in shift as they have no substantial animal reservoir. (94)*

Trade name	Manufacturer	Presentation	Age indication
Inactivated influenza vaccines, quadrivalent (IIV4s), standard-dose[†]			
Afluria Quadrivalent	Seqirus	0.5 mL prefilled syringe	≥18 years
		5.0 mL multidose vial	≥18 years (by needle/syringe) 18 through 64 years (by jet injector)
Fluarix Quadrivalent	GlaxoSmithKline	0.5 mL prefilled syringe	≥3 years
FluLaval Quadrivalent	ID Biomedical Corp. of Quebec (distributed by GlaxoSmithKline)	0.5 mL prefilled syringe	≥6 months
		5.0 mL multidose vial	≥6 months
Fluzone Quadrivalent	Sanofi Pasteur	0.25 mL prefilled syringe	6 through 35 months
		0.5 mL prefilled syringe	≥3 years
		0.5 mL single-dose vial	≥3 years
		5.0 mL multidose vial	≥6 months
Inactivated influenza vaccine, quadrivalent (ccIIV4), standard-dose,[†] cell culture-based			
Flucelvax Quadrivalent	Seqirus	0.5 mL prefilled syringe	≥4 years
		5.0 mL multidose vial	≥4 years
Inactivated influenza vaccine, quadrivalent (IIV4), standard-dose, intradermal[¶]			
Fluzone Intradermal Quadrivalent	Sanofi Pasteur	0.1 mL single-dose prefilled microinjection system	18 through 64 years
Inactivated Influenza Vaccines, trivalent (IIV3s), standard-dose[†]			
Afluria	Seqirus	0.5 mL prefilled syringe	≥5 years
		5.0 mL multidose vial	≥5 years (by needle/syringe) 18 through 64 years (by jet injector)
Fluvirin	Seqirus	0.5 mL prefilled syringe	≥4 years
		5.0 mL multidose vial	≥4 years
Adjuvanted inactivated influenza vaccine, trivalent (aIIV3),[†] standard-dose			
Fluad	Seqirus	0.5 mL prefilled syringe	≥65 years
Inactivated Influenza Vaccine, trivalent (IIV3), high-dose[§§]			
Fluzone High-Dose	Sanofi Pasteur	0.5 mL prefilled syringe	≥65 years
Recombinant Influenza Vaccine, quadrivalent (RIV4)[¶¶]			
Flublok Quadrivalent	Protein Sciences	0.5 mL prefilled syringe	≥18 years
Recombinant Influenza Vaccine, trivalent (RIV3)[¶¶]			
Flublok	Protein Sciences	0.5 mL single-dose vial	≥18 years
Live Attenuated Influenza Vaccine, quadrivalent (LAIV4)[***] (not recommended for use during the 2017–18 season)			
FluMist Quadrivalent	MedImmune	0.2 mL single-dose prefilled intranasal sprayer	2 through 49 years

Table 1*: Currently licensed flu vaccines in the United States for the 2017-2018 influenza season. The general standard of care is the intradermal quadrivalent inactivated vaccine which is recommended for all people between 6 months and 65 years of age, including pregnant women and the immunocompromised. The recombinant vaccine, FluBlok™, was approved in 2013 and does not use an egg-based manufacturing scheme. Previously, the live attenuated vaccine marketed as FluMist™ was not recommended due to poor efficacy data but is now available to some patients. Also offered are high dose formulations for patients over 65 years of age. (17)*

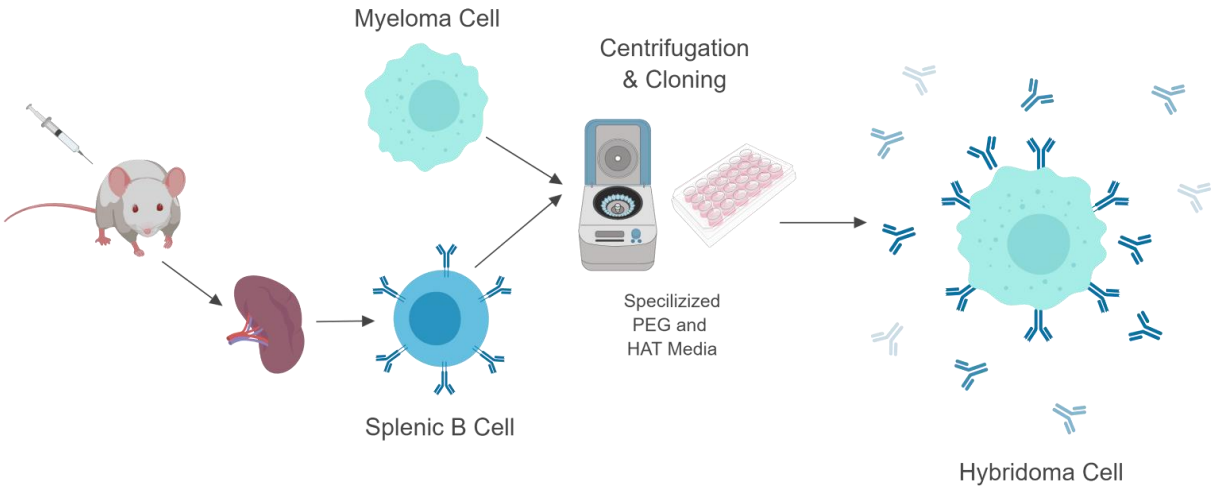

***Figure 8**: Hybridoma cells are generated via the fusion of splenic B cells isolated from an immunized mouse and myeloma cells to form stable antibody producing cell lines using specialized fusion and selection media. Hybridomas can divide indefinitely and serve as a renewable source of standardized and specific monoclonal antibodies. (56, 71, 88) Image created with BioRender©*

SPECIFIC AIMS

Aim 1. Develop and purify anti-Flu Monoclonal Antibodies (mAbs)

1. Generate candidate mAbs via hybridoma technology following mouse immunization
    1.1. Immunization Protocol Alpha: Immunization with A/Puerto Rico/8/1934 (H1N1) and NYMC X-162 (H3N1, A/Wisconsin/67/2003 HA donor) HA and NA protein preparations
    1.2. Immunization Protocol Beta: Co-immunization of A/Puerto Rico/8/1934 (H1N1) and NYMC X-162 (H3N1) HA and NA protein preparations with anti-HA head mAb 2A6 (IgG1)
2. Identify potential candidate mAbs
    2.1. Neuraminidase Inhibition (NI) assay against A/Puerto Rico/8/1934 (H1N1) and NYMC X-162 (H3N1) using both hybridoma supernatant and purified antibody candidates
    2.2. Hemagglutinin Inhibition (HAI) assay against A/Puerto Rico/8/1934 (H1N1) and NYMC X-162 (H3N1) using purified antibody candidates
3. Isotype and purify candidate mAbs

Aim 2. Characterize binding profile and epitope of candidate mAbs

1. Investigate binding profile of candidate mAbs
    1.1. Western blotting against infected allantoic fluid and purified viruses; including immunizing viruses A/Puerto Rico/8/1934 (PR8, H1N1) and NYMC X-162 (H3N1) in addition to heterosubtypic viruses (H1N1, H1N1 pandemic, H3N2 viruses, influenza B viruses)

2. Map the epitope(s) of each candidate mAb using
    2.1. *In silico* sequence alignment of bound viruses from Aim 2.1.1
    2.2. Epitope mapping via overlapping peptide array

Aim 3. Evaluate candidate mAbs efficacy *in vitro* and *in ovo*

1. Demonstrate quantitative *in vitro* inhibition of viral activity by candidate mAbs via Plaque Reduction and Neutralization Tests (PRNT)
    1.1. Testing plaque number and size reduction capability of antibody candidates as hybridoma supernatants against immunizing viruses A/Puerto Rico/8/1934 (PR8, H1N1) and NYMC X-162 (H3N1) in addition to heterosubtypic viruses (H1N1, H1N1 pandemic, H3N2 viruses, and influenza B viruses)
2. Demonstrate qualitative *in vitro* inhibition of viral activity by candidate mAbs via fluorescent microscopy of infected cells
    2.1. Fixed fluorescent staining of A/Puerto Rico/8/1934 (PR8, H1N1) HA following infection then treatment with candidate mAbs or isotype control
3. Compare viral growth curves *in ovo* of immunizing viruses A/Puerto Rico/8/1934 (PR8, H1N1) and NYMC X-162 (H3N1) in addition to an influenza B virus following co-incubation of virus and candidate mAbs

MATERIALS AND METHODS

Mouse Immunizations

Eight six month old female BALB/C mice (POCONO FARMS) were immunized for hybridoma preparation. On Day 0 mice were bled were for a pre-immunization baseline and then injected intraperitoneally with 25 μg purified A/Puerto Rico/8/1934 (H1N1) hemagglutinin and neuraminidase antigen in Freund's adjuvant. This was repeated on Day 14. On Day 28 mice were injected with 25 μg purified NYMC X-162 (H3N1, A/Wisconsin/67/2014 HA parent) hemagglutinin and neuraminidase antigen in Freund's adjuvant. On Day 40, mice were bled and sera tested for response to A/Puerto Rico/9/1934 antigen by ELISA. On Day 45 mice were given a final 25 μg A/Puerto Rico/8/1934 hemagglutinin and neuraminidase antigen boost intravenously before being sacrificed on Day 47 or 48.

Hybridoma Preparation

Following sacrifice, murine spleens are harvested and splenic cells are suspended in serum free hybridoma media (THERMO FISHER) and counted. X63 murine myeloma cells (ATCC) are added directly at a ratio of 1:2 and centrifuged together. 1.5 mL polyethylene glycol (PEG) for every $3x10^8$ mixed cells is very slowly added before centrifuging the solution again at 1000 rpm for 5 minutes. Hypoxanthine-aminopterin-thymidine (HAT) media (THERMO FISHER) is added and the fused cell suspension is divided into flasks prepared with warmed HAT media. Flasks are gently swirled to ensure an even cellular distribution and then cells and 2mL media are aliquoted into 24 well plates to be incubated at 5% CO_2 and 37 ^{0}C. After 10-14 days wells with visible color change from acidic cellular replication by-products are tested for antibody production by ELISA. ELISA positive wells

are sub-cloned into 96 well plates for primary screening and then transferred to flasks for continuing culture.

Antibody Isotyping

Antibody isotyping is done via Murine Antibody Isotyping Kit (PIERCE). Candidate hybridoma cell culture supernatant is diluted with the sample diluent to a final concentration of 1:1000 and vortexed. 150 µl of the diluted sample is added to the testing cassette and incubated at room temperature for 10 minutes. A successful typing is characterized by a red band at the control mark and a dark band at one of the isotypes markered on the cassette.

IgG Antibody Purification

The cell culture supernatant of candidate hybridomas is centrifuged at 6000g for 5 minutes to remove any cellular debris. The G protein column is equilibrated with 75 ml PBS and the supernatant is diluted two fold with PBS to a final volume of 600 mL and directly applied to the column followed by 100 mL PBS to wash the column. Bound monoclonal antibody is eluted from the column with 75 mL 0.1 M glycine (pH 2.7) and approximately 2 mL per fraction is collected in 5 mL tubes with 40 µl 1 M Tris-HCl (pH 9.0). Absorbance at 280 nm is measured for each fraction, and all fractions with an absorbance more than 0.5 are pooled into a clean 15 ml conical tube. The pH of the purified mAb is determined by pH paper and adjusted to 7.0 by neutralizing buffer. Antibody solutions are then run by Western blot in reducing and non reducing conditions and stained with Coomassie blue to assure purity.

Antibody Concentration Measurement

The concentration of purified monoclonal antibodies is determined by Bradford assay (BIO-RAD). Five linear-range dilutions of the bovine gamma immunoglobulin standard and

purified antibody are prepared. 800 µl of each standard and sample solution is incubated with 200 µl dye reagent concentrate at room temperature for 5 minutes. Absorbance is then measured at 595 nm. The concentration of purified antibody is calculated from the standard curve. All protein solutions are assayed in duplicate.

Virus Amplification

Viruses are amplified in 11 day old embryonated Specific Pathogen Free (SPF) chicken eggs. A virus dilution of 10^{-5} is prepared in phosphate buffered saline (PBS) with 25 µg/ml gentamicin (SIGMA). 0.1 mL of the viral dilution is injected into each egg. After incubation at 35 ^{0}C for 48 hours, the eggs are placed at -20 ^{0}C for 1 hour and then 4 ^{0}C for at least 2 hours. Then allantoic fluid containing virus is harvested from the eggs. The titer is determined by hemagglutination assay and plaque forming units per mL (PFU/mL) is determined by plaque assay.

Neuraminidase Assay

50 µl of hybridoma cellular supernatant is first added to a glass 16 X 125 mm tube (FISHER). 50 µl virus diluted to desired concentration in PBS supplemented with 2mM calcium. PBS with calcium without virus is used as a negative control. Following 30 mins incubation at room temperature, 100 µL of fetuin diluted in 0.4M phosphate buffer (pH 5.9) is added to each tube. Tubes are vortexed and incubated in a 37 ^{0}C water bath for 16-18 hours. 0.1 mL periodate is then added to each tube. Following a 20 minute incubation at room temperature, 1 mL arsenite is added. Tubes are agitated by hand until the solution turns from dark brown to clear or opaque. 2.5 mL of thiobarbituric acid is added and tubes are vortexed. Tubes are then placed in a boiling water bath for 15 mins. The mixture is allowed to reach room temperature before 4 mL acid butanol is added. Tubes are briefly

vortexed and then centrifuged for 2 mins at 1000 RPM. The optical density read at 549 nanometers by spectrophotometer.

Hemagglutination Assay

50 µl phosphate buffered saline (PBS) is added to each well of a V bottomed 96-well microtiter plate. 50 µl of purified virus or virus suspended in allantoic fluid is added into the first well of each row. A 2-fold serial dilution (1:2, 1:4, 1:8, etc.) is made by carrying 50 µl of solution from well to well across the plate. 50 µl PBS and virus left in each well are incubated with 50 µl 0.5% chicken red blood cells at room temperature for 30 minutes after 30 seconds of agitation. The virus titer is read as the lowest dilution ratio of virus without visible hemagglutination.

Western Blotting

0.1 µg viral protein or 10 µL of infected allantoic fluid is loaded into NuPAGE Novex 4-12% Bis-Tris precast gel and separated using the XCell SureLock Mini-Cell electrophoresis system (INVITROGEN). The proteins are transferred onto polyvinylidene difluoride (PVDF) membrane and probed with antibody containing hybridoma cellular supernatant overnight at 4 °C. Near infrared fluorescent anti-mouse IgG secondary antibody (LICOR) diluted in blocking buffer (LICOR) is then incubated with the membrane for 1 hour at room temperature. Blots are washed four times before scanning using an Odyssey membrane scanner (LICOR).

Cell Culture

Madin-Darby canine kidney (MDCK) cells were purchased from American Type Culture Collection (ATCC). Cells are grown in Eagle's Minimum Essential Medium (EMEM,

GIBCO) supplemented with 10% fetal bovine serum (FBS, GIBCO), 10 units/mL penicillin (SIGMA), and 10 μg/mL streptomycin (SIGMA) at 5% CO_2 and 37 ^{0}C. FBS is denatured at 56^{0}C for 30 minutes prior to use. For subculture, cells are grown to 80% confluency before detached from culture flask using trypsin-EDTA (SIGMA).

In vitro Plaque Reduction Neutralization Test

MDCK cells are seeded in 6-well plates (CORNING) at a density of 0.5-1x10^5 cells per well in 4 ml of growth medium. When approximately 80-90% confluency is achieved after 48 hours, the growth medium is removed and wells are washed with 2 ml PBS supplemented with 0.2% bovine serum albumin (BSA, SIGMA). Each well is then inoculated with 0.2 mL virus diluted to desired PFU. After incubation at 5% CO_2 and 37 ^{0}C for 30 minutes the virus inoculum is removed. Each well is then covered with an agar overlay composed of Minimal Essential Medium (MEM, ATCC), 2 μg/mL trypsin (WORTHINGTON), and 0.01% Diethylaminoethyl (DEAE) dextran supplemented with hybridoma cell culture supernatant or purified monoclonal antibody. 72 hours post infection the overlay is removed and plaques are visualized by staining with 0.1% crystal violet in 20% ethanol for 15 minutes at room temperature.

Indirect Immunofluorescence

MDCK cells are seeded into 6 or 8 well chamber slides (NUNC). Cells are incubated at at 5% CO_2 and 37 ^{0}C and reach 80 to 90% confluency at 12-18 hours. Each well is then inoculated with 0.2 mL A/Puerto Rico/8/1934 (H1N1) diluted to desired PFU in PBS supplemented with 0.2% bovine serum albumin (SIGMA). Following 30 mins at 37 ^{0}C, the viral inoculum is removed and replaced with growth media or growth media supplemented with purified monoclonal antibody. The chamber slides are incubated at 5% CO_2 and 37 ^{0}C

for 48 hours. The cellular monolayer is fixed with 3.7% paraformaldehyde for 30 mins at 4 ^{0}C and then rinsed with PBS. Cells are incubated with 5% bovine serum albumin (SIGMA) in PBS for 1 hour at room temperature. Primary antibody is diluted in 1% bovine serum albumin (SIGMA) and incubated with the cells overnight at 4 ^{0}C. Next, the cells are washed with PBS and incubated with the anti-mouse IgG Alexa Fluor 488 secondary antibody (JACKSON LAB) for 1 hour at room temperature. Following a final wash, the cells are incubated with 4'6,-diamidino-2-phenylindole (DAPI, THERMO FISHER) for 5 mins and mounted with coverslip.

In ovo Inhibition Test

11 day embryonated Specific Pathogen Free chicken eggs (CHARLES RIVER) are first "windowed" by removing a 1 cm square portion of the shell. Virus is diluted to 10^{-8} in PBS supplemented with 25 μg/mL gentamicin (SIGMA) and then incubated with purified monoclonal antibodies for 30 mins at 37 ^{0}C. 0.1 ml of the virus-antibody solution is injected into each windowed egg and the window is sealed UV sterilized parafilm sealed to the intact shell with melted paraffin wax. The parafilm is removed and 150 μl of allantoic fluid collected every 12 hours before resealing the window. Eggs are incubated for a total of 72 hours at 37 ^{0}C for influenza A viruses, or 96 hours at 33 ^{0}C for influenza B viruses. The viral titer of allantoic fluid is determined by hemagglutination assay.

EXPERIMENTAL RESULTS

Aim 1. Develop and purify anti-Flu Monoclonal Antibodies (mAbs)

During the completion of his dissertation in our laboratory, Dr. Yu He began experiments with the intention of generating monoclonal antibodies (mAbs) targeting the hemagglutinin (HA) and neuraminidase (NA) proteins of A/Puerto Rico/8/1943 (PR8) for use during the generation of candidate vaccine viruses. MAb secreting hybridomas were produced from the harvested spleens of animals enrolled in an immunization protocol referred to as Alpha (**Figure 9**). Briefly, eight female BALB/C mice were immunized intraperitoneally with PR8 H1N1 HA and NA protein preparation followed by heterosubtypic NYMC X-162 H3N1 preparation. NYMC X-162 is a high yield reassortant (HYR) virus which has the HA gene from A/Wisconsin/67/2005 (H3N2) but the NA and remaining internal genes of PR8. Antigen was prepared for injection by amplification in specific pathogen free embryonated chicken eggs. HA and NA proteins were co-purified using high speed centrifugation and sucrose gradient. Following inoculation, mouse sera was then collected and screened via ELISA against PR8 HA and NA on Day 40 post injection. Animals with positive ELISA results were given a final PR8 HA+NA protein boost intravenously on Day 45 and then sacrificed. Isolated spleen cells were fused with myeloma cells to form stable antibody producing hybridoma cells which were then cloned and screened (**Figure 8**).

From Immunization Protocol Alpha, we were able to establish 114 hybridoma cell lines targeted to influenza surface glycoproteins HA or NA. The antibody containing (conditioned) supernatant of these cells was then screened for reactivity against HA or NA by Western blot using recombinant PR8 HI HA (rHA). Initially, we were interested in an

antibody to the PR8 NA as Dr Yu He had previously characterized several HA antibodies. Of 114 hybridoma supernatants tested, 25 appeared to be targeted to NA as they showed a positive HANA ELISA but a negative Western blot against rHA.

All 25 of these antibodies were tested, but only seven showed the ability to inhibit NA activity in a Neuraminidase Inhibition (NI) assay (**Figure 12**). The NI assay allows us to determine if an antibody (present in sera, in hybridoma supernatant, or as purified protein) has the ability to inhibit the viral NA by measuring the enzymatic activity of NA in the presence of antibody vs that of an uninhibited control. This is accomplished via colorimetric assay which measures available N-acetyl neuraminic acid following incubation of antibody (or control buffer), live virus, and NA substrate in the form supplemented of bovine fetuin (93). Following overnight incubation, free N-acetyl neuraminic acid is measured by the addition of arsenite and 2-Thiobarbituric Acid. The resulting hot pink color is then extracted into the organic phase through the addition of Warrenoff reagent (acid butanol). Absorption at 549 nanometers is determined using a fetuin blank to equilibrate the spectrophotometer. NA enzymatic activity is shown normalized to an uninhibited virus control and experiments were performed in duplicate. Supernatant from 2H9 secreting hybridoma cells, one of the anti-HA antibodies developed by Dr Yu He, was used as a conditioned supernatant control. It is likely the cellular supernatant contains sialic acid beyond the fetuin used in the assay, thus explaining why supernatant containing mAb 2H9 shows NA activity above 100% when normalized to the viral control. Supernatant containing mAb 2G5 (IgM) was the most successful inhibitor of PR8 NA enzymatic activity followed by all three IgG candidates: 1G3, 2A7, and 1G9 (**Figure 12**).

Following primary screening via NI assay of hybridoma supernatants, the seven

mAb candidates from Immunization Protocol Alpha with NI activity were isotyped and purified for further study (**Table 2**). MAb candidates were typed using a commercially available isotyping cassette. IgG mAbs were then purified by Protein G column chromatography. Concentrations were determined by Bradford assay and calculated from the standard curve. Antibodies 1G3 and 1G9 originate from the same immunized mouse, although the parent splenic B cell of each lineage is unique. 2A7 shares mouse origin and parent cell with 1G9, although they are distinct clones from that line. It's possible that 1G9 and 2A7 have the same epitope, but very unlikely 1G3 and 1G9 do.

IgG purification necessitates elution in a low pH solution that can compromise the integrity and efficacy of an antibody. Therefore establishing NI activity following purification is not only valuable in determining concentration dependence, but also in establishing continued functional relevance. 2H9 is a PR8 specific anti-HA mAb developed by Dr Yu He that binds the HA globular head and was selected as an antibody control. As before, NA enzymatic activity is shown normalized to an uninhibited virus control and all experiments were performed in duplicate. Where 2G5 (IgM) appeared the most successful in supernatant, its NA inhibition was ablated following purification. It's unknown if this reflects nonspecific inhibitors present in the cellular media or perhaps a loss of function during the purification process. However all three of the IgG mAb containing conditioned hybridoma supernatants which showed NA inhibition, 1G3, 2A7, and 1G9, continued to inhibit PR8 NA once purified (**Figure 13**). Of these, 1G3 was the most efficient, followed by mAbs 2A7 and 1G9. These data are indicative of the ability to interfere with the enzymatic activity of NA. This can be attributed to one of two possible mechanisms, the first being direct binding to NA. However, it has also been shown that some HA targeted

antibodies can indirectly inhibit NA via steric hindrance (68). We observed this phenomenon experimentally with mAb 2H9. Despite its confirmed globular head/HA1 epitope, 2H9 was still was able to reduce PR8 NA activity by nearly 20% (**Figure 13**).

NA inhibition assays were then repeated in the presence of Triton X-100. The design of this experiment was most recently outlined by Yewdell's group (68) in an attempt to distinguish true NA targeted antibodies vs HA antibodies which may also be able to inhibit NA enzymatic activity. By solubilizing viral membranes, they aimed to spatially separate HA and NA thus removing the contribution of steric hindrance. Their lab was able to use this technique to show that the addition of Triton X-100 significantly lowers or completely eliminates the ability of known HA antibodies to inhibit NA function measured by NI assay. A/Puerto Rico/8/1934 (PR8, H1N1) suspended in infected allantoic fluid and 0.5% Triton X-100 were co-incubated for 10 mins before the completion of the NI assay as described previously. We performed this experiment with cloned hybridoma supernatant containing antibodies 1G9 and 1G3 as well as with a 2H9 antibody control. Triton X-100 has been shown to stabilize NA (13), and as expected it's addition did increase NA activity in the PR8 control to above 100% relative activity of insolubilized virus. However, we found that the addition of detergent eliminated NA inhibition by 1G3 and 1G9 previously seen. Triton treatment also removed 2H9 mediated NA inhibition. (**Figure 14**). According to the hypothesis set forth by Yewdell *et al*, these data imply that 1G3 and 1G9 inhibit NA indirectly.

The most well studied and common neutralizing antibodies to influenza A are those like 2H9 and 2A6 which target the globular HA head. These antibodies prevent virus from binding and entering the host cell during infection as well as prevent the HA mediated

agglutination of red blood cells (102). In contrast, antibodies which target NA or the HA stem have been shown to lack the ability to inhibit hemagglutination (69, 125). MAb 1G3 showed the most significant NI as a purified antibody (~50% reduction in NA activity in the absence of detergent) and was next tested for its ability to inhibit the activity of the viral HA head through a Hemagglutinin Inhibition (HAI) assay. Briefly, columns 1, 2, and 3 of a 96 well microtiter plate are loaded with antibody. Virus suspended in infected allantoic fluid at an experimentally determined HA titer of 1:16 is then added to columns 2-12. Virus is not added to column 1 to assess any possible nonspecific hemagglutination. Column 2 contains virus with no antibody as a positive control for virus mediated agglutination. Starting in column 3, purified antibody is serially diluted across the plate and an equal volume of 0.5% chicken red blood cells is added to each well. While some viruses require the use of alternative blood sources, like guinea pig or turkey, both PR8 and NYMC X-162 readily agglutinate chicken red blood cells. Agglutination is seen as an opaque well while the absence of agglutination is visualized by the pooling of red blood cells at the bottom of the well, forming a "button" (64).

HAI assays were performed with purified 1G3 and 1G9 against both immunizing viruses which carry different HA proteins; PR8 (H1N1) and NYMC X-162 (H3N1, A/Wisconsin/67/2005 HA parent) **(Figure 15**). Experiments were performed twice, each in duplicate. HA mediated agglutination of red blood cells was clearly seen in all columns 3-12, despite the presence of purified mAb 1G3 or 1G9 at concentrations as high has 1 mg/mL in column 3. These data show that mAbs 1G3 and 1G9 cannot inhibit the agglutination of red blood cells of either the H1 or H3 proteins and therefore likely does not bind to the globular HA head.

A second panel of hybridoma cell lines from an alternative immunization protocol were also developed, referred to as Immunization Protocol Beta. HA is immunodominant in natural and laboratory infections as well as following vaccination (80). Immunization Protocol Beta (**Figure 10**) differs from Alpha in that HA+NA preparations were co-injected with a mAb specific for PR8 HA, 2A6. 2A6 has been mapped by Dr Yu He to bind the HA globular head of PR8. This protocol was designed with the intention of encouraging an immune response to the PR8 NA, as HA would be theoretically occluded from immune recognition due to the presence of bound 2A6. During Immunization Protocol Beta, sera on Day 40 was collected for ELISA and for NA specificity testing via an NA inhibition assay. Sera from all seven animals enrolled in Immunization Protocol Beta showed the ability to inhibit PR8 NA (**Figure 11**). Fusions of splenic B cells from those animals with the most significant ELISAs to generate hybridomas for further screening are currently ongoing.

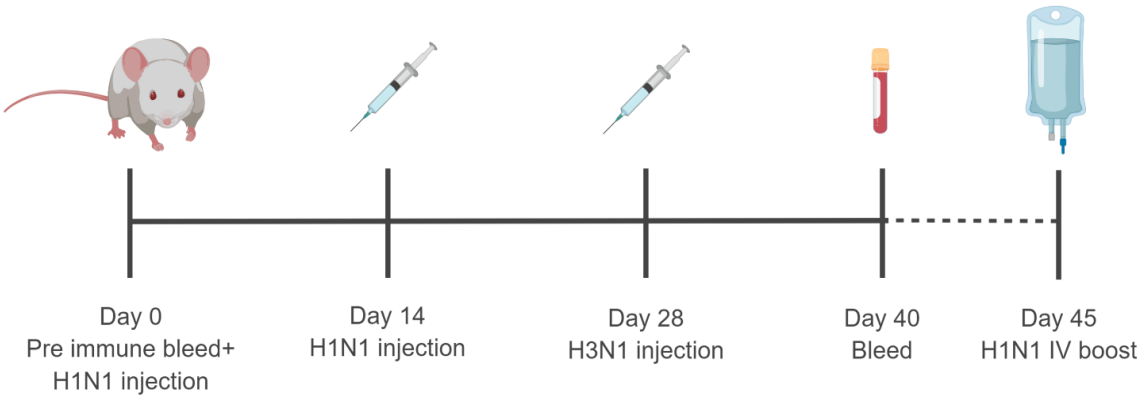

***Figure 9**: Immunization Protocol Alpha. N=8 female BALB/C mice (3 months old at D.0) were immunized intraperitoneally first with A/Puerto Rico/8/1934 (PR8, H1N1) HA + NA protein on days 0 and 14 followed by NYMC X-162 (H3N1, A/Wisconsin/67/2005 parent) HA + NA protein preparation on day 28. Sera from immunized animals were screened by ELISA against PR8 HA+NA on Day 40 and hybridoma fusions performed post intravenous antigen boost and sacrifice on D.45. Image created with BioRender©*

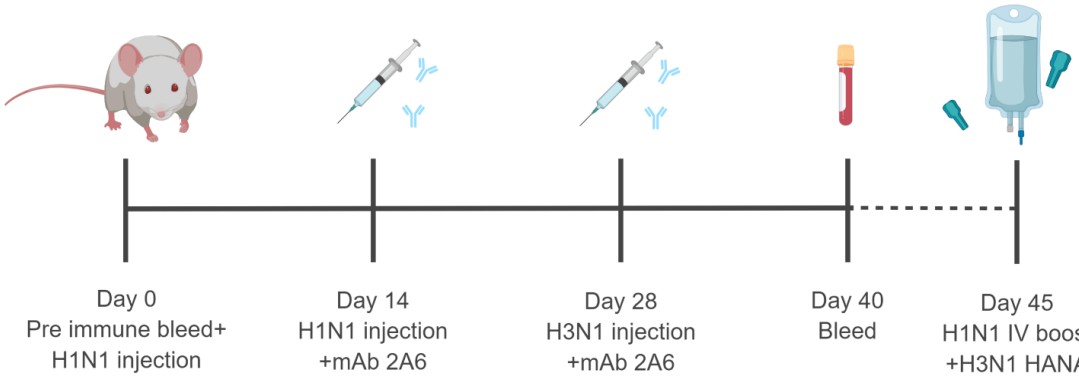

***Figure 10**: Immunization Protocol Beta. N=7 female BALB/C mice (3 months old at D.0) intraperitoneally immunized with A/Puerto Rico/8/1934(PR8, H1N1) and NYMC X-162 (H3N1, A/Wisconsin/67/2005 parent) HA+NA purified protein preparation co-injected with PR8 HA head specific mAb 2A6 developed by Dr. Yu He. Sera were screened by ELISA on Day 40 and hybridoma fusions performed post intravenous antigen boost and sacrifice on D.45. Image created with BioRender©*

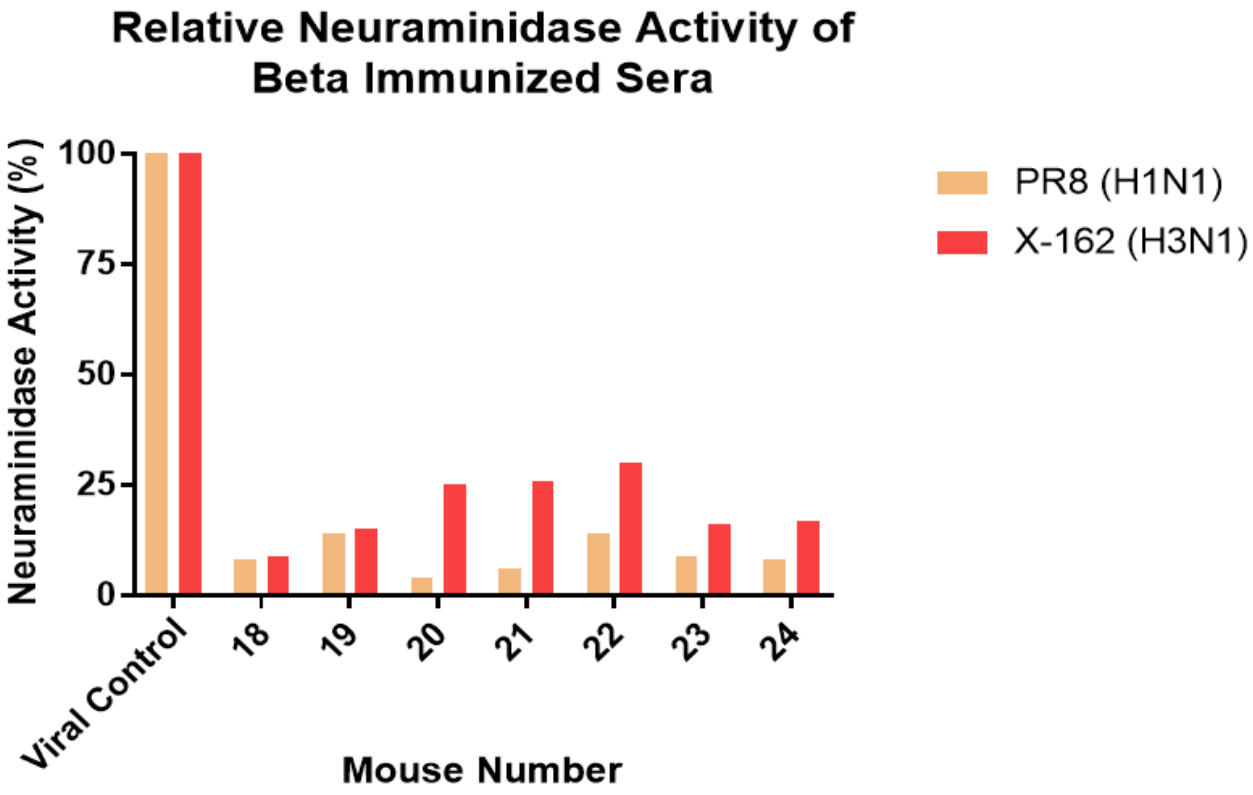

Figure 11*: Relative neuraminidase Activity of sera collected from animals enrolled in Immunization Protocol Beta (n=7). Sera from immunized animals was tested for the ability to inhibit NA activity using a Neuraminidase Inhibition (NI) assay against both immunizing viruses, A/Puerto Rico/8/1934(PR8, H1N1) and NYMC X-162 (H3N1, A/Wisconsin/67/2005). NA Activity is shown relative to uninhibited viral controls. Sera from each animal showed the ability to significantly inhibit the activity of NA of both PR8 (orange) and NYMC X-162 (red). Experiments performed in duplicate.*

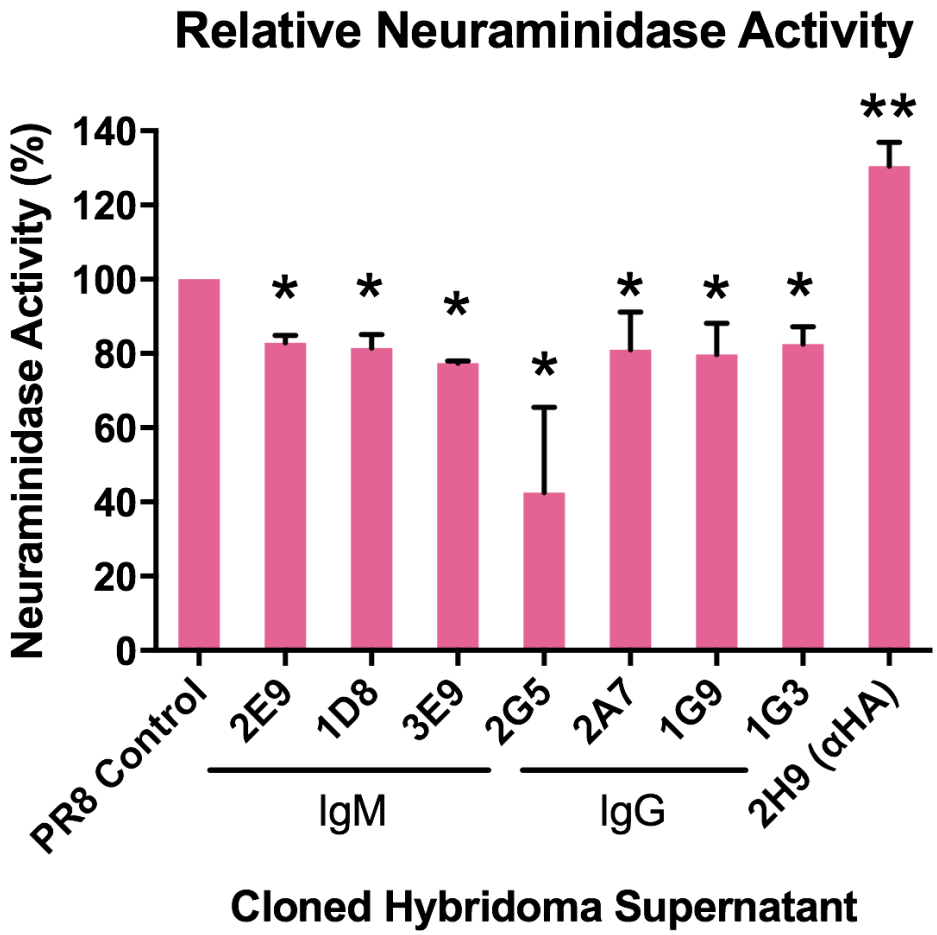

***Figure 12**: Relative neuraminidase activity following incubation of A/Puerto Rico/8/1934(PR8, H1N1) with seven antibody candidates developed from Immunization Protocol Alpha as conditioned hybridoma supernatant. Data shown are relative to viral PR8 control and PR8 specific anti HA mAb 2H9 supernatant control. Supernatant from each of seven hybridoma fusions negative for rHA binding by Western blot showed the ability to inhibit the NA of PR8 by an average of 20%. Cellular supernatant likely contains additional NA substrate above the supplemented fetuin, therefore the HA targeted 2H9 showed NA activity above the viral control. Experiments performed in duplicate. * = $p<0.05$, ** = $p<0.01$, *** = $p<0.001$*

Candidate mAb	Isotype
2E9	IgM
3E9	IgM
1G3	IgG1
2A7	IgG1
1G9	IgG1
2G5	IgM
1D8	IgM

***Table 2**: Candidate monoclonal antibodies identified following Immunization Protocol Alpha then subsequently purified. Antibodies shown failed to bind recombinant PR8 HA on Western Blot but reacted with PR8 HA+NA protein by ELISA. Of seven antibody candidates, four were of the IgM subclass while the remaining three were IgG1. 1G3, 2A7, and 1G9 are from the same parental mouse. However 1G3 and 1G9 were derived from different parental splenic B cells.*

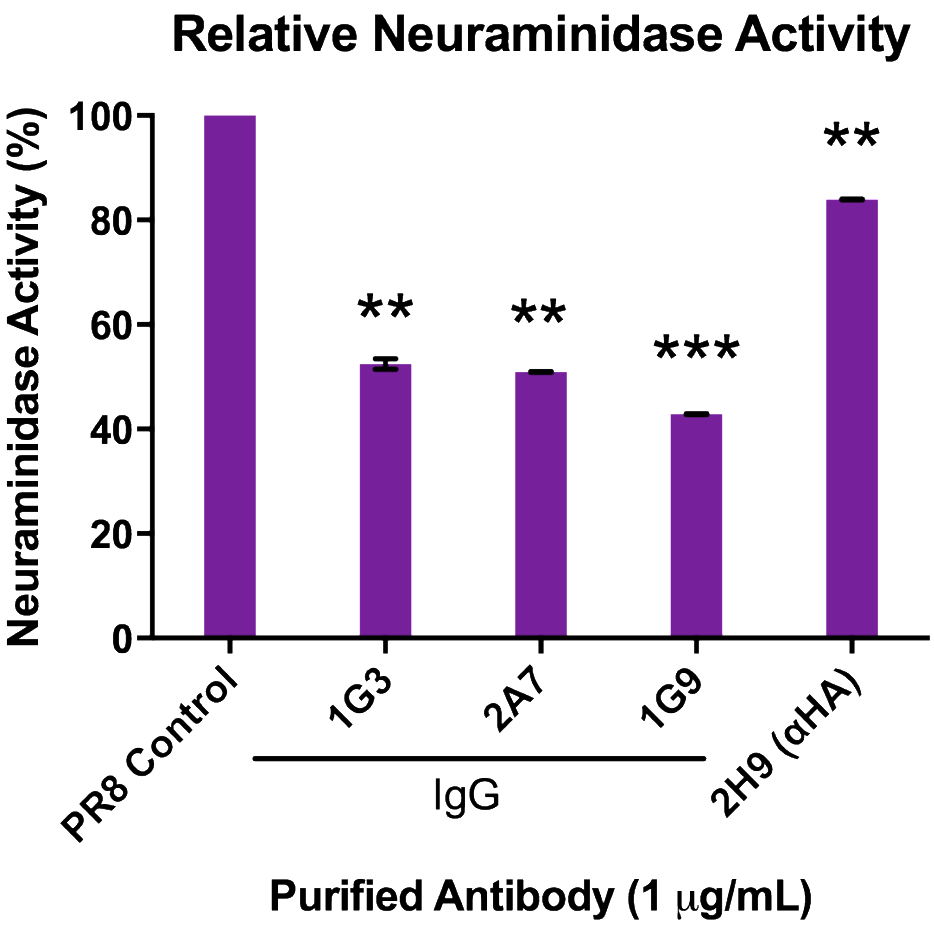

Figure 13: *Relative neuraminidase activity following incubation of virus and purified antibody at a concentration of 1μg/mL, shown compared to viral PR8 (A/Puerto Rico/8/1934, H1N1) control and anti-HA head mAb 2H9 antibody control. MAbs 1G3, 2A7, and 1G9 (IgG1) each resulted in roughly a 50% reduction in NA enzymatic function. HA targeted mAb 2H9 (IgG1) showed a reduction of almost 20% despite being targeted to the HA head, likely due to steric hindrance. Experiments performed in duplicate. * = $p<0.05$, ** = $p<0.01$, *** = $p<0.001$*

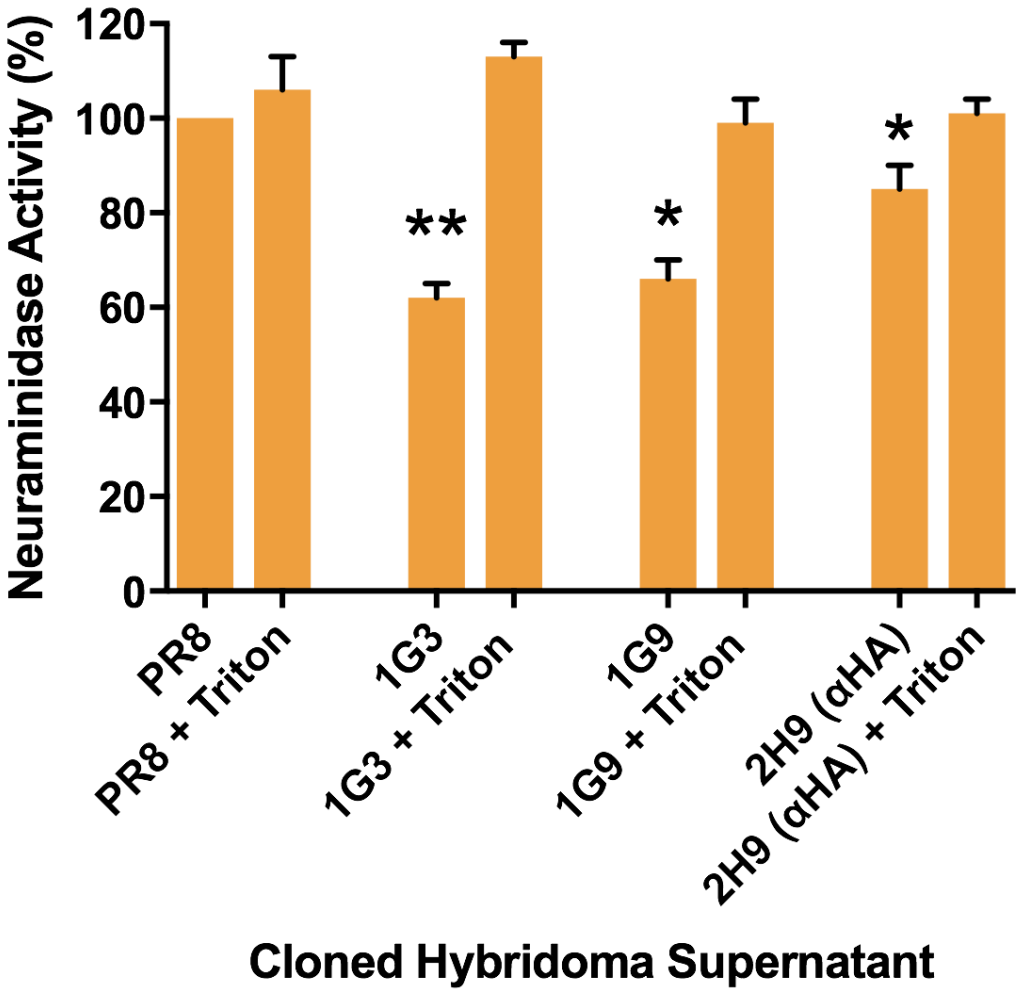

Figure 14*: Neuraminidase (NA) activity following incubation of virus and antibody containing hybridoma supernatant shown relative to PR8 (A/Puerto Rico/8/1934, H1N1) viral control. Virus suspended in allantoic fluid was pretreated with 0.5% Triton X-100 prior to assay to solubilize virion membranes. Triton has been shown to stabilize NA, therefore an increase in NA activity was expected with the uninhibited PR8 virus control treated with Triton. Antibodies 1G3 and 1G9 showed a reduction of roughly 40%, which was completely reversed upon detergent treatment. 2A6 is an HA head targeted antibody control, which again showed some inhibition of PR8 NA that was similarly ablated following triton treatment. Experiments performed in quadruplicate. : * = p<0.05, ** = p<0.01, *** = p<0.001*

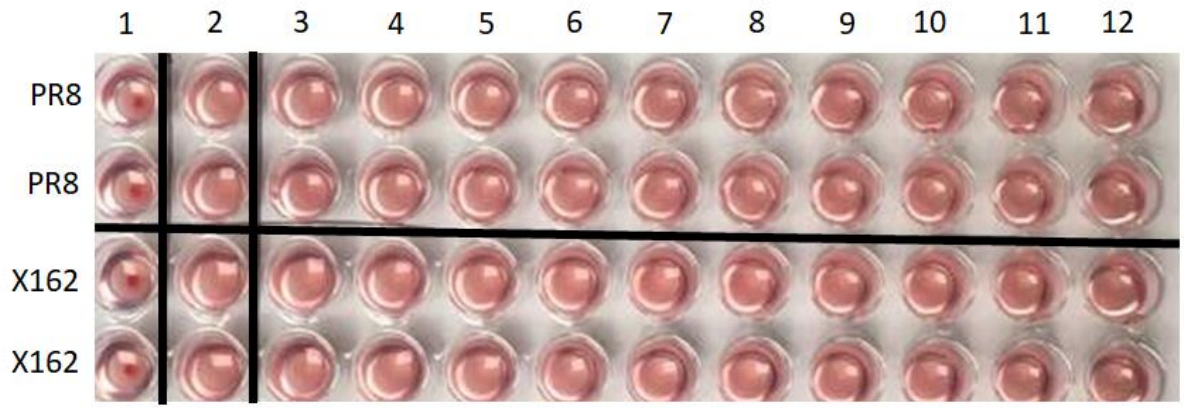

Figure 15: *Representative hemagglutination inhibition (HI) assay plate following incubation of virus and purified 1G3 antibody with chicken red blood cells. Antibody candidate 1G3 was tested at a high starting concentration of 1 mg/mL (column 3) and serially diluted to column 12. Column 1 contains no virus as a negative control to assess nonspecific agglutination. Column 2 contains no antibody as a positive control of agglutination activity by the virus. Both immunizing viruses were tested, A/Puerto Rico/8/1934 (PR8, H1N1, top rows) and NYMC X-162 (A/Wisconsin/67/2005 HA parent, H3N1, bottom rows). Agglutination of the red blood cells by both viruses was seen in all rows of columns 2-12, demonstrating that mAb 1G3 lacks the ability to inhibit either the H1 or H3 HA head.*

Aim 2. Characterize binding profile and epitope of candidate mAbs

Candidate mAb 1G3 is an IgG1 antibody that displayed an interesting activity profile in our primary screen. 1G3 showed NA inhibition in an NI assay (**Figures 12, 13**) which is indicative of an antibody that can block NA enzymatic function. However, 1G3 lacked NA inhibition activity following virus pre-treatment with detergent (**Figure 14)** and additionally lacked the ability to inhibit HA head mediated agglutination (**Figure 15**). These data together suggest an epitope outside of NA and away from the HA head, possibly on the HA stem. In order to confirm mAb 1G3's viral target, Western blots were performed.

First, commercially available recombinant A/Puerto Rico/8/1934 HA H1 (PR8, H1N1) (rHA) as well as both immunizing viruses NYMC X-162 (H3N1, A/Wisconsin/67/2005 HA parent), and native PR8 (H1N1) as infected allantoic fluid were run on a 4-12% gradient Bis Tris gel in non-reducing conditions (**Figure 16**). MAb 1G3 containing conditioned hybridoma supernatant was used as the primary probing antibody at a dilution of 1:128,000. An infrared goat anti-mouse secondary was incubated with the membranes and all blots were visualized using an Odyssey Scanner. Candidate mAb 1G3 showed the ability to bind both NYMC X-162 and native PR8. Bands were seen at roughly 70, 125 and 260 kDA for PR8 and 85, 100, and 130 kDA for NYMC X-162. When repeated in reducing conditions, a faint band could also be seen around 25 kDa for both immunizing viruses in addition to a larger, significant band between 55 and 75 kDa (**Figure 17**). In both reducing and non-reducing conditions, 1G3 was not able to bind to the recombinant PR8 HA H1 subunit despite displaying excellent affinity for native PR8 in allantoic fluid.

MAb 2A6 containing hybridoma supernatant was used as the primary probing antibody as a blotting control. 2A6 is a PR8 specific anti-HA head antibody previously

identified by Dr Yu He. 2A6 showed excellent affinity for native PR8 in non-reducing conditions, with a band visible at roughly 70 kDa (**Figure 16**). 2A6 produced no bands in reducing conditions (**Figure 17**).

The band pattern on the 1G3 probed blot was consistent with what was seen when probing with anti-HA mAb 2A6 – both produced a major signal at roughly 70 kDA for PR8. 2A6 has been mapped to bind HA1, the larger component of the HA0 monomer. We therefore hypothesized that 1G3 also bound HA, not NA, consistent with what we observed in the primary screen. HA in infected allantoic fluid exists as cleaved HA1 and HA2 subunits, the uncleaved HA0 monomer, and the functional HA trimeric unit. We conjectured that the bands seen on 1G3 probed non-reducing blot corresponded to HA1, HA0 monomer, the HA trimer, as well as heavy oligomeric forms at the top of each well.

In reducing conditions, mAb 1G3 produced a significant band at roughly 55 kDa for PR8 (H1N1) and very near to 70 kDa for NYMC X-162 (H3N1), as well as a faint second band at 25 kDa for each (**Figure 17**). For PR8 (H1N1), these two bands match known molecular weights for glycosylated HA1 and HA2, the two peptide components of the cleaved monomer that in reducing conditions are resolved into two bands (117). However, the slightly larger molecular weight for the dominant band observed for NYMC X-162 (H3N1) could be as a result of increased glycosylation on H3 or because mAb 1G3 is binding uncleaved HA0 present in the fluid. It is important to note that the size of HA seen on Western blots varies greatly between virus subtypes as a result of major differences in glycosylation patterns (63, 132).

The non-reducing and reducing blots taken together with comparison to the 2A6 control bands make an NA target for mAb 1G3 unlikely. The influenza NA monomer has a

smaller molecular weight of roughly 60 kDa in non-reducing conditions but can form higher molecular weight oligomers. However, NA is a single polypeptide lacking distinct subunits and does not separate into separate bands in reducing conditions (104).

Molecular weights and banding patterns corresponding to HA were initially surprising, as PR8 (H1N1) and NYMC X-162 (H3N1) share an NA protein but differ in their HA components. NYMC X-162 is a 7:1 reassortant virus, meaning it has all PR8 genes except the HA which is derived from A/Wisconsin/67/2005 (H3N2). The HA head is extraordinarily immunodominant in natural and laboratory infections and these head antibodies are characterized by strict strain specificity (82). However, these blots would appear to suggest that 1G3 was binding both H1 (group 1 IAV) and H3 (group 2 IAV). We next performed a series of several Western blots to confirm the unique heterosubtypic binding character of mAb 1G3. MAb 1G3 was first tested against the NYMC X-162 wild type HA parent, A/Wisconsin/67/2005. We also tested the ability of 1G3 to bind A/California/07/2009, which is a pandemic H1N1 virus still circulating in people and the causative virus of the 2009 "Swine Flu" (73). MAb 1G3 successfully bound each of these viruses at a molecular weight corresponding with HA, despite the fact they each carry a different HA protein (**Figure 18**). The banding pattern observed was similar as in the previous reducing blot, however neither A/California/07/2009 (H1N1pdm) nor A/Wisconsin/67/2005 (H3N2) appeared to show the second lower weight molecular band.

Candidate mAb 1G3 thus far has shown the ability to recognize various putative HA targets, including wild type H1, H1 pandemic, and H3 viruses in addition to an H3 reassortant virus, which represent members of both Groups 1 and 2 influenza A viruses. Because HA is known to drift significantly over time, we were interested to determine if this

broadly binding character was limited temporally to relatively recently emerged viruses or if 1G3 was capable of binding H1 and H3 viruses from decades past.

We used mAb 1G3 to probe two additional H1N1 viruses of non-pandemic lineage, A/Hong Kong/50/2014 and A/New Caledonia/20/1999. We also tested two additional H3N2 viruses, A/South Dakota/06/2009 and A/Moscow/10/1999. Viruses were chosen to be representative of circulating wild type viruses from both H1 and H3 subtypes (Groups 1 and 2 respectively) over the last two decades. This is in addition to previously tested immunizing virus PR8, which was isolated in 1934. We also elected to include two influenza B viruses, B/Massachusetts/02/2012 (Yamagata) and B/Brisbane/60/2008 (Victoria). These are both wild type viruses, representing the two major lineages of influenza B viruses. Using uninfected allantoic fluid as a protein background control, we found that mAb 1G3 was able to successfully bind all viruses tested (**Figure 19**). Each virus, including both influenza B strains, showed a strong band at roughly 70 kDa, consistent with previous blots. A/South Dakota/06/2007 also showed the second smaller band at roughly 25 kDa that was observed with PR8 and NYMC X-162.

These results were startling, as a mAb that can bind multiple viruses not only within a subtype but across IAV groups is a relatively rare occurrence. There are roughly of dozen of these cross reactive antibodies in the literature, some isolated from isolated patients and some developed following successive immunization of animals with multiple HA subtypes (29, 121, 140). An antibody that can bind both influenza A and influenza B is the rarest of influenza antibodies. To date, there is one antibody published and recently patented that can inhibit both influenza A and B *in vivo,* CR9114 (32).

Despite not binding to uninfected allantoic fluid, we next assessed the possibility that the 1G3 epitope in part or in whole consisted of glycan motifs. An antibody to sugar motifs may be able to bind a wide range of viruses, but would negate its relevance as a reagent, as a means of epitope discovery, or as a potential treatment modality. Previous isotyping of 1G3 described in *Specific Aim 1* revealed it to be IgG1, making an entirely glycan epitope unlikely as class switching from IgM to IgG had occurred in the immunized mouse. Class switching in a murine model, as in humans, is most often as a result of protein stimulation (30). In order to establish the molecular character of the epitope target, we decided to treat previously blotted viruses PR8 (H1N1), A/California/07/2009 (H1N1pdm), and A/Wisconsin/67/2005 (H3N2) with PNGase F. PNGase F is commercially available enzyme purified from *Flavobacterium meningosepticum* that cleaves N-linked glyco-motifs from protein (72, 116). Subsequent to overnight enzyme treatment of infected allantoic fluid, mAb 1G3 was still capable of binding each virus, but with diminished affinity (**Figure 20**). These data supported our hypothesis that the 1G3 epitope is modulated by glycan, either by direct binding to some critical carbohydrates or most likely to a conformational epitope supported by glycan scaffolding. However, because the signal was indeed present after enzyme treatment these data also demonstrate that the epitope is not entirely composed of sugars and 1G3 does in fact interact with amino acids of HA. Candidate mAb 1G3 thus far was shown to bind wild type and reassortant H1, H1pdm H3, and B viruses (from both lineages) spanning the last 20 years. The 1G3 epitope was not present in uninfected allantoic fluid and was not dependent on glycans alone.

In order to confirm candidate mAb 1G3 was indeed binding the viral HA target and not a identically sized protein present as a result of propagation in eggs, we next performed a

series of blots with purified HA+NA from PR8 as well as whole purified virus NYMC X-187 and HA+NA from NYMC X-179A. Both NYMC X-187 and NYMC X-179A are high yield reassortant viruses prepared via classical reassortment by Jean Marie Silverman and Barbara Pokorny in our lab as candidate vaccine seeds. NYMC X-187 is an H3N2 virus with HA and NA genes from A/Victoria/201/2009 and six internal genes of PR8. NYMC X-179A is an H1N1pdm virus with the HA, NA, and PB1 genes of A/California/07/2009 and the five remaining genes from PR8.

Virus purification is a multistep process that begins with amplifying and harvesting virus from infected embryonated chicken eggs. Allantoic fluid was pooled and spun to remove cellular debris, and then centrifuged at high speed in an ultracentrifuge to pellet virus. Finally, the viruses were purified using a sucrose gradient whereby virus collects at the 30%-60% interface. This solution was again centrifuged at high speed (20,000 rpm) before being soaked overnight in a calcium containing buffer to maintain the structural and enzymatic integrity of HA and NA (13). Viral protein content was measured by a standard Lowry assay.

First, 10 µg of each purified virus or viral HA+NA were blotted in non-reducing conditions with 50 µg purified Bovine Serum Albumin (BSA, Sigma) as a binding control. As anticipated from previous blots, mAb 1G3 bound purified PR8 (H1N1) HA+NA, NYMC X-187 (H3N2), and NYMC X-179A (H1N1pdm) HA+NA, but not the BSA control. PR8 specific anti-HA mAb 2A6 only bound purified PR8 (H1N1) HA+NA, failing to bind the other HA subtypes and the BSA control (**Figure 21**). This blot was repeated using 1 µg of each purified virus to prevent overexposure. Purified ovalbumin was used as an additional binding control. Consistent with blots done from allantoic fluid, major bands were seen at

roughly 55 kDa for the H1 and H1pdm viruses (PR8, NYMC X-179A) and 70 kDa for the H3 virus (NYMC X-187) in reducing conditions. Additionally, both the H1 and H1pdm viruses showed the second putative HA2 band at 25 kDa. No binding to either control (BSA or ovalbumin) was observed despite high protein load (**Figure 22**). This blot was repeated using PR8 specific anti-HA mAb 2A6 as the primary antibody control with ovalbumin as a protein binding control. As expected, major banding was only observed for purified PR8 HA+NA in non-reducing conditions (**Figure 23**). Again, it was observed that the banding pattern for PR8 was identical either with known HA antibody 2A6 and our candidate 1G3.

We also observed that in reducing conditions bands produced with 1G3 were of diminished intensity compared to equivalent blots in non-reducing conditions. This is a pattern commonly associated with discontinuous epitopes, contrasted with linear epitopes wherein binding should produce an identical signal regardless of protein shape (45, 61). While conventional wisdom held that antibodies used to probe Western blots could only recognize linear epitopes, it has since been established that some proteins may undergo renaturation following transfer. Therefore positive results on a Western blot, especially when signal is diminished by reduction, can also be indicative of recognition of a discontinuous or conformational epitope (143).

By using purified virus or viral protein devoid of cellular or host derived debris, we were able to confirm a unique pattern where the major band from both H1 and H1pdm viruses appeared to be of lower molecular weight than that seen with the H3 virus (70 kDa vs 50 kDa). This could be as a result of increased glycosylation of the H3 virus making the HA heavier, or because mAb 1G3 binds HA1 of H1 viruses and the larger HA0 monomer of H3 viruses. We hypothesized that the 1G3 epitope lies on HA1 subunit, but the 3D

conformation necessary for binding is only present in the HA0 monomer of H3 viruses. In order to test this hypothesis, the same three purified viruses were subject to overnight treatment with trypsin to cleave any HA0 monomers present in solution and then blotted in reducing conditions to resolve all HA0 into its two subunits, HA1 and HA2. NYMC X-187 (H3N2) treated with trypsin could no longer be bound by 1G3 while PR8 HANA (H1N1) and NYMC X-179A (H1N1pdm) retained identical banding pattern (**Figure 24**). These data support that the 1G3 target epitope is slightly altered for the H3 viruses, as was suggested by differences in banding weight. This also suggests that although the epitope is retained in reducing conditions, it is dependent on conformation of the HA subunits as we suspected from the observed decrease in affinity following reduction or the removal of glycans by PNGase F.

As another approach to confirming a shared HA epitope as the target of 1G3, next decided to test a panel of recombinant HA proteins. Previously we had demonstrated that mAb 1G3 did not bind recombinant PR8 H1 HA. However, the PR8 specific 2A6 antibody also showed low affinity in Western blot and we suspected that recombinant protein may have been compromised in storage (**Figure 16**). Additionally, we tested a recombinant HA from A/Perth/16/2009 (H3) as well as A/Vietnam/1194/2004 (H5). The recombinant protein from A/Perth/16/2009 (H3) was sourced from baculoviral cells and was not full length, instead encoding only the HA1 domain. Binding would demonstrate not only that 1G3 could bind this particular H3 virus, but that it bound the glycosylated HA1 subunit as opposed to the H3 HA0 monomer as we suspected was the case from the trypsin blots. A/Vietnam/1194/2004 is an H5 virus and is a Biosafety Level 3 highly pathogenic avian influenza (HPAI) (3, 99). Its HA component alone as a recombinant protein can be used at

BSL-1 for Western blotting, allowing us the opportunity to test this previously untested HA subtype. Both the recombinant HA from PR8 (H1) and A/Vietnam/1194/2004 (H5) were the extracellular domains secreted from HEK293 cells. MAb 1G3 was not able to bind these recombinant proteins in reducing or non-reducing conditions (**Figure 25**), despite previously binding PR8 in allantoic fluid and as purified protein. This is most likely explained by the baculoviral or HEK293 cell systems being incapable of maintaining proper shape for 1G3 binding, either in terms of epitope fidelity or 3D conformation. It's also possible that either as only HA1 or only the extracellular domain, there are amino acids in the membrane proximal portion of the HA stem that were missing or incomplete. Finally, it's also possible that as recombinant proteins they are not available in the active HA trimer formation, which may be necessary for 1G3 binding. While recombinant proteins are useful, they have been cited as poor antibody validation tools (12, 128).

While we previously established that the 1G3 epitope is not glycan alone, next we chose to test two control viruses for 1G3 binding: Sendai Virus and Respiratory Syncytial Virus (RSV). The Paramyxovirus group includes parainfluenza viruses (Sendai), Metapneumonia virus, and RSV. These viruses are responsible for a growing number of hospitalizations in the United States, especially among children and elderly. Often these infections are misdiagnosed as influenza, as symptoms are largely overlapping (21, 110). Paramyxoviruses are closely related to Orthomyxoviruses. Like influenza, RSV and Sendai are enveloped viruses with a single stranded negative sense RNA genome. However, unlike flu their genomes are contiguous and undergo replication in the cytoplasm of infected cells (37). While Sendai virus does not infect humans, it is often used as an animal model for human parainfluenza infections. Sendai is a well-documented agricultural blight, as it can

cause death in chicken stocks (78). Because mAb 1G3 failed to bind any of the recombinant proteins tested, we analyzed Sendai and RSV as sucrose gradient purified native protein. The Sendai virus used was amplified in the same eggs from the same distributor we use internally for influenza, allowing it to serve as a control for egg propagation effects in addition to a binding control as a closely related virus. 1G3 did not bind native RSV or Sendai in either reducing or non-reducing conditions (**Figure 26**).

These blots suggest that candidate mAb 1G3 is a unique antibody that can bind HA of H1, H1 pandemic, and H3 viruses of influenza A as well as the HA of two distinct lineages of influenza B viruses. Banding pattern and molecular weight analysis suggests that the epitope of 1G3 is conformational and lies predominantly on HA1, as each virus tested shows a high molecular weight band between 70 and 80 kDA. However at least a part of the epitope may be found on HA2 for some viruses, observable as a second lower molecular weight band at 25 kDa. Trypsin cleavage ablates the consensus sequence for H3 virus NYMC X-187, implying that some part of the antibody footprint lies in or around the HA1/HA2 cleavage site located at the C terminal end of HA1. It's also possible that cleavage disrupts necessary conformation for H3 binding, but not H1 binding. Interestingly, mAb 1G3 was not able to bind any recombinant proteins; further supporting a conformational epitope that may not be easily recapitulated by non-native protein. Blot results are summarized in **Figure 27**.

To investigate whether there was any apparent sequence homology between heterosubtypic viruses at this predicted HA1/HA2 epitope, we completed an *in silico* sequence alignment of the HA segments of A/Puerto Rico/8/1934 (PR8, H1N1, ID CY045764), A/California/07/2009 (H1N1pdm, ID CY121680) and A/Victoria/201/2008

(H3N2, ID KM821344). Analysis was performed using sequences from the NCBI Influenza Database using LaserGene Suit MegAlign software following alignment by Clustal W method.

We observed that these three viruses share significant homology centered about the HA1/HA2 cleavage site despite their different IAV grouping **(Figure 28**). This is unsurprising, as every wild type IAV HA subtype (with the exception of HA14) share the same P4-P1 sequence for recognition by trypsin-like proteases in the host. Cleavage consistently occurs at the same invariant arginine residue shared by nearly every influenza virus, including these three (109). Only HPAI viruses, which contain a multibasic cleavage site, differ (112). The fusion peptide at the N terminal region of HA2 is one of the most highly conserved peptide sequences across all influenza viruses, however our blotting data suggested the majority of the 1G3 epitope is on the HA1 peptide as only some viruses displayed the lower molecular weight HA2 band. While sequence hormonology around and upstream of the cleavage site present on HA1 is encouraging, most epitopes are not continuous. It's likely that the true epitope of mAb 1G3 is dependent on the conformation of the C terminal domain of HA1 both in the context of the monomer and as a resolved subunit.

Epitope mapping of mAb 1G3 against PR8 HA was completed by PEPperPRINT via PEPperMAP® linear epitope mapping using a peptide microarray chip. The sequence of A/Puerto Rico/8/1934 (ID B4UPA6) HA was submitted and elongated with neutral linkers (GSGSGSG) at both the N and C termini to prevent truncated peptides. The sequence was then translated into 15 amino acid peptides with an overlap of 14 amino acids, yielding 565 unique peptides printed in duplicate (**Appendix 2: Peptide Map**). Unlike similar technologies, peptides were synthesized directly unto the chip to eliminate the need for

immobilization. Between different printing steps, "amino acid toners" were melted to release amino acids and initiate synthesis. Following washing, the N-terminal Fmoc group was unprotected to allow for the next round of toners to be printed and coupled. Control c-myc (EQKLISEEDL) peptides were spotted along the perimeter of the chip. The chip was then incubated with purified 1G3 at concentrations of 10 µg/mL and 100 µg/mL and stained with a DyLight 680 goat anti-mouse secondary before being scanned with a LI-COR Odyssey Imaging System. Quantification of spot intensities was done with a proprietary software, PepSlide® Analyzer.

Following analysis, peaks of fluorescence associated with binding failed to reach statistical significance. This is mostly likely attributed to our conformational epitope being analyzed by a software program which is designed to detect linear binding. Linear binding is seen as peaks of neighboring peptides in a tight bell curve centered on the epitope, as opposed to several distinct peaks along the protein as we observed. However, the raw data provides some valuable insight into a proposed 1G3 epitope. At both 10 and 100 µg/mL, 1G3 showed nine significant peaks in fluorescent intensity (**Figure 29**). There was perfect agreement regarding the location of these peaks between the two concentrations. Two of these, corresponding with peptides LSSVSSFERFEIFPK and GKEVLVLWGIHHPSN, fall in the receptor binding domain and are unlikely to be involved in the neutralizing mechanism of 1G3 in context with the lack of observed HA inhibition activity. However, two of the remaining seven peaks were consistent with our predicted epitope based on Western blotting and *in silico* analysis. Peptides PVTIGECPKYVRSAKL and YAADQKSTQNAINGIT fall at the C terminus of HA1 and N terminus of HA2 within the fusion peptide sequence, straddling the protease cleavage site (**Figure 30**). These epitopes

were visualized on the HA HA) monomer and active HA trimer using iCn3D, a web-based protein structure viewer hosted by NCBI (**Figure 31**). These peaks tracked to the HA stem, sitting below the globular head and surrounding the fusion peptide located on the interior of the trimer.

The predicted 1G3 epitope was then compared with the published epitopes of previously identified broadly neutralizing stem antibodies: CR9114 (32), F16 (14), C05 (36), and C179 (85). While we were limited to 15 amino acid peptide sequences, epitopes of these other antibodies have been established to a single amino acid resolution using X-ray crystallography. Our epitope appeared to correspond remarkably well with two known HA stem antibodies, CR9114 and C179 (**Figure 30**). CR9114 is the only published antibody that can protect mice from lethal challenge of both groups of influenza A as well as both lineages of influenza B (32). C179 was discovered in 1993 and is the first antibody identified that could neutralize multiple subtypes of influenza A, however only within Group 1 (85). While their epitopes are similar, and in fact overlap at several positions, the binding of C179 is rotated 45° from CR9114. Interestingly, C179 has a similar approach angle to the epitopically distinct F16 which targets the protease recognition site. It has been experimentally determined that group and subtype specific differences at amino acid position 111 of HA2 prevent C179 from binding Group 2 IAV (31). While Group 1, like A/Puerto Rico/8/1934 (H1N1), feature a histidine; Group 2 strains instead code for threonine or alanine. This results in a subtly different conformation of an indole side chain located at position 21 on HA2 that prevents interaction with a phenylalanine at the tip of the heavy chain complementarity determining region 3 of C179. Mutating His111Thr on HA2 abrogated C179 binding and underlies its inability to bind Group 2 viruses (31, 66, 85). We

hypothesize that because of the more broadly neutralizing character of 1G3, its angle of approach is likely more similar to CR9114 which is unaffected by an amino acid change at position 111. Both Cr9114 and C157 antibodies target the HA fusion peptide located in the stem domain. Functionally, they prevent low pH induced conformational changes to HA1/HA2 necessary for release of the virion into the cytoplasm *in vitro* (22, 115, 137).

While the linear peptide mapping was performed with the HA sequence of A/Puerto Rico/8/1934, we also saw that 1G3 can efficiently bind to heterologous viruses. In order to identify any specific amino acids that may be major contributors to the epitope, we performed a sequence alignment of PR8 (H1N1), A/Hong Kong/4801/2014 (H3N2) and B/Brisbane/60/2008 (Victoria) (**Figure 32**). Interestingly, over half of the amino acids in the proposed 1G3 binding site were conserved between these three very distinct influenza viruses, 16 out of 30 residues in total. This demonstrates that although these viruses represent both groups of influenza A as well as influenza B, there is significant conservation in the stem that can be exploited for broad neutralizing potential.

Antibody candidate 1G3 has a conformational epitope that may lie at the C terminal region of HA1 and the N terminal region of HA2. It appears to share many amino acids with the published epitopes of similarly broadly neutralizing stem targeted antibodies, like CR9114 and C179. However, mAb 1G3 is a unique antibody that is epitopically similar to both C179 and CR9114, sharing amino acids in both HA1 and HA2 footprints, but like CR9114 is able to bind both groups of influenza A as well as influenza B.

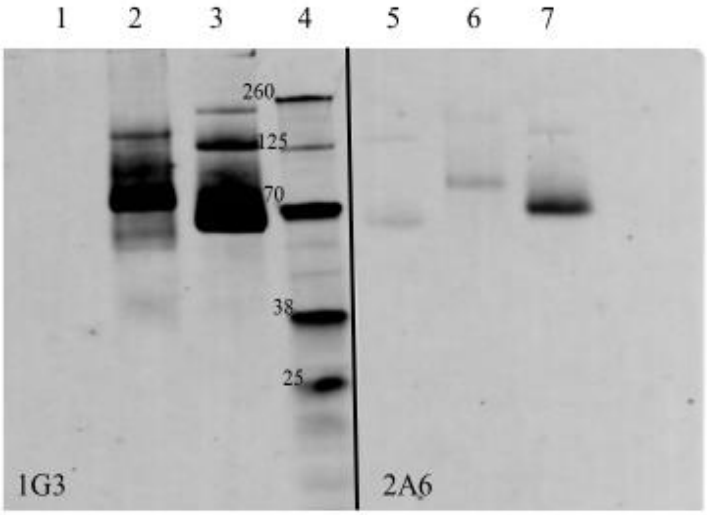

Lane	Virus	HANA
1	Recombinant PR8 HA	H1
2	NYMC X-162	H3N1
3	PR8	H1N1
4	Ladder	-
5	Recombinant PR8 HA	H1
6	NYMC X-162	H3N1
7	PR8	H1N1

***Figure 16**: Non-reducing Western blot of Recombinant A/Puerto Rico/8/1934 HA (PR8, rHA, H1), NYMC X-162 (H3N1, A/Wisconsin/67/2005 HA parent) and native PR8 (H1N1) in allantoic fluid. 1G3 (left) or anti-H1 HA head antibody 2A6 (right) containing hybridoma supernatant was used as primary antibody and an infrared goat anti mouse secondary was used to visualize bands. Each lane was loaded with 20 µL infected allantoic fluid or 0.1 µg rHA as noted. 1G3 successfully bound both PR8 and X-162 to the exclusion of recombinant PR8 H1 HA.*

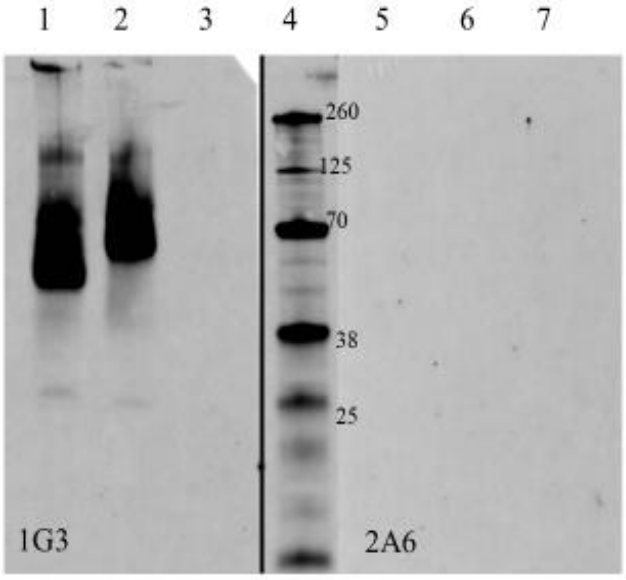

Lane	Virus	HANA
1	PR8	H1N1
2	NYMC X-162	H3N1
3	Recombinant PR8 HA	H1
4	Ladder	-
5	PR8	H1N1
6	NYMC X-162	H3N1
7	Recombinant PR8 HA	H1

***Figure 17**: Reducing Western blot of Recombinant A/Puerto Rico/8/1934 HA (PR8, rHA, H1), NYMC X-162 (H3N1, A/Wisconsin/67/2005 HA parent) and native PR8 (H1N1) in allantoic fluid. 1G3 (left) or anti-H1 mAb 2A6 (right) containing hybridoma supernatant was used as primary antibody and an infrared goat anti mouse secondary was used to visualize bands. Each lane was loaded with 20 µL infected allantoic fluid or 0.1 µg rHA. Where 2A6 does not bind in reducing conditions, 1G3 bound native PR8 and X-162 with both a high (60-70 kDA) and lower (25 kDA) molecular weight band.*

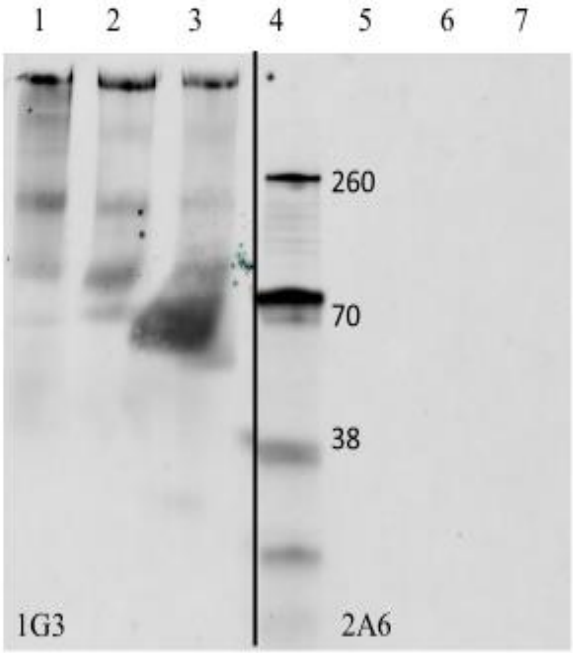

Lane	Virus	HANA
1	A/California/2009	H1N1pdm
2	A/Wisconsin/2005	H3N2
3	PR8	H1N1
4	Ladder	-
5	A/California/2009	H1N1pdm
6	A/Wisconsin/2005	H3N2
7	PR8	H1N1

Figure 18: *Reducing Western blot of A/California/07/09(H1N1pdm), A/Wisconsin/67/05(H3N2), and A/Puerto Rico/8/1934 (PR8, H1N1) in allantoic fluid using 1G3 (left) or anti-H1 HA mAb 2A6 (right) containing hybridoma supernatant as primary antibody. An infrared goat anti mouse secondary was used to visualize bands. Each lane was loaded with 10 µL infected allantoic fluid. 1G3 successfully bound the H1, H1pdm, and H3 wild type viruses.*

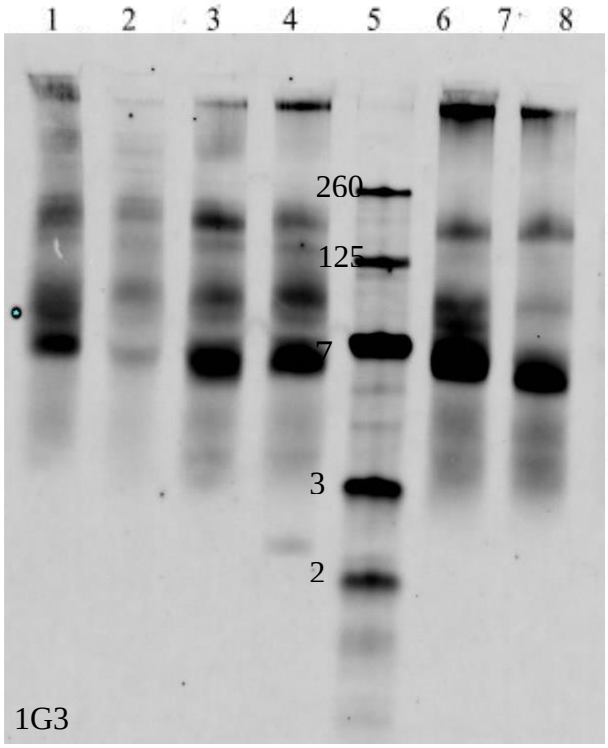

Lane	Virus	HANA
1	A/Hong Kong/2014	H3N2
2	A/Moscow/1999	H3N2
3	A/New Caledonia/1999	H1N1
4	A/South Dakota/2007	H1N1
5	Ladder	-
6	B/Brisbane/2008	Victoria
7	B/Massachusetts/2012	Yamagata
8	Allantoic Fluid (Uninfected)	-

Figure 19*: Reducing Western blot of two H3N2, two H1N1, and two influenza B viruses in allantoic fluid. Viruses from left to right (lanes 1-8): A/Hong Kong/50/2014 (H3N2), A/Moscow/10/1999 (H3N2), A/New Caledonia/20/1999 (H1N1), A/South Dakota/06/2007 (H1N1), B/Brisbane/60/2008 (Victoria), B/Massachusetts/02/2012 (Yamagata Lineage). MAb 1G3 containing hybridoma supernatant was used as primary antibody and an infrared goat anti mouse as the secondary to visualize bands. 1G3 bound both the influenza A and influenza B viruses tested, despite varying HA proteins across subtype, group, and lineage.*

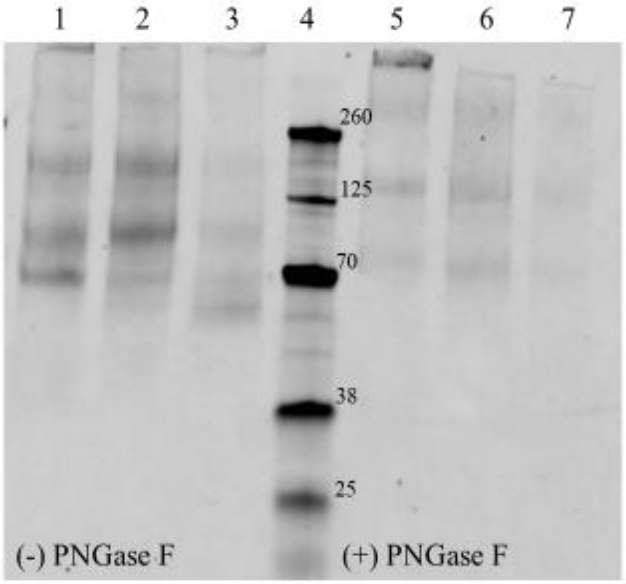

Lane	Virus	HANA
1	PR8	H1N1
2	A/California/2009	H1N1pdm
3	A/Wisconsin/2005	H3N2
4	Ladder	-
5	PR8	H1N1
6	A/California/2009	H1N1pdm
7	A/Wisconsin/2005	H3N2

***Figure 20**: Non-reducing Western blot A/Puerto Rico/8/1934 (PR8,H1N1), A/California/07/2009 (H1N1pdm), and A/Wisconsin/67/2005(H3N2) using 1G3 containing hybridoma supernatant as primary antibody and an infrared goat anti mouse as the secondary to visualize bands. Each lane was loaded with 20 µL infected allantoic fluid. Left panel shows virus treated with a buffer control while viruses in lanes 5, 6, and 7 were treated with PNGase F, an enzyme that removes N-linked glycosylation. All viruses were incubated overnight at 37°C prior to blotting. While affinity was lower, 1G3 still bound viruses devoid of sugar groups.*

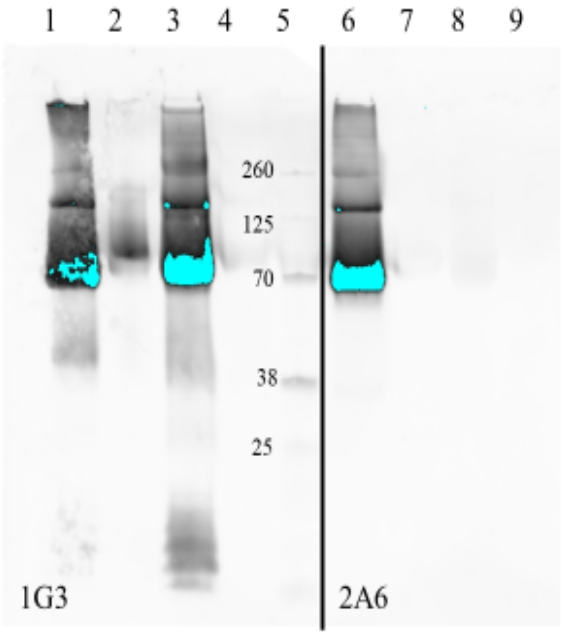

Lane	Purified Virus	Conc (µg)
1	PR8 HANA	10
2	X187 (H3N2)	10
3	X179A (H1N1pdm) HANA	10
4	Bovine Serum Albumin	50
5	Ladder	-
6	PR8 HANA	10
7	X187 (H3N2)	10
8	X179A (H1N1pdm)	10
9	Bovine Serum Albumin	50

***Figure 21**: Non-reducing Western blot of purified A/Puerto Rico/8/1934 (PR8, H1N1) HANA, NYMC X-187 (H3N2), and NYMC X-179A (H1N1pdm) HANA. MAb candidate 1G3 (left) or anti-PR8 HA 2A6 (right) containing hybridoma supernatant were used as primary antibodies followed by an infrared goat anti mouse secondary to visualize bands. Each lane was loaded with 10 µg purified virus/viral protein or bovine serum albumin control (lanes 4 and 9). 1G3 successfully bound virus purified from egg protein. Blue signal is an artifact of overexposure during membrane scanning.*

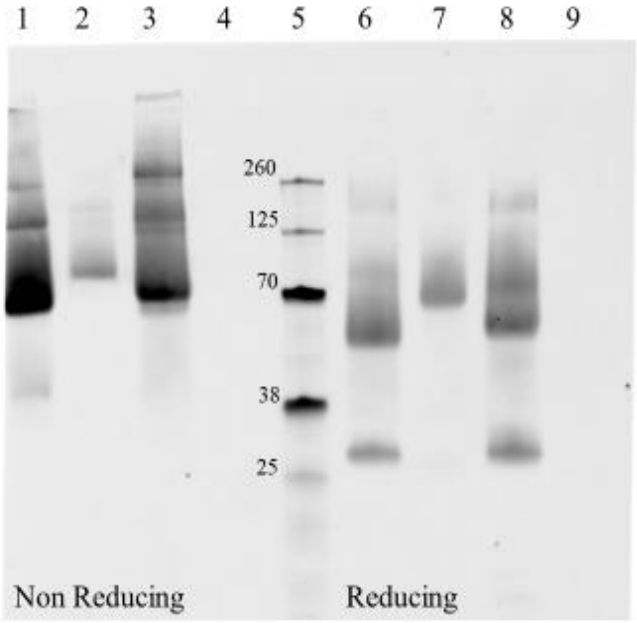

Lane	Purified Virus	Conc (µg)
1	PR8 HANA	1
2	X187 (H3N2)	1
3	X179A (H1N1pdm) HANA	1
4	Ovalbumin	80
5	Ladder	-
6	PR8 HANA	1
7	X187 (H3N2)	1
8	X179A (H1N1pdm)	1
9	Ovalbumin	80

***Figure 22**: Non-reducing (left) and reducing (right) Western blot with purified A/Puerto Rico/8/1934 (PR8, H1N1) HANA, NYMC X-187(H3N2), and NYMC X-179A (H1N1pdm) HANA using 1G3 hybridoma supernatant as primary antibody, followed by an infrared goat anti mouse secondary to visualize bands. Each lane was loaded with 1 µg purified viral protein or 80 µg Ovalbumin control.*

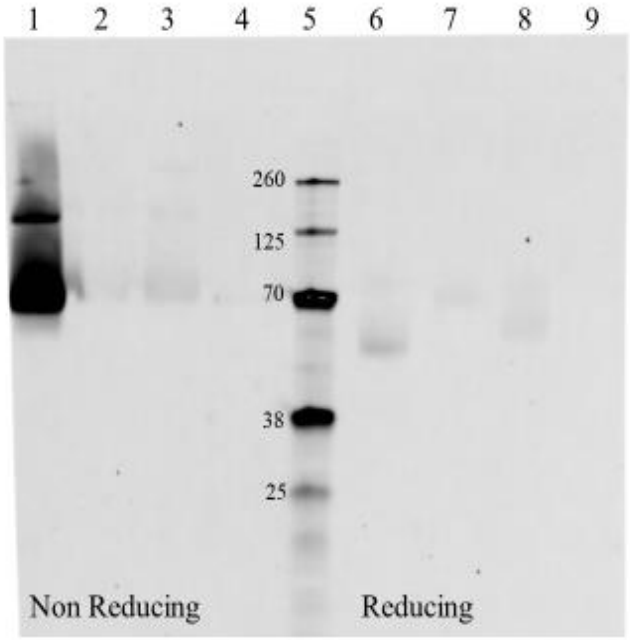

Lane	Purified Virus	Conc (µg)
1	PR8 HANA	1
2	X187 (H3N2)	1
3	X179A (H1N1pdm) HANA	1
4	Ovalbumin	80
5	Ladder	-
6	PR8 HANA	1
7	X187 (H3N2)	1
8	X179A (H1N1pdm)	1
9	Ovalbumin	80

***Figure 23**: Non-reducing (left) and reducing (right) Western blot with purified A/Puerto Rico/8/1934 (PR8, H1N1) HANA, NYMC X-187(H3N2), and NYMC X-179A (H1N1pdm) HANA using PR8 specific anti-HA 2A6 hybridoma supernatant as primary antibody, followed by an infrared goat anti mouse secondary to visualize bands. Each lane was loaded with 1 µg purified viral protein or 80 µg Ovalbumin control. Unlike 1G3, blotting control 2A6 did not show hetero-HA reactivity.*

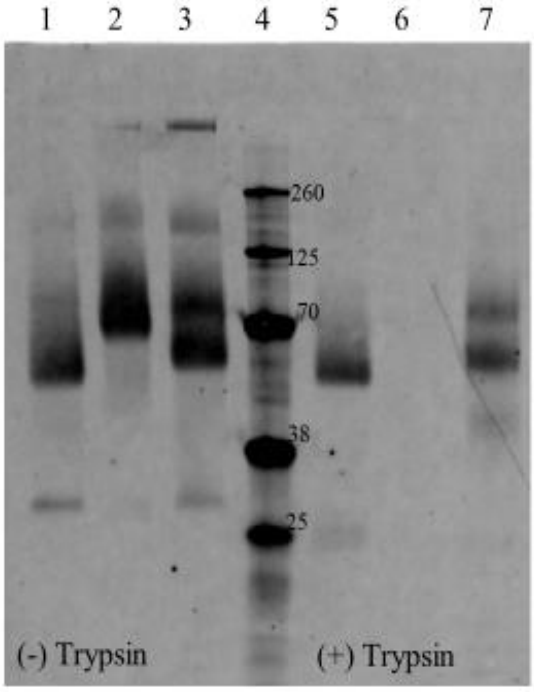

Lane	Purified Virus	Conc (µg)
1	PR8 HANA	1
2	X187 (H3N2)	1
3	X179A (H1N1pdm) HANA	1
4	Ladder	-
5	PR8 HANA	1
6	X187 (H3N2)	1
7	X179A (H1N1pdm)	1

***Figure 24**: Reducing Western blot of purified A/Puerto Rico/8/1934 (PR8, H1N1) HANA, NYMC X-187 (H3N2), and NYMC X-179A (H1N1pdm) HANA. MAb candidate 1G3 containing hybridoma supernatant was used as primary antibody followed by an infrared goat anti mouse secondary to visualize bands. Each lane was loaded with 1 µg purified virus or viral protein. Lanes 1, 2 and 3 were subject to a buffer control while lanes 5, 6 and 7 were treated with trypsin. Trypsin cleavage removes HA0 monomers present in the sample, leaving only HA1 and HA2. All samples were incubated overnight at 37°C prior to blot. 1G3 was no longer able to bind H3N2 virus following treatment with trypsin.*

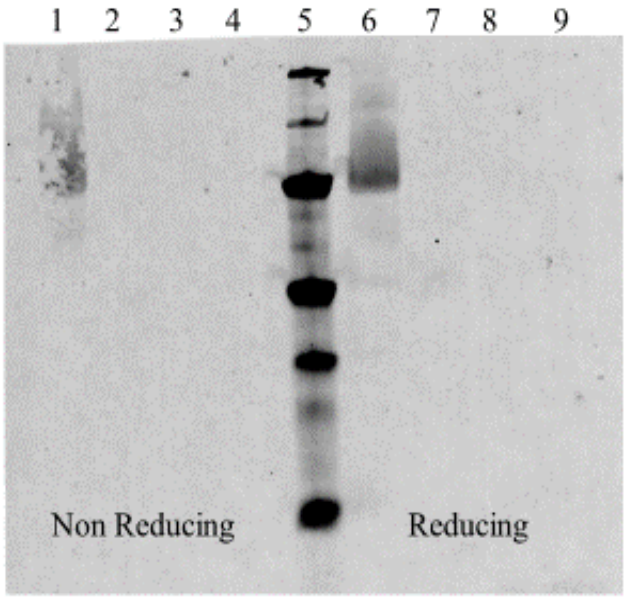

Lane	Purified Virus	HA
1	Purified PR8	H1
2	rHA PR8	H1
3	rHA A/Perth HA1	H3
4	rHA A/Vietnam	H5
5	Ladder	-
6	Purified PR8	H1
7	rHA PR8	H1
8	rHA A/Perth HA1	H3
9	rHA A/Vietnam	H5

***Figure 25**: Non-reducing (left) and reducing (right) Western blot using recombinant HA (rHA) proteins from A/Puerto Rico/8/1934 (PR8, H1), A/Perth/16/2009 (H3) and A/Vietnam/1194/2004 (H5). Recombinant PR8 and A/Vietnam HA consists of the secreted extracellular domain and was isolated from HEK293 cells. Recombinant A/Perth HA consists of only the HA1 domain and was isolated from a baculoviral system. MAb candidate 1G3 containing hybridoma supernatant was used as primary antibody followed by an infrared goat anti mouse secondary to visualize bands. Each lane was loaded with 1 µg recombinant viral protein. 1G3 successfully bound purified native PR8 protein but showed no reactivity with any recombinant HA.*

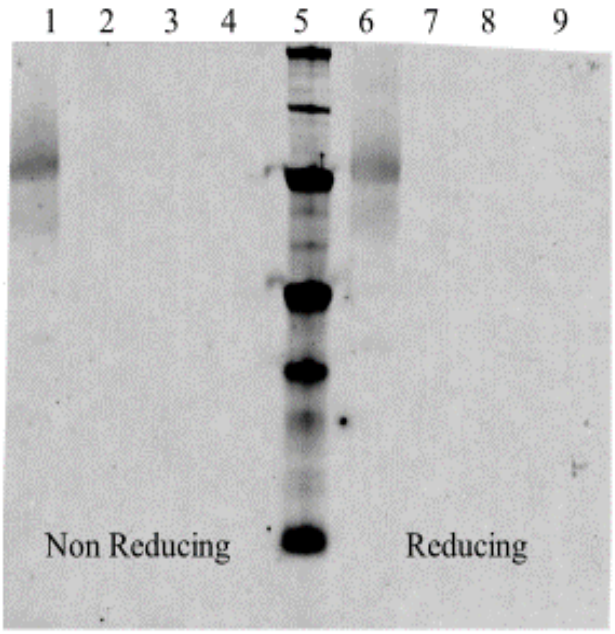

Lane	Purified Virus	Conc (µg)
1	Purified PR8	1
2	Purified Sendai Virus	1
3	Purified RSV Virus	1
4	Allanotic Fluid	1
5	Ladder	-
6	Purified PR8	1
7	Purified Sendai Virus	1
8	Purified RSV Virus	1
9	Allanotic Fluid	1

Figure 26: *Non-reducing (left) and reducing (right) Western blot using sucrose gradient purified antigen from Sendai and Respiratory Syncytial Virus as well as an uninfected allantoic fluid control. MAb candidate 1G3 containing hybridoma supernatant was used as primary antibody followed by an infrared goat anti mouse secondary to visualize bands. Each lane was loaded with 1 µg viral protein. 1G3 successfully bound native PR8 to the exclusion of the closely related Sendai and Respiratory Syncytial viruses. 1G3 showed no reactivity for allantoic fluid alone.*

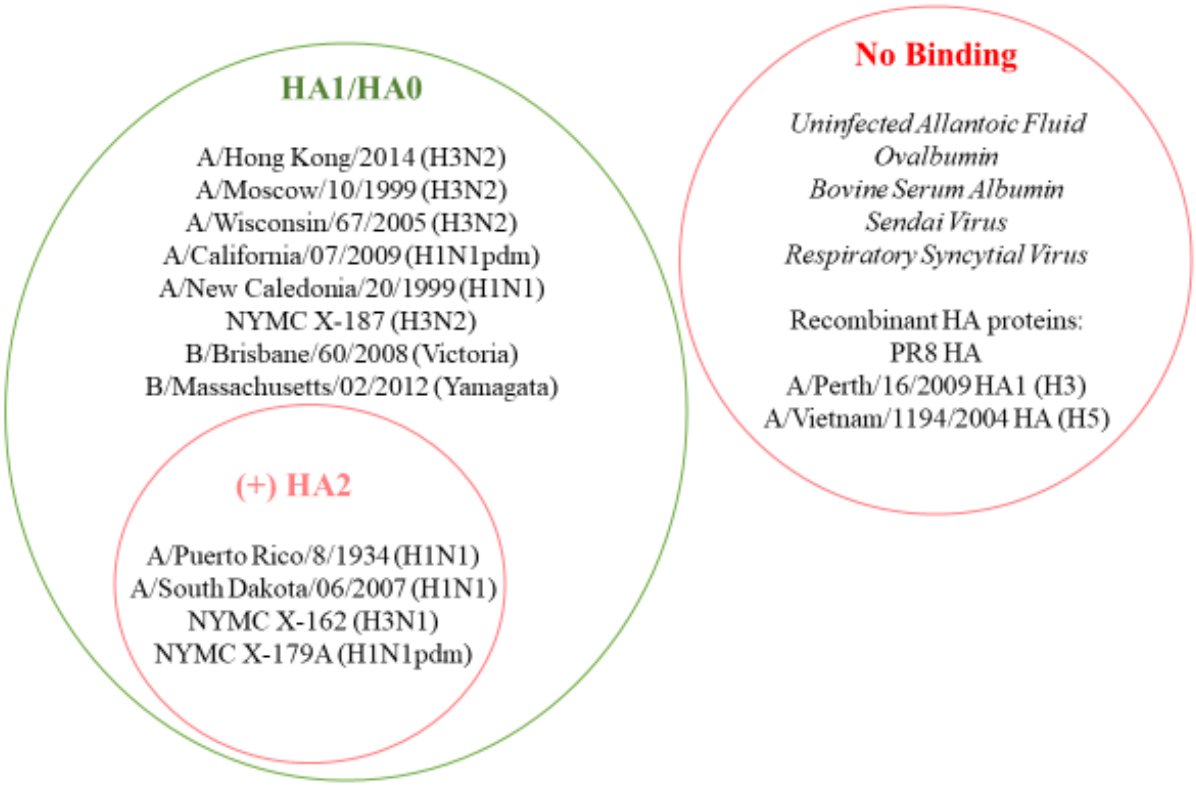

***Figure 27**: Summary of Western blot results. Viruses in the green circle showed an HA0 or HA1 band between 60 – 80 kDa in both reducing and non-reducing conditions. Those listed in the nested pink circle showed an HA0 or HA1 band plus an additional HA2 band at ~25 kDa in reducing conditions. MAb 1G3 was not able to bind controls in italics as well as recombinant proteins listed in the red circle. Control viruses Sendai and RSV were tested as purified whole virus, not recombinant proteins.*

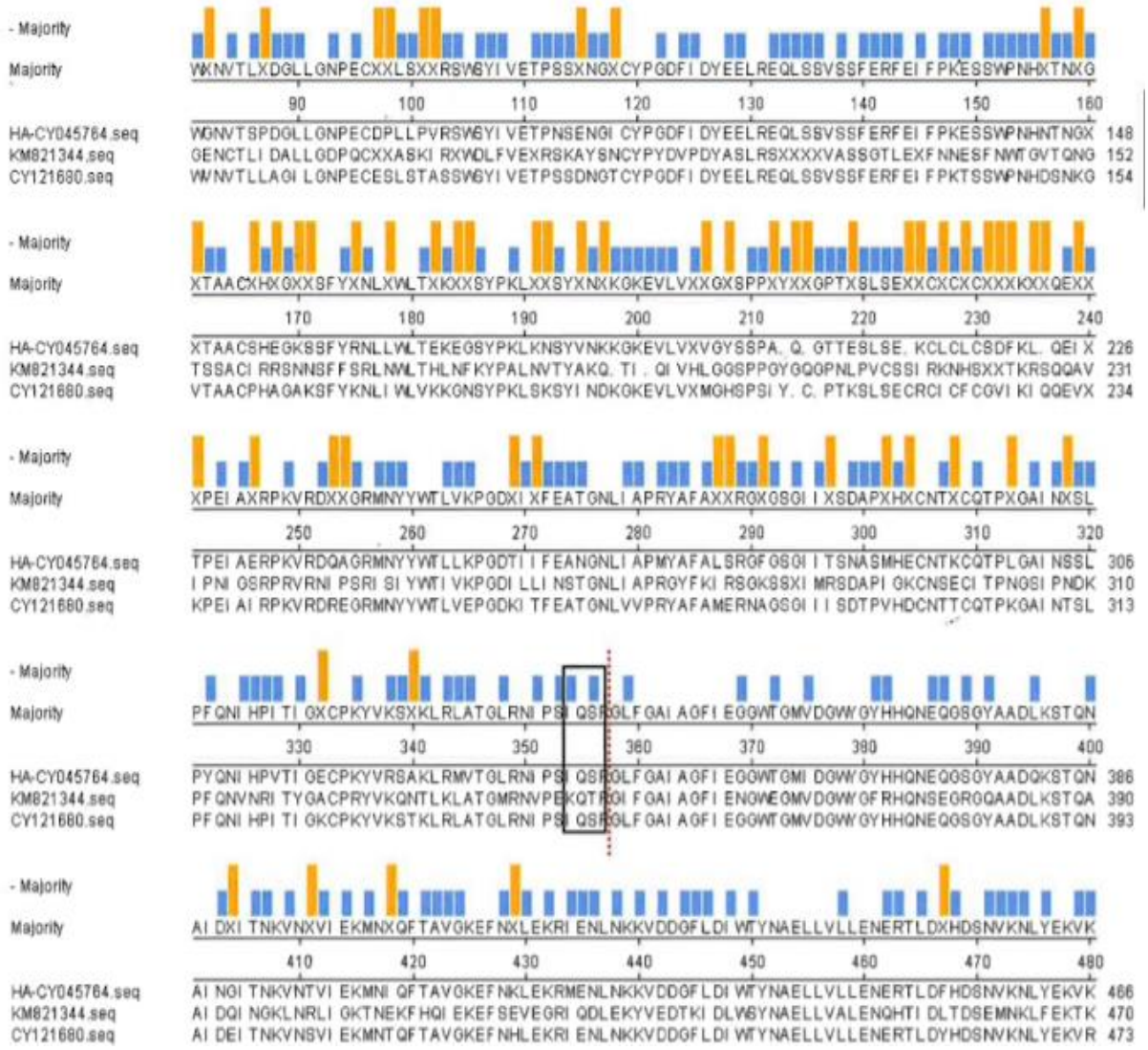

***Figure 28**: Sequence alignment of the HA segments of PR8 (H1N1, HA-CY045764, top row), A/Victoria/201/2008 (H3N2, KM821344, middle row), and A/California/07/2009 (H1N1pdm, CY121680, bottom row). Box highlights the P4-P1 loci of the trypsin cleavage site. Red dotted line delineates HA1 and HA2 where HA2 N terminus begins with consensus sequence G-L/I-F. Blue highlight shows amino acids where H1 and H1pdm viruses agree to the exclusion of the H3 virus. Gold highlights amino acids where all three viruses diverge. Generally, the area of highest conservation lies around the fusion peptide downstream of the trypsin recognition sequence.*

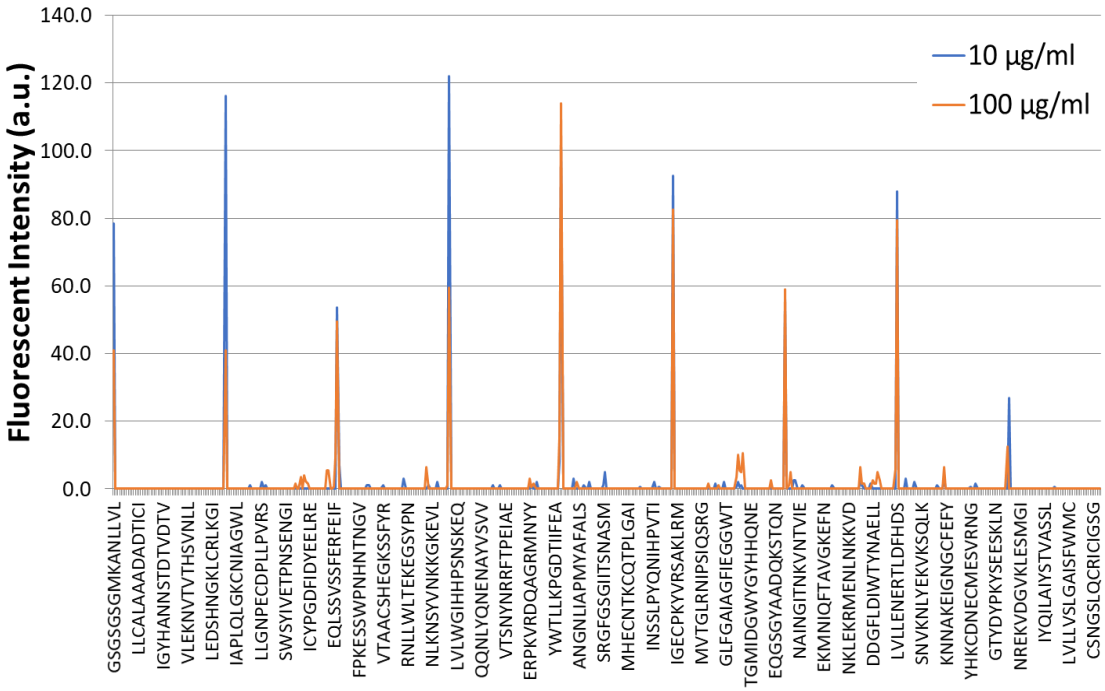

***Figure 29**: 15 amino acid peptides with 14 amino acid overlaps were generated from the HA sequence of A/Puerto Rico/8/1934 and synthesized directly on to a PEPperMap linear peptide array. Fluorescent intensity measured in arbitrary units (a.u.) following peptide chip incubation with mAb 1G3 at a concentration of 10 and 100 µg/mL and a fluorescent secondary antibody. Where a linear epitope would appear as a bell curve around a single sequence, we observed 9 distinct peaks along the length of the HA protein. Full peptide map can be found in the appendix.*

Figure 30*: HA amino acid sequence of A/Puerto Rico/8/1934 (UniProt ID B4UPA6). Binding peaks of 1G3 from epitope mapping are shown in the top row in purple. Epitope sequences of known HA stem antibodies determined by X-ray crystallography (bottom row) are noted in blue for CR9114 and pink for C179. GLF, highlighted in yellow, are the first amino acids at the N terminus of HA2.*

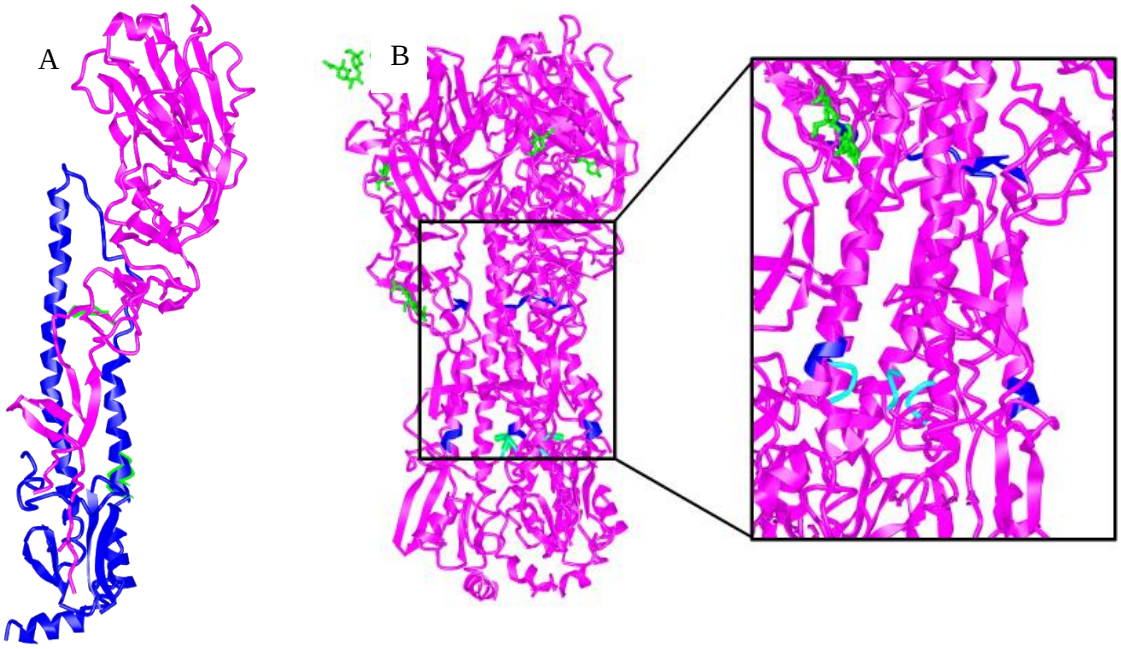

Figure 31*: 3D visualization of A/Puerto Rico/8/1934 HA with predicted 1G3 epitope via iCn3D. A: HA monomer with HA1 in magenta and HA2 in blue. Portions of predicted 1G3 epitopes PVTIGECPKYVRSAKL and YAADQKSTQNAINGIT are highlighted in cyan on the HA stem. B: HA trimer with HA protein in magenta, predicted 1G3 epitopes in blue, and the linker sequence of the HA fusion peptide in cyan on the interior of the HA trimer. Sialic acid interactions at the receptor binding head are shown in green.*

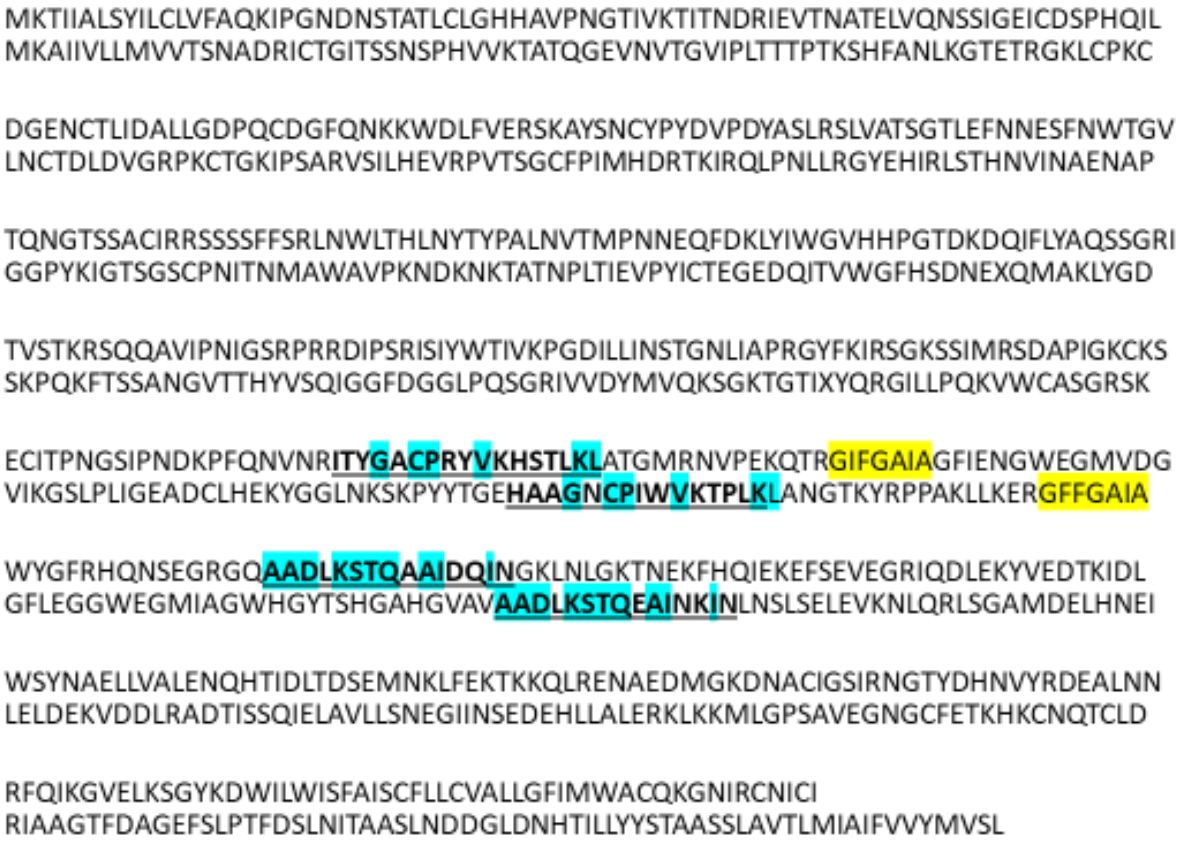

Figure 32*: HA amino acid sequence of A/Hong Kong/4801/2014 (top) and B/Brisbane/60/2008 (bottom). The two putative binding sites of 1G3 of interest are underlined and bolded. Amino acids within that footprint which are conserved between A/Puerto Rico/8/1934 as well as A/Hong Kong/4801/2014 and B/Brisbane/60/2008 are highlighted in cyan. GLFGAIA, highlighted in yellow, are the first amino acids of the N terminus of the HA2 subunit.*

Aim 3. Evaluate candidate mAbs efficacy *in vitro* and *in ovo*

Despite the breadth of viral subtypes bound by mAb 1G3 on Western blot, interaction with a viral target does not necessarily translate to inhibition or neutralization of virus during an infection. In order to assess mAb 1G3's ability to inhibit virus replication we performed Plaque Reduction and Neutralization Tests (PRNTs) coupled with fluorescence microscopy *in vitro* as well as time course inhibition assays *in ovo*.

PRNTs are complementary to previously described NI and HAI assays in that they measure the functional impact of mAb 1G3 on virus. Where NI and HAI assays quantify effect on viral protein, PRNTs instead look only at live, actively replicating virus. Madin Darby Canine Kidney (MDCK) cells were seeded into a 6-well plate and allowed to reach 80-90% confluency. Following 30 mins of viral exposure, inoculum is removed and an oxoid agar overlay applied. The overlay itself serves several chemical and physical roles in propagating infection. MDCK cells do not possess the necessary cellular proteases for productive influenza replication (4, 66). HA on the virion surface must be cleaved into its active subunits HA1 and HA2 to allow for entry into the cell as well as exit from the endosomal compartment (10, 42, 112). Therefore, the overlay contains TPCK treated free trypsin to ensure budding virions display mature HA and are infection competent. The overlay also serves to restrict virus to lateral movement to adjacent cells following the initial infection while allowing cells to participate in oxygen exchange. Resulting localized foci of cell death and detachment are known as "plaques". 1G3 was applied in the overlay media as purified mAb and also Receptor Destroying Enzyme (RDE) treated hybridoma conditioned supernatant. RDE is a commercially available enzyme purified from *Vibrio cholerae* that works to eliminate any non-specific inhibitors of viral replication that may be present in the

supernatant (60, 65). 72 hours post infection the overlay is removed and plaques visualized with 0.1% crystal violet in 20% ethanol to fix and stain what remains of the surviving cellular monolayer.

Initially, all seven candidate monoclonal antibodies with positive NI were screened for plaque reduction *in vitro*. NYMC X-162 (H3N1, A/Wisconsin/67/2005 HA parent) was chosen as the first experimental virus because it was one of two of the immunizing viruses during Immunization Protocol Alpha. But unlike PR8, NYMC X-162 produces lytic plaques with defined edges that are easily quantified - making it an ideal choice for screening. Data are shown as a percent reduction relative to total plaque number calculated for virus controls to account for heterogeneity inherent in viral infection. Anti-HA mAb 2H9 was used as a conditioned hybridoma supernatant control as it is known to target the HA head and inhibit viral entry. Of the seven flu mAbs identified in the preliminary Protocol Alpha screen, all showed some degree of inhibition against NYMC X-162 prior to RDE treatment (**Figure 32**). However, after treatment with RDE mAb 2G5 conditioned supernatant failed to inhibit virus at all (**Figure 33**). Only the 2H9 control and 3 of our candidate antibodies 1G3, 3E9, and 2A7 retained the ability to inhibit NYMC X-162 following RDE treatment. Next to the control antibody 2H9, 1G3 containing hybridoma supernatant was the most successful inhibitor, reducing plaque number by over 50% and 20% at 1:100 and 1:1000 respectively. (**Figure 33**).

Due to heterosubtypic binding profile of 1G3 observed in Western blotting, we next tested 1G3's ability to inhibit viruses of other subtypes *in vitro.* In addition to NYMC X-162 (H3N1), three viruses were selected; immunizing virus PR8 (H1N1) as well as an H1N1 pandemic virus (A/California/07/2009) and a wild type H3N2 virus (A/Hong

Kong/50/2016). These viruses showed reactivity with mAb 1G3 by Western blot and represent two subtypes of HA currently circulating from each influenza A group. MAb 1G3 containing hybridoma supernatant at a dilution of 1:100 was able to neutralize these viruses with considerable efficiency, reaching well over 50% neutralization rates for both of the non-immunizing viruses A/Hong Kong/50/2016 (H3N2) and A/California/07/2009 (H1N1) (**Figure 34**). The plaques that developed following infection with A/Hong Kong/50/2016 were observed to be pinpoint sized. We hypothesize that the almost 100% plaque reduction seen against this virus is as a function of plaques that may not have been observable to the naked eye. These data indicate that the binding seen on Western blot has functional relevance in the context of *in vitro* replication and infection capacity for these viruses. MAb 1G3 not only binds Group 1 and 2 influenza A viruses, but can also inhibit their ability to form plaques in cell culture.

Canonically, it was thought that a hallmark of antibodies that bind NA was a reduction in plaque size. This results from targeting the virus toward the end of the life cycle and limiting egress of progeny virions. However more recently it has been seen that HA stem antibodies can also limit plaque size via restricting virus to the endosomal compartment (133, 137). HA head antibodies function almost exclusively at the attachment stage and therefore only limit overall plaque number (4, 44). Our antibody candidate 1G3 was first tested for plaque size reduction against NYMC X-162 and demonstrated the ability to significantly limit plaque size at dilutions of 1:100 and 1:1000 of RDE treated hybridoma supernatant. 1G3 reduced overall plaque size from an average of 4.3 mm to 1.9 mm and 3.5 mm respectively (**Figure 35**).

In addition to NYMC X-162 (H3N1), plaque size was also assessed for heterosubtypic viruses PR8 (H1N1) and A/California/07/2009 (H1N1pdm) (**Figure 36**). Plaque size was not calculated following infection with A/Hong Kong/50/2016 (H3N2), as infection yielded very small plaques with ill-defined borders. Candidate mAb 1G3 was able to reduce plaque size following infection with PR8 (H1N1) and A/California/07/2009 (H1N1pdm) as it had for NYMC X-162 (H3N1), suggesting a conserved mechanism of action across distinct IAV groups.

Elution of a monoclonal antibody during purification is a process that necessitates reestablishing efficacy to ensure low pH conditions didn't distort the conformation or character of an antibody. Results seen with hybridoma supernatant were recapitulated with purified antibody to ensure data collected was not a result of inhibitors in supernatant that may survive RDE treatment. Therefore, PRNTs were repeated with multiple concentrations of purified 1G3 against immunizing virus A/Puerto Rico/8/1934 (PR8, H1N1). Plaque reduction was maintained and shown to be dose dependent, where the lowest concentration tested (0.1µg/mL) resulted in a 30% reduction in plaque number (**Figure 37**). In this model of infection, 100% plaque reduction is not expected because the initial infection period (30 mins) occurs in the absence of antibody. These results allowed for us to conclude that plaque number and size reduction upon treatment with 1G3 was as a direct result of antibody activity and not an inherent property of the hybridoma supernatant.

Finally, we expanded our experimental viral panel to include B/Brisbane/60/2008. This virus has been the dominant Victoria lineage B virus since its introduction and has been recommended in vaccine composition by the WHO every year from 2008 till 2018 (24). Because MAb 1G3 was shown to bind B/Brisbane/60/2008 on Western blot, it was selected

to be a representative B virus to test via PRNT. We found that RDE treated 1G3 supernatant was able to significantly reduce plaque number by roughly 50% at a dilution of 1:1000 (**Figure 38**), demonstrating that 1G3 indeed has functional activity against this B virus. Like wild type H3 viruses, B plaques have pinpoint morphology with individual diameters that cannot be measured. Representative images of plaque morphology in virus controls as well as in the presence of candidate mAb 1G3 can be seen in **Figure 39**.

Taken together, these PRNT data show that binding on Western blot is indeed correlated with *in vitro* neutralization activity of mAb 1G3 against H1, H1pdm, and H3 viruses as well as a wild type B Victoria virus. We can therefore categorize candidate mAb 1G3 as not only broadly binding, but broadly neutralizing. To date, only one other antibody with activity against influenza A and B, CR9114, has been published (32).

As a qualitative complement to the PRNT data, we next looked at infection in the presence and absence of mAb 1G3 on the cellular level via indirect fluorescent (IFA) staining. MDCK cells were seeded into chamber slides and allowed to reach 80-90% confluency. Cells were then infected with immunizing virus A/Puerto Rico/8/1934 (H1N1) at a multiplicity of infection (MOI) equal to one. Following 30 mins for viral absorption, viral inoculum was removed and replaced with cellular growth media, cellular growth media supplemented with 10 μg/mL purified mAb 1G3, or a commercial isotype control (**Figure 40**). Unlike a PRNT where an agar overlay is applied to contain virus to plaques, liquid media was used to allow virus to move into solution and infect the monolayer in a manner more representative of a natural infection. 24 hours post infection cells were fixed and stained via IFA. The primary antibody used was 1B3, a PR8 specific anti-HA head mAb developed in our lab by Dr Yu He. The secondary antibody was an anti-mouse heavy chain

conjugated with Alexa Fluor 488, allowing infected cells positive for the presence of PR8 HA to be visualized with green fluorescence. We observed that the quality of the cellular monolayer was greatly improved with the application of neutralizing 1G3 noted as almost no areas of cell death were seen. Instead the DAPI stained monolayer looked indistinguishable from the uninfected control. Additionally, positive HA staining was restricted to very few isolated cells as opposed to the outward spreading in large patches observed in both the virus and isotype controls (**Figure 40**). The number of HA positive cells in 1G3 treated chambers was significantly fewer, while no difference was detected qualitatively or quantitatively between virus and isotype control cells (**Figure 41**).

These qualitative data provide further support that mAb 1G3 can not only bind but also neutralize virus during active *in vitro* infection**.** Because these data were obtained with purified mAb 1G3, we can also conclude that inhibition of viral replication is as a direct result of antibody 1G3 and not any other components of the hybridoma supernatant.

We have thus far established that candidate mAb 1G3 has functional neutralization activity *in vitro* against H1, H1pdm, and H3 viruses as well as influenza B using a PRNT model. We also have shown using liquid media and fluorescent staining that purified 1G3 significantly alters infection dynamics. We next investigated the ability of purified 1G3 to inhibit viral replication and growth *in ovo* against both immunizing viruses, A/Puerto Rico/8/1934 (PR8, H1N1) and NYMC X-162 (H3N1, A/Wisconsin/67/2005 HA parent) as well as a representative influenza B virus (BX-31B). The natural reservoir of IAV is aquatic birds, this combined with the use of chicken eggs in vaccine manufacturing makes the efficacy of influenza antibodies in infected eggs an important parameter for evaluation (94).

Influenza A or B viruses at a dilution of 10^{-8} and purified mAb 1G3 at two concentrations were co-incubated at 37°C for 30 mins prior to infection. All virus stocks were diluted in PBS with calcium and gentamicin to maintain virion stability and prevent bacterial contamination. 11 day Specific Pathogen Free (SPF) embryonated chicken eggs were first candled to ensure embryonic viability. Eggs were then "windowed" to allow for ease of allantoic fluid collection without compromising the relative sterility of the egg. Windowing is done by cutting a 1 cm^2 hole in the shell of the egg below in the air sac and opposite to the embryo in aseptic conditions. Allantoic fluid is collected and the window covered with UV sterilized parafilm sealed to the intact shell with heated paraffin wax. Harvested fluid is then assayed for viral content by HA titer and streaked unto Sheep Red Blood Cell plates to check for any possible confounding bacterial contamination. Fluid was collected every 12 hours for 72 hours for influenza A viruses and 96 hours for influenza B starting at time 0, immediately prior to infection. Titers for each experimental run were done simultaneously in duplicate following final fluid collection to limit variance due to individual lots of chicken red blood cells. Pre-incubation of virus and antibody at 37°C allows an antibody to bind any available epitopes prior to inoculation of the egg. It was observed by Dr Yu He that antibodies that target the HA (head or stem) applied in high concentrations can prevent infection due to targeting virus at the beginning of the life cycle, similarly to what is seen in PRNTs. In cells, antibodies that target NA may allow for viral entry but inhibit egress and are typically associated with a delayed onset of titer as opposed to total inhibition.

Antibody candidate 1G3 was tested at two concentrations, 1 and 5 µg/mL. At both concentrations tested, 1G3 prevented rapid PR8 (H1N1) expansion at 36 hours and delayed

onset of positive viral titer by at least 12 hours. 1G3 at a concentration of 5 µg/mL was able to suppress viral growth for almost the entirety of the experimental duration (**Figure 42**). 1G3 was also tested against NYMC X-162 (H3N2) and again delayed the positive onset of viral titer by at least 12 hours and prevented the virus from reaching its uninhibited max at 72 hours post infection. Unlike what was seen with PR8 infection, 1G3 was not able to contain NYMC X-162 expansion completely at the higher concentration tested (**Figure 43**).

Encouraged by the *in vitro* results, we also tested BX-31B (Victoria). BX-31B is a high yield reassortant virus prepared by Dr Shiroh Onodera from B/Lee/40 with the HA and NA components from B/Brisbane/60/2008. Unlike influenza A viruses, influenza B is slower growing in eggs therefore the infection was allowed to continue for 96 hours total. Similarly to what was seen with PR8 infection, 5 µg/mL purified 1G3 inhibited infection totally for the duration of the experiment. Where the uninhibited virus showed considerable expansion 48 hours post infection, virus pre-incubated with 1 µg/mL 1G3 showed no positive titer for another 12 hours (**Figure 44**).

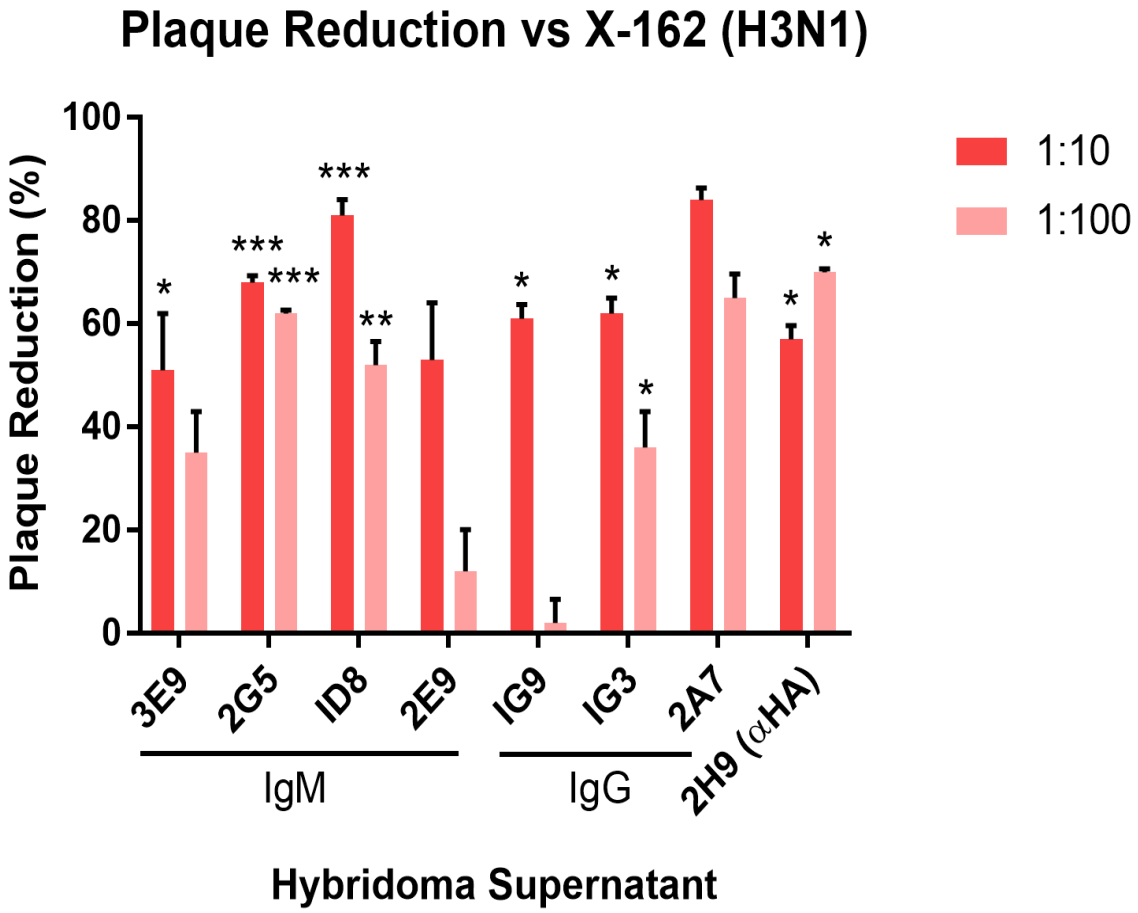

***Figure 33**: Percent plaque reduction relative to NYMC X-162 (H3N1, A/Wisconsin/67/2005 HA parent) uninhibited controls of seven hybridoma supernatants prior to treatment with receptor destroying enzyme. 2H9, a characterized anti-HA head mAb, was used as a hybridoma supernatant control. Data are shown with supernatants at a final dilution factor of 1:10 or 1:100. N ≥ 6 wells/condition, shown ± standard deviation, Student's T Test to viral control: * = p<0.05, ** = p<0.01, *** = p<0.001*

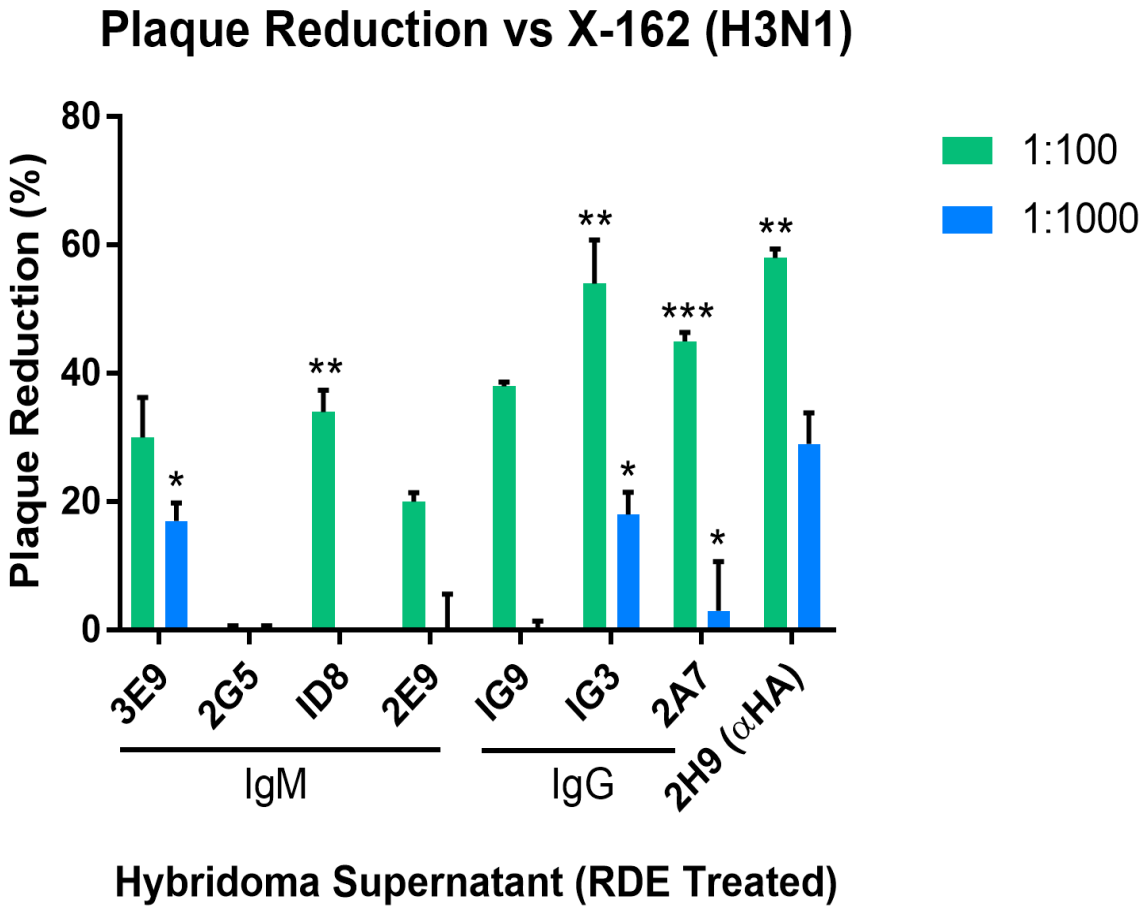

Figure 34: *Percent plaque reduction relative to NYMC X-162 (H3N1, A/Wisconsin/67/2005 HA parent) uninhibited controls of seven receptor destroying enzyme treated hybridoma supernatants. 2H9, a known anti-HA head mAb, was used as a hybridoma supernatant control. Data are shown with supernatants at a final dilution factor of 1:100 or 1:1000. 1G9, 1D8, and 2E9 showed no inhibition activity at 1:1000. 2G5 showed no in vitro inhibition at either dilution. N ≥ 6 wells/condition, shown ± standard deviation, Student's T Test to viral control: * = p<0.05, ** = p<0.01, *** = p<0.001*

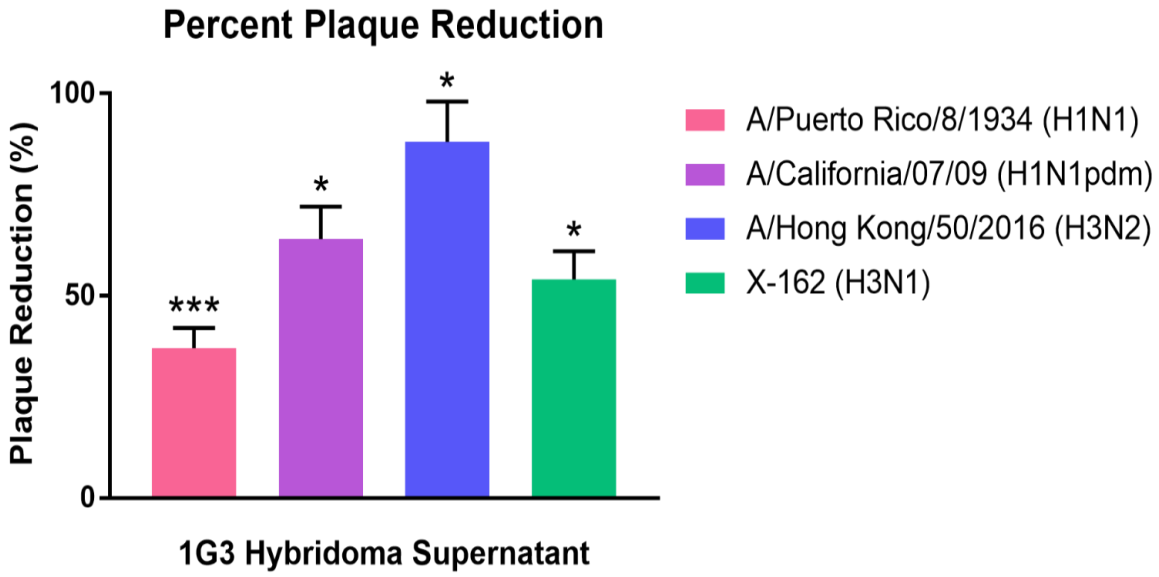

*Figure 35: A/Puerto Rico/8/1934 (PR8, H1N1), A/California/07/2009 (H1N1pdm), A/Hong Kong/50/2016 (H3N2) and NYMC X-162 (H3N1, A/Wisconsin/67/2005 HA parent) were used at a concentration of ~40 PFUs/ well. Overlay contained growth media in oxoid agar or growth media in oxoid agar supplemented with receptor destroying enzyme treated 1G3 hybridoma supernatant at a final dilution of 1:100. N ≥ 6 wells/condition, shown ± standard deviation, Student's T Test to respective viral control: * = p<0.05, *** = p<0.001*

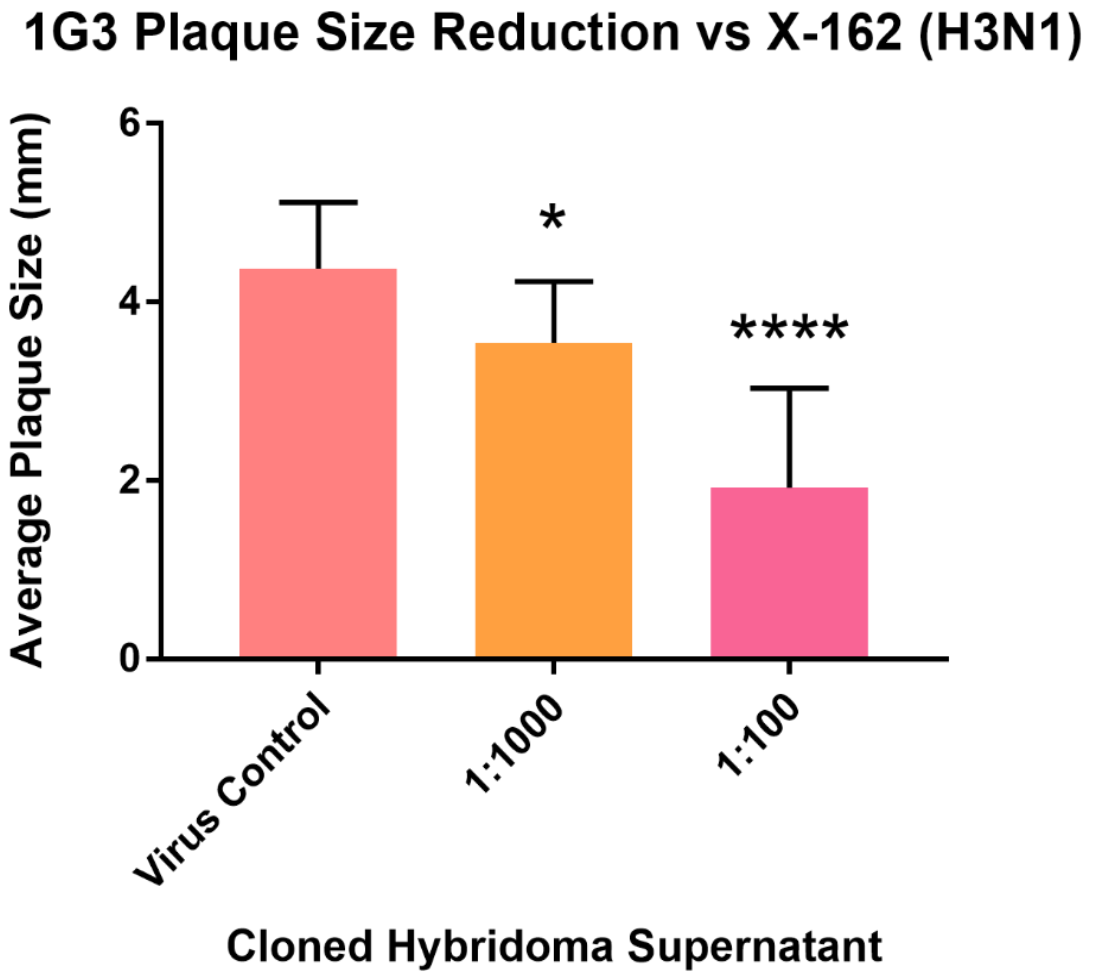

***Figure 36**: Plaque size reduction mediated by mAb 1G3 vs NYMC X-162 (H3N1, A/Wisconsin/67/2005 HA parent) at a dilution of 1:1000 and 1:100. N ≥ 6 wells/ condition; bars show average plaque size ± standard deviation. Student's T Test: * =p < 0.05, **** p= <0.0001*

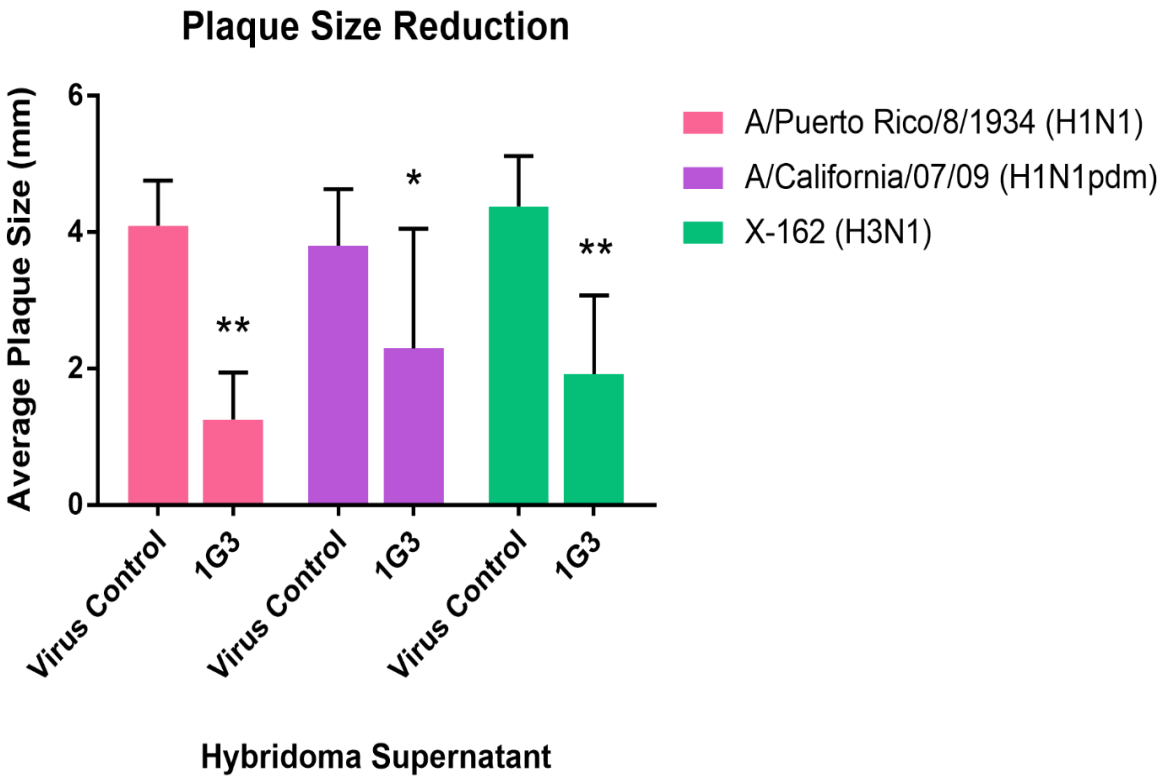

***Figure 37**: Average plaque size following infection with A/Puerto Rico/8/1934 (PR8, H1N1), A/California/07/2009 (H1N1pdm), and NYMC X-162 (H3N1, A/Wisconsin/67/2005 HA parent) at a concentration of ~40 PFUs/ well. Overlay contained growth media agar or growth media agar supplemented with 1G3 containing hybridoma supernatant at a dilution of 1:100. Plaques were visualized with crystal violet and diameter measured in mm. $N \geq 6$ wells/condition, shown ± standard deviation, Student's T Test: * = $p<0.05$, ** = $p<0.01$*

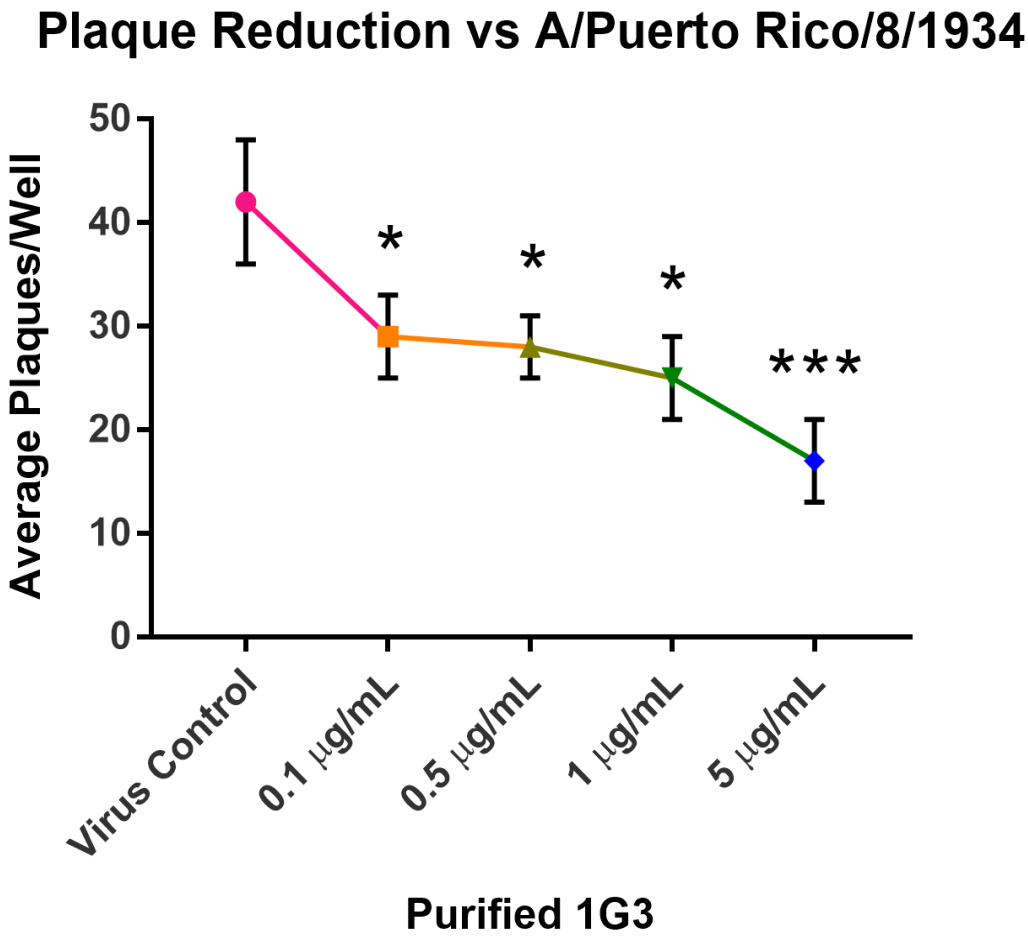

***Figure 38**: Plaque Reduction and Neutralization Test completed with purified mAb 1G3. A/Puerto Rico/8/1934 (PR8, H1N1) was applied to 6 well plates at a concentration of ~40 PFUs/ well. Overlay contained control growth media agar or growth media agar supplemented with purified 1G3 at concentrations shown. N ≥ 6 wells/condition, shown ± standard deviation, Student's T Test: * = $p<0.05$, *** = $p<0.001$*

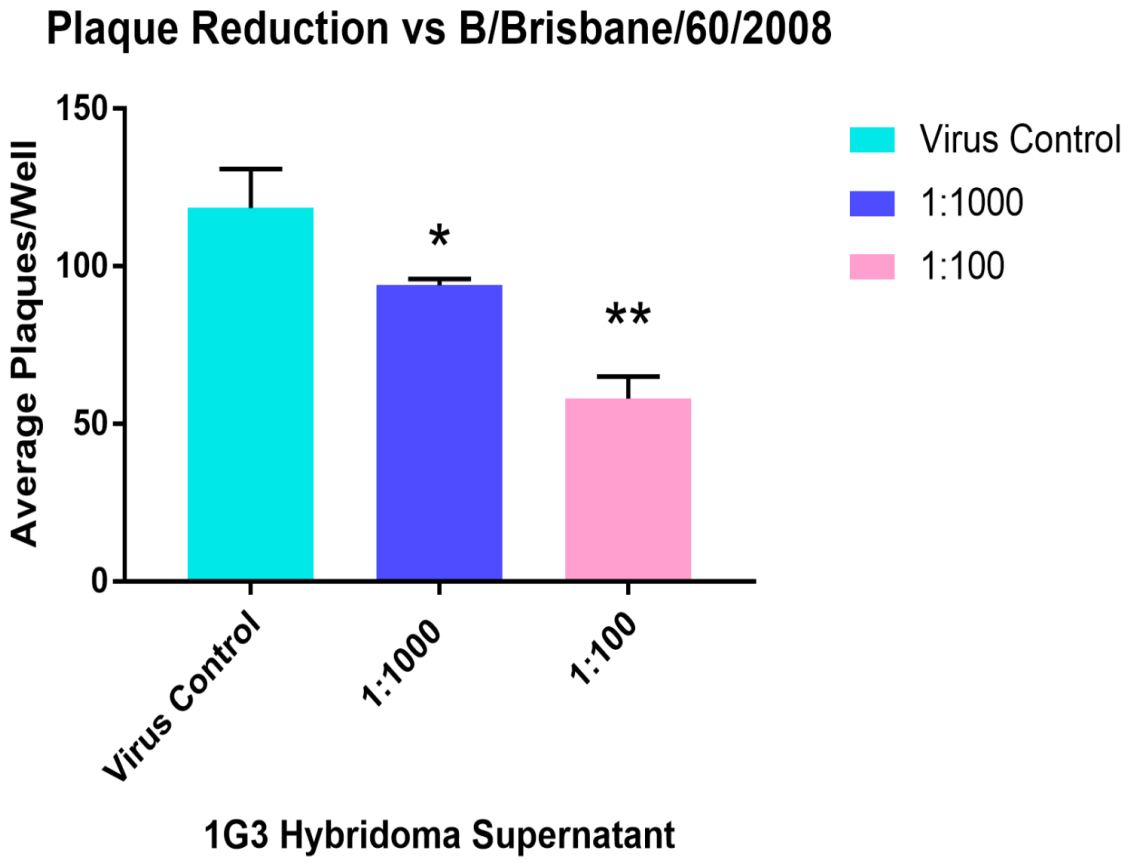

***Figure 39**: Average plaque number following infection with B/Brisbane/60/2008 (Victoria). Overlay contained growth media agar or growth media agar supplemented with 1G3 containing hybridoma supernatant at a dilution of 1:1000 or 1:100. N ≥ 6 wells/condition, shown ± standard deviation, Student's T Test: * = $p<0.05$, ** = $p<0.01$*

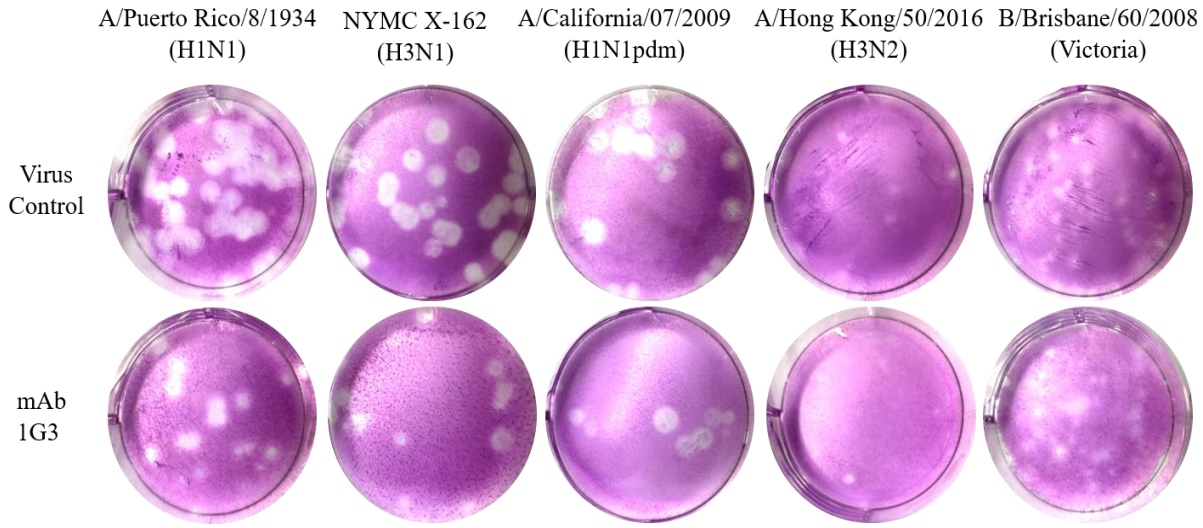

***Figure 40**: Representative images of plaque morphology following infection with (from left to right) A/Puerto Rico/8/1934 (H1N1), NYMC X-162 (H3N1), A/California/07/2009 (H1N1pdm), A/Hong Kong/50/2016 (H3N2), and B/Brisbane/60/2008 (Victoria). Below are representative images of plaques formed in the presence of candidate mAb 1G3 showing plaque number and average plaque size reduction.*

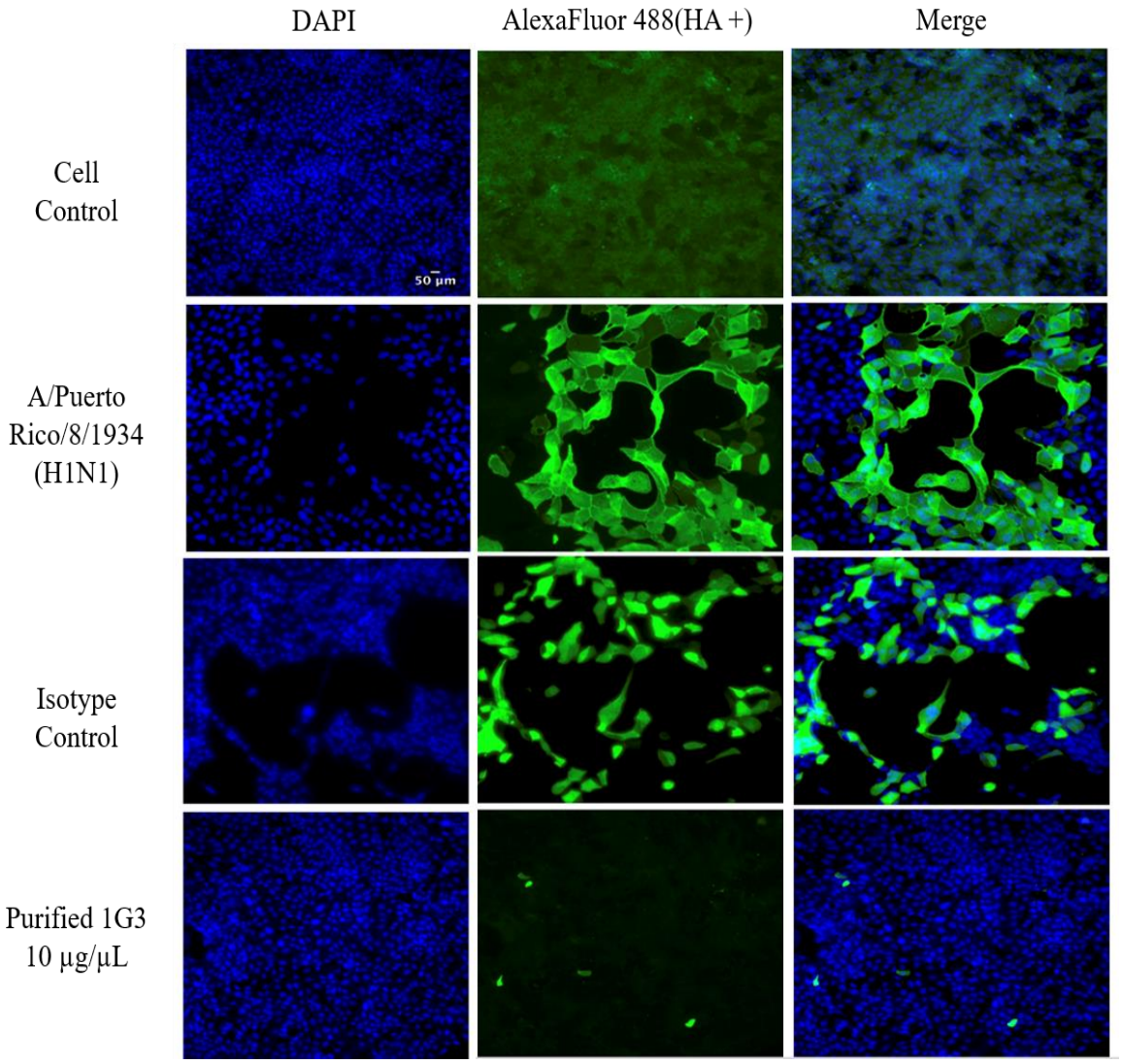

Figure 41: Indirect fluorescent staining of A/Puerto Rico/8/1934 (PR8, H1N1) HA in infected MDCK cells. Primary antibody for stained was 1B3, an PR8 specific anti-HA mAb. An AlexaFluor488 conjugated secondary was used to visualize infected cells positive for PR8 HA. Cellular nuclei were stained with DAPI (blue). Images at 20X.

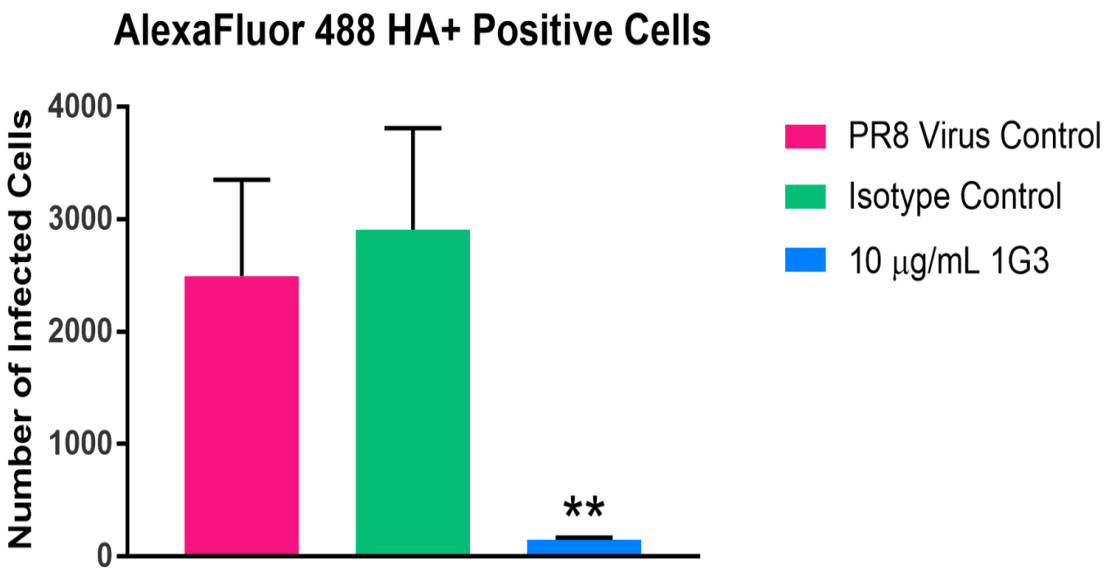

***Figure 42**: Following indirect fluorescent staining of MDCK cells, AlexaFluor488 HA+ cells were counted following A/Puerto Rico/8/1934 infection. No significant difference was observed between virus and isotype controls. N ≥ 3 wells/condition, shown ± standard deviation, Student's T Test: ** = p<0.01*

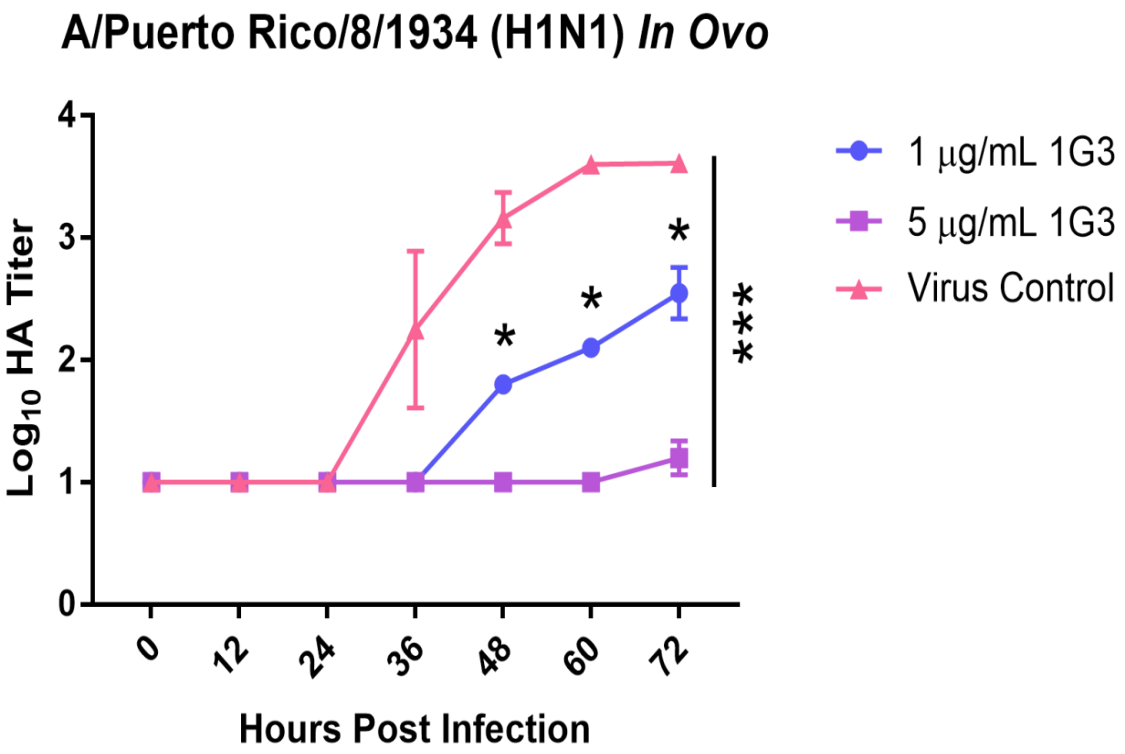

***Figure 43**: A/Puerto Rico/8/1934 (PR8, H1N1) viral growth represented by the Log of HA titer. Titer was measured every 12 hours for 72 hours following injection at time point 0 of PR8 diluted to 10^{-8} in PBS and gentamicin. 1G3 was pre-incubated with virus at 37°C at concentrations of 1 or 5 µg/mL. N ≥ 6 eggs/condition, shown ± standard deviation, Student's T Test to viral control for each time point: * = p<0.05, *** = p<0.001*

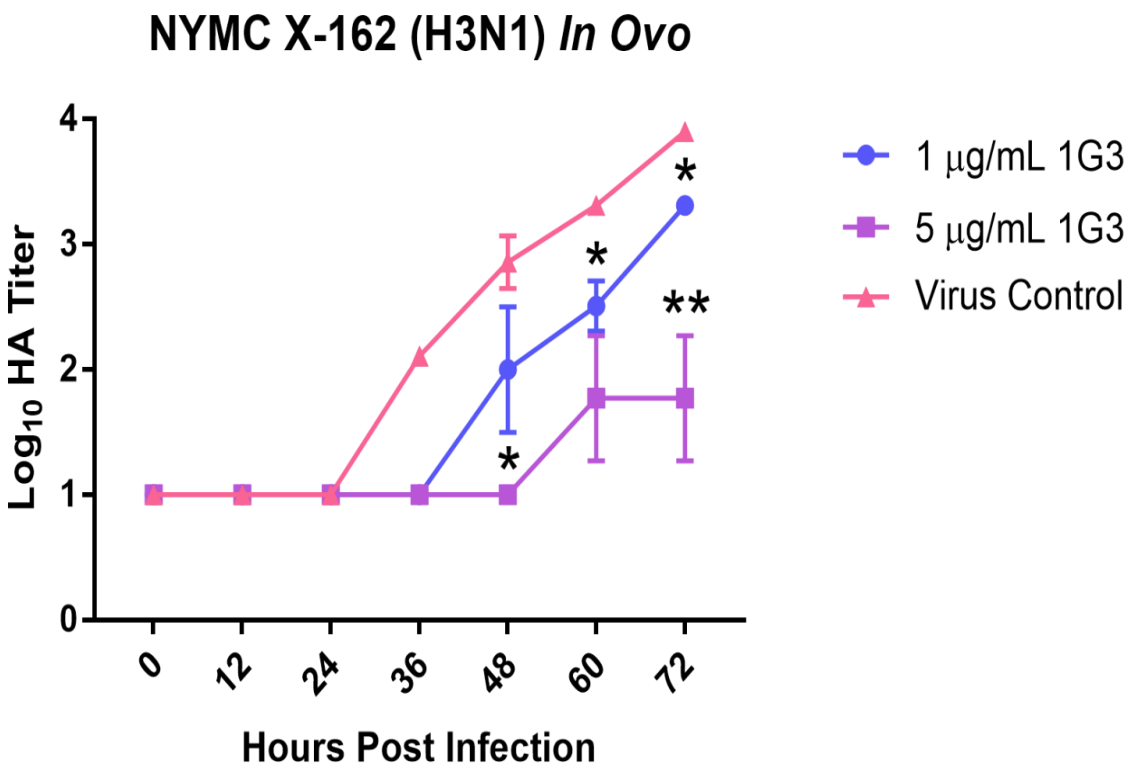

***Figure 44**: NYMC X-163(H3N1) viral growth represented by the Log of HA titer. Measured every 12 hours for 72 hours following injection at time point 0 of X-162 diluted to 10^{-8} in PBS and gentamicin. 1G3 was pre-incubated with virus at 37°C at concentrations of 1 or 5 µg/mL. N ≥ 6 eggs/condition, shown ± standard deviation, Student's T Test to viral control for each time point: * = p<0.05, ** = p<0.01*

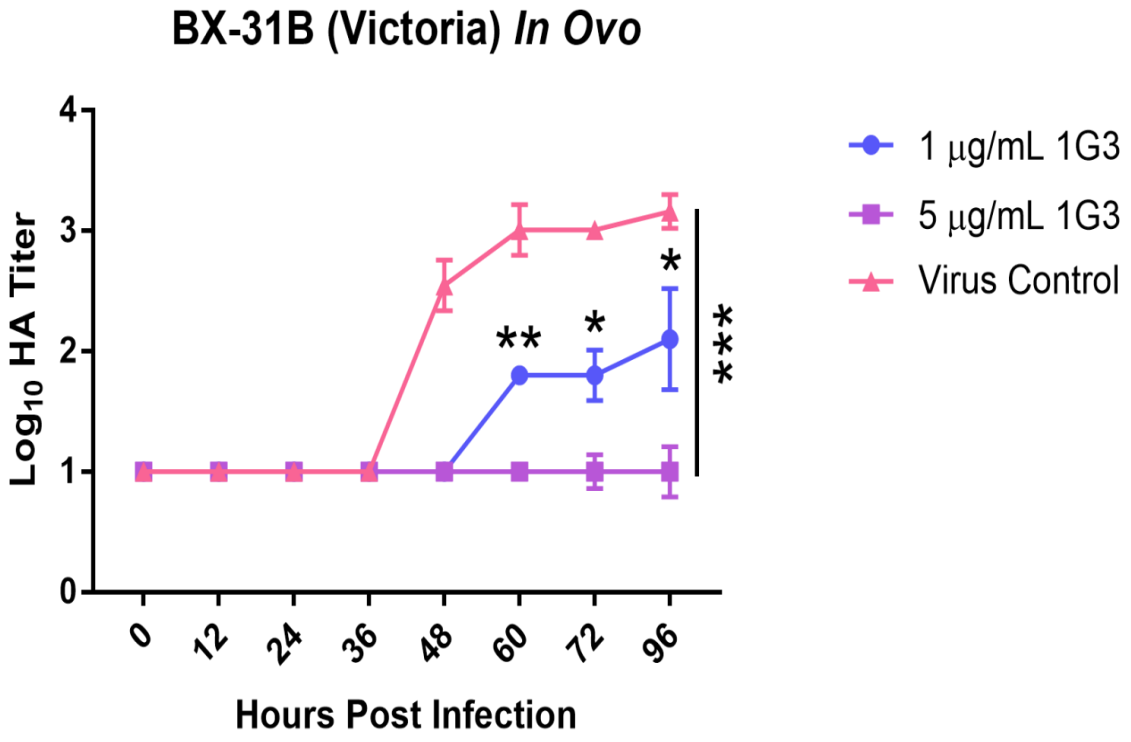

Figure 45: *BX-31B (Victoria) viral growth represented by the Log of HA titer. Measured every 12 hours for 96 hours following injection at time point 0 of BX-31B diluted to 10^{-8} in PBS and gentamicin. 1G3 was pre-incubated with virus at 37°C at concentrations of 1 or 5 µg/mL. N ≥ 6 eggs/condition, shown ± standard deviation, Student's T Test to viral control for each time point: * = p<0.05, ** = p<0.01, *** = p<0.001*

CONCLUSIONS

Through the immunization of mice with varied influenza hemagglutinin (HA) proteins, we have generated a novel murine monoclonal antibody 1G3 (IgG1). MAb 1G3 can bind viruses from group 1 and group 2 of influenza A as well both major lineages of influenza B, Yamagata and Victoria. Using plaque assays, fluorescent staining, and time course studies, we have shown that mAb 1G3 can also neutralize heterosubtypic viruses to successfully inhibit infection *in vitro* and *in ovo*.

1G3 binds a conformational epitope, making traditional linear mapping difficult. However, using a peptide array paired with 3D modeling we propose that 1G3 binds the HA stem near the fusion peptide and across the C terminus of HA1 and the N terminus of HA2. Although distinct, this putative epitope appears to share many features with the published epitopes of known broadly neutralizing influenza antibodies. Through sequence alignment we have also shown that critical residues therein show a high degree of conservation between different influenza A and B viruses, reflecting strong conservation of the stem domain.

Influenza's ability to both drift and shift away from immune recognition makes vaccination and treatment challenging (24). Antibodies to influenza have been studied in human and animal sera since the 1970's (93). Following the advent of hybridoma technology and various recombinant techniques, hundreds of labs around the world have attempted to find and target common epitopes. To date, dozens of antibodies have been identified, published, and patented, that can bind across strains and subtypes. However only one antibody, CR9114, can protect mice *in vivo* from lethal challenge with both influenza A and B (32). Our mAb 1G3 is the first to show activity against A and B viruses *in vitro*.

Therefore, mAb 1G3 joins an exclusive class of broadly neutralizing influenza antibodies. Because of this extremely rare reactivity profile, we believe that 1G3 has the potential to work in concert with other advances in the field to improve upon currently available therapies and/or support a universal vaccine.

DISCUSSION

Influenza epidemics are a major public health concern. Worldwide it is estimated that annual seasonal infection results in at least 3 million cases of severe illness (requiring hospitalization) and as many as 650,000 deaths (131). At the height of the 2017-2018 flu season, 11% of all deaths in the United States were attributed to influenza and influenza like illness in addition to 185 reported pediatric deaths. This was the highest number of pediatric deaths since infant and child mortality from influenza became a reportable illness. 80-90% of these deceased patients were unvaccinated (17). Influenza pandemics can result from the introduction of novel flu proteins into an immunologically naive human population. The most recent "Swine Flu" pandemic in 2009 infected an estimated 65 million people and caused a significant amount of morbidity in typically lower risk groups, especially young adults (109). The 1918 "Spanish Flu" was even more devastating, estimated to have killed roughly 5% of the global population at the time.

Unfortunately, treatment for influenza infection is significantly limited. Until very recently only two classes of drugs were approved for the management of flu, M2 ion channel inhibitors and NA inhibitors (NAIs) (77). M2 ion channel inhibitors were developed first and function to prevent the acidification of the viral core and subsequent uncoating (100, 124). Although initially effective, over time their use has selected for resistant strains that maintain pathogenicity - which now predominate the infection landscape (124). The CDC recommends against their use as efficacy is at an all-time low (17). NAIs like Tamiflu™ and Relenza™ interfere with the activity of the viral neuraminidase, allowing virus to gain entry into host cells but preventing progeny virion release. Several large-scale retrospective studies have demonstrated that NAIs are effective as prophylaxis for those

populations most at risk of complications from influenza infection. However, as treatment NAIs are limited and have been met with mixed success (73, 87). Replication in the respiratory tract generally peaks 24-48 hours post infection. Therefore NAIs have to be prescribed very early in disease course, representing a significant hurdle to their continued use and success (77). NAIs have also been used as a therapeutic modality for patients who are already hospitalized with severe illness, although this is considered off label and most studies show no advantage of the use the NAIs over traditional supportive therapies (39, 59). Resistance mutations are rare but have been recorded in some seasonal H1N1 viruses (73).

Regular vaccination remains both the most operative and cost-effective way to control influenza. Current seasonal influenza vaccines are effective against infection but are not without shortcomings. Due to constant antigenic drift and occasional shift of circulating viruses, vaccines need to be reformulated and redistributed to the general public each year. Despite significant effort, mismatches do occur that may leave even vaccinated individuals vulnerable to illness. Trivalent and tetravalent vaccines are only partially effective in the most susceptible target populations, including the elderly and immunocompromised. (24, 121, 141). Crucially, seasonal vaccines provide no protection against novel strains, significantly limiting pandemic preparedness (82).

Perhaps the most significant limitation in our current vaccination strategy is that it generally induces a narrow and strain specific response (7, 48). Antibodies developed following vaccination are most often targeted to the highly variable loops on the globular HA head that surround the receptor binding site (127). HA head binding antibodies are very adept at neutralization because they prevent the virus from binding to the sialic acid receptors necessary for the virus to gain entry into a host cell. Some HA head antibodies can

also interfere with the function of the viral NA through steric hindrance, preventing viral egress as well as endocytosis (80, 130). However, in addition to being largely strain specific these antibodies readily select for escape mutations and lose efficacy quickly against drifted strains (11).

New prevention and treatment modalities for influenza are needed. Recently several human antibodies with wider neutralizing activity have been isolated using single B cell identification techniques, phage display libraries, and hybridoma cell lines (123). These broadly neutralizing monoclonal antibodies (bnmAbs) have been characterized following vaccination with heterosubtypic HA, but are comparatively rare following natural infection (133).

Broadly neutralizing influenza antibodies are divided into three types based on the breadth of viruses they have been demonstrated to inhibit. Type 1 are effective against several group 1 influenza A viruses, Type 2 against several group 2, and Type 3 which are effective many HA subtypes belonging to both groups 1 and 2 (137). There are also a handful of broadly neutralizing antibodies which target influenza B, these are characterized as having activity against a subset of viruses of both the major B lineages (32). Many of these antibodies have been shown to be of therapeutic or prophylactic benefit in animal models and are summarized in **Figure 45**.

Therapeutic Antibodies

There is a significant existing framework for the use of targeted monoclonal antibodies in the treatment of human diseases, including autoimmune disorders, cardiovascular pathologies, cancer, and some bacterial infections. The earliest iterations of antibody therapy were murine antibodies developed using hybridoma cell lines and were

largely disappointing. Unfortunately mouse derived molecules failed to interact as predicted in a human immunological context and were not only ineffective, but dangerous as they were recognized as foreign by the patient resulting in inflammation and their subsequent elimination (19). The era of antibody engineering quickly followed with the advent of the first chimeric and then humanized mAbs. Chimeric antibodies are generated by fusing the murine variable domain with a human constant domain and are roughly 70% human origin. In addition to being less immunogenic, chimeric antibodies can bind their intended target while still interacting with the patient's own Fc receptors (67). Humanized antibodies were developed shortly thereafter by replacing the antigen binding hypervariable loops of a human antibody with the targeted murine loops – a process known as "complementarity-determining region grafting". Humanized antibodies are nearly 90% human but cost more to produce as often mutagenesis via a phage library is needed post hoc to restore high affinity binding. Almost all of the mAbs approved in the United States currently are either chimeric or humanized (19).

Despite the over 60 FDA approved mAbs to date there is only a single antiviral antibody widely available; Palivizumab for Respiratory Syncytial Virus (RSV) prophylaxis in high risk infants (123). The reason for the limited development of virally targeted antibodies is a combination of factors, including high production cost, difficulties related to administration, and the belief that antibodies are most effective prior to exposure - which for many viruses is made redundant by vaccination. However there is a growing appreciation of the potential of many novel antiviral mAbs, including the now infamous Ebola virus mAb Porgaviximab, also known as Zmapp (95). More antiviral antibodies will continue to come to market as the increased potency of superior antibodies reduces the cost of production and

makes patient compliance more feasible and less expensive by also reducing the number of treatments needed. This coupled with a new generation of technologies for antibody generation, including humanized animals, single B cell cloning, and combinatorial display libraries, is the cause of much cautious optimism for combatting notoriously difficult viruses like HIV as well as emerging threats like MERS coronavirus (123).

Antibodies can act against viruses in several defined ways but are generally divided into two categories: those which act on viral particles and those which target infected cells. The best measure of activity on free virus is known as neutralization; or the ability of an antibody to prevent viral entry. Neutralization is measured *in vitro* and has been shown to be a strong correlate of *in vivo* protection for a wide range of viruses (74). Neutralization for influenza viruses is measured as blockade of either HA or NA through HI, NI, or PRNT assays (28). However for some viruses, and for influenza viruses in particular, activity against infected cells in the intact host immunological context appears to be critical for antibody efficacy - as *in vitro* neutralization titers often do not predict *in vivo* protection (26, 51, 105, 113). These antibodies interact with the host Fc receptors and may incite a number of complex downstream processes including antibody-dependent cytotoxicity (ADCC), complement-dependent cytotoxicity (CDC), and antibody-dependent cellular phagocytosis (ADCP) (36, 106, 123, 127). Meaning that despite commonly held wisdom, the constant regions of these antibodies are as critical for *in vivo* protection, if not more so, than the antigen binding variable region.

There is growing evidence for the role of ADCC in the influenza immune response as mediated by some HA antibodies. ADCC is a mechanism by which Fc receptor bearing natural killer (NK) cells recognize antibody bound cells and release cytotoxic granules into

an immunological synapse formed between the NK cell FcγRIIIa and its target. These granules generally contain a combination of perforin and granzyme B and their release results in the apoptosis of the infected cell (19, 76). It has been demonstrated that stalk mAb efficacy is dependent on the presence of functioning Fcγ receptors, as transgenic mice lacking Fcγ receptors on murine NK cells are not protected from lethal challenge by anti-HA stalk mAbs (28, 57). Interestingly, this same requirement has not been seen for strain specific HA head antibodies, which are effective regardless of NK cell presence (29).

The basis of this observation lies in a difference of mechanism for head and stalk antibody function. While head antibodies prevent virus binding similarly *in vitro* and *in vivo*, most stalk antibodies show a very different mechanistic profile in cells and in animals. Anti-HA stalk antibodies may primarily inhibit endocytic membrane fusion *in vitro*, but in the complete immunological context of an animal these same antibodies function primarily through the activation of ADCC (29, 57, 122). These data may provide a framework of understanding why our mAb 1G3 was more effective at lower concentrations *in ovo* than in PRNT cellular assays against the same A/Puerto Rico/8/1934 virus. Chicken embryos produce T and B cells by day 11 and 12 of development and do have an avian NK cell homologue known as TCRO (58, 83). Therefore, our *in ovo* studies may be more representative of the true neutralizing potential of 1G3 which like other stalk mAbs may interact with NK cells to target and destroy virally infected cells. These observations also support the data obtained with mAb CR9114 where *in vitro* neutralization was absent against those viruses whereas CR9114 did protect against in mice with functioning NK cells (32). However, it is important to note that were CR9114 failed to inhibit influenza B viruses in cells, our mAb 1G3 was successful. Therefore 1G3 activity is not dependent on ADCC

alone.

Despite their many advantages, monoclonal antibodies are subject to more than a few major limitations and therapeutic considerations. First there are several practical issues, namely cost. Because monoclonal antibodies are complex molecules that require extensive eukaryotic machinery in order to be properly synthesized, production relies on very large cultures of mammalian cells followed by many steps of purification in order to be approved for infusion or injection into a human patient (19, 34, 136). High cost is also directly proportional to the high concentration of mAbs needed for human efficacy. For example, Natalizumab, also known as Tysabri, is a humanized IgG4 developed to treat Multiple Sclerosis. Natalizumab is given to patients as 300 mg IV infusion every 28 days for an indefinite period of time, often many years, requiring at least 4 grams of antibody per patient per year (8). This scheme is common among current therapeutic models for chronic disease, however dosing for acute conditions is less clear. As reference, Palivizumab is given prophylactically at 15 mg/kg of body weight every 28 days during the RSV season until the child reaches 2 years old or is no longer considered at risk (110).

Interestingly, the high effective serum concentration needed of human antibodies might be because of Fc receptor dependent mechanisms of action. Some therapeutic antibodies saturate ADCC function *in vitro* at concentrations as low as 10 ng/μL but require effective serum concentrations between 10 and 100 μg/μL (19). Its hypothesized that this may be as a result of competition from a patient's own circulating IgG for available FcγRIIIa receptors, as IgG1 has a very high mean serum level in adults (55). It has also been demonstrated that affinity between a therapeutic antibody and a patients Fc receptor may be a predictive measure of efficacy. Unfortunately, about 80% of the world's population

expresses FcγRIII-F158, a low affinity variant of the receptor which may also contribute to high antibody effective concentrations (127). Another consideration is that like natural human IgG1, therapeutic IgG1 can interact with both classes of Fcγ receptors. ADCC occurs through activating receptors, but inhibitory receptor FcγRIIb is expressed on B-cells, macrophages, and dendritic cells. Where FcγRIII possesses a tyrosine activation motif, FcγRIIb does not and binding to this receptor sequesters and decreases the overall efficacy of exogenous mAbs (19).

Influenza Monoclonal Antibodies

There are currently eight anti-influenza antibodies listened as in clinical trials in the US. Of these, seven target HA while one targets the extracellular domain of the M2 ion channel. Most have been developed within the last 10 years using single B cell isolation from vaccinated patient volunteers. These are summarized in **Figure 46**.

The HA protein is encoded by RNA segment 4 and is moved across the host rough endoplasmic reticulum during translation. HA is synthesized as a monomer, HA0, which is composed of 549 amino acids and undergoes significant N linked glycosylation. HA0 is assembled into trimers at the virion surface and then must be cleaved into its active subunits HA1 (327 amino acids) and HA2 (222 amino acids) in order to be active (109). HA0 cleavage is a major determinant of tissue tropism and occurs via a trypsin-like serine protease at a cleavage site encoded by a single arginine residue (R329) in most influenza A viruses (117). HPAI viruses have well characterized mutations at this cleavage site that result in the insertion of several basic residues near the requisite arginine, resulting in the ability to be cleaved intracellularly by more ubiquitous enzymes like furin (112). Following cleavage, the hydrophobic fusion peptide on the N terminal domain of HA2 relocates to the

trimer interior forming the fusion peptide pocket and becomes fusogenic (25, 66). However, HA1 and HA2 stay associated via disulphide bonds throughout viral entry. HA then undergoes significant conformational change in response to the acidification of the endocytic vesicle, including the disassociation of the HA1 domain from the HA2 fusion domain (42). This results in the extrusion of the fusion peptide from the interior pocket while the C terminal domain of HA2 stays anchored in the viral membrane. This structure collapses by "zipping up" and drives the fusion of the endosomal and virion membranes, necessary for the release of viral contents into the cytoplasm (25).

HA can be divided into two structural domains, the globular head and the stem. The globular head contains the receptor binding domain, as well as part of a vestigial esterase, while the stem contains the fusion peptide and the remaining esterase residues. The receptor binding domain is located at the top of the globular head and is composed of the 130 loop, 190 helix, and 220 loop; all encoded by HA1 along with the proximal antigenic sites (69, 109). In contrast, the fusion domain includes residues from both HA1 and HA2. The fusion domain sits in the stem is encoded by the N and C terminal domains of HA1 (amino acids 11-64, 276-329) as well as the N terminal domain of HA2 (amino acids 1-160) (132).

Traditional HA head targeted antibodies subvert the propagation of infection by preventing the HA receptor binding pocket from appropriately interacting with its sialic acid ligand and are associated with positive experimental hemagglutinin inhibition (97). However broadly neutralizing HA stem antibodies have been shown to be effective against influenza *in vitro* and *in vivo* by several mechanisms, irrespective of sialic acid binding (**Figure 47**). Of these, inhibition of fusion between the virus and endosome has been observed in relation to all broadly neutralizing stem MAbs (11). It was previously hypothesized that stem mAbs

are internalized together with virus and reach the late endosome where binding to their epitope prevents the fusion peptide from responding to low pH (71). Indirect evidence for this reasoning has been the lack of detectable HAI activity, inhibition of conformational changes in recombinant HA, and the prevention of syncytia formation in HA expressing cells (35, 85, 111). Friessen *et al* have demonstrated using single particle tracking technology that mAb CR8020, a stem antibody which neutralizes multiple Group 2 flus, is in fact internalized by live cells during infection and are capable of reaching the late endosomes (11). CR8020 was developed through human B cell isolation by Crucell and is currently in phase II clinical trials supported by Johnson and Johnson (32, 123)

Due to the close structural relationship between the fusion peptide and cleavage site that separates HA1 and HA2, epitopes that prevent endosomal fusion may also prevent proteolytic activation of HA exterior to the cell and prior to receptor mediated endocytosis. While fusion inhibition is widely reported as the dominant mechanism of virus neutralization, this second means of inhibiting virus has been shown to add to the strength of some broadly neutralizing mAbs (68, 109, 112). Our own data for mAb 1G3 suggests that both of these mechanisms may be involved. Linear epitope mapping and 3D protein visualization show that the most likely epitope is near the fusion peptide, at the C terminus of HA1 and N terminus of HA2. Additionally, for Group 2 viruses trypsin treatment disrupted 1G3 binding; suggesting that the cleavage site could plays an integral role in recognition of H3 viruses.

The third mechanism by which stem antibodies may inhibit cellular viral infection is through the interference of viral egress. It was previously accepted that only NA targeted antibodies prevented the release of progeny virions, as the primary function of NA is to

cleave sialic acid at the surface and prevent HA cross linking (47, 77, 129). Recent studies using scanning electron microscopy have shown that some HA targeted antibodies may also inhibit virion escape, although there is some debate about the exact mechanism (28, 57). It appears that antibodies with specific VH regions may participate directly in cross-linking bound virions at the surface of the cell while others may function indirectly through steric hindrance of NA activity (68, 130). We found that mAb 1G3 does in fact limit virion egress, as evidenced by significant plaque size reduction against both H1 and H3 influenza A viruses. Furthermore, we believe this is through indirect inhibition of the viral NA, as 1G3 mediated NA inhibition is ablated by treating virus with a strong detergent.

The only antibody described to date that can bind and neutralize both influenza A Groups 1 and 2 as well as influenza B viruses is CR9114 (32). CR9114 was generated using single B cell isolation from human volunteers who received regular season vaccination and constructing combinatorial phage display libraries. CR9114 has been shown to be capable of neutralizing H1, H2, H3, H4, H5, H6, H7, H8, H9, H10, H12 viruses *in vitro*. CR9114 initially showed no activity against any influenza B viruses. However, they found CR9114 fully protected mice from lethal challenge with B/Florida/4/2006 and B/Malaysia/2506/2004 when given prophylactically 24 hours post infection at a concentration of 15 mg/kg. Lower concentrations were needed for 100% survival against influenza A viruses, as low as 1.7 mg/kg for both A/Puerto Rico/8/1934 (H1N1) and A/Hong Kong/1/1968 (H3N2) (35). Recently CR9114 was also evaluated prophylactically against a panel of H2 viruses, which although not currently circulating in humans remains a threat due to a persistent animal reservoir. As with influenza B, CR9114 showed weak activity in cells but was protective against a lethal challenge with both A/Ann Arbor/6/1960 and A/swine/MO/4296424/2006 at

a concentration of 5 mg/kg (113). These effects were dependent on the presence of Fcγ receptors and again demonstrate the importance of ADCC within *in vivo* studies for analyzing stalk mAbs which may not neutralize efficiently in cells. While 1G3 shares some epitopic features with CR9114, it has been shown to be broadly neutralizing *in vitro*, therefore the role of ADCC in 1G3 efficacy remains to be seen.

Future Directions

Monoclonal antibody 1G3 represents a new member in the broadly neutralizing group. While its epitope is similar, and indeed overlaps with that of other known HA stem antibodies, its *in vitro* neutralization profile is unrivaled. Further work will focus on establishing the 1G3 epitope with a higher resolution, exploring the possible mechanism or mechanisms of action with respect to different lineages of influenza, as well as establishing *in vivo* relevance.

The gold standard for establishing antibody epitopes is X-ray crystallography. Here the target protein and antibody are allowed to bind and then purified in high concentrations in a crystalline form. When a single X-ray beam is applied, the resulting pattern of diffraction can be used to obtain data on "crystal packing" which can be translated into electron density and therefore atoms and amino acids (38, 108). This method has yielded an incredible amount of data, including the discovery of the structure of DNA by Rosalind Franklin for which Watson, Crick, and Wilkins received the Nobel prize in 1962. Images of experimental antibody bound to purified HA obtained using X-ray crystallography allow the researcher to identify single amino acids that contribute to affinity. Unfortunately, as a technique crystallography is expensive and exceedingly difficult. Crystalizing a protein can take upwards of one year which is compounded in our use by crystalizing a protein-antibody

interaction. Crystals need to be of the highest purity and in large concentrations to have regular repeating unit cells that can be easily interpreted. Proteins are generally crystalized in solution, although discerning the best conditions for nucleating high quality crystals is almost always a process of trial and error (1). While X-ray crystallography is accepted as the ideal, we may instead consider site directed mutagenesis to complement the data obtained from our linear array. When comparing the mapping data across group 1, group 2, and influenza B viruses we found some highly conserved amino acids within the predicted 1G3 footprint on both HA1 and HA2. We could systematically mutate these single amino acids and then retest 1G3's ability to bind HA antigen either via ELISA or Western blot and thereby identify those sites which may contribute the most to affinity. Although site directed mutagenesis is also time intensive, it is significantly less costly than X-ray crystallography and would improve our resolution from 15 amino acid long stretches, instead highlighting a few critical residues.

One important observation from our data is that although 1G3 is effective *in vitro* and *in ovo* against both H1 and H3 viruses, the banding pattern on Western blot is different; especially with respect to trypsin treatment. While performing an additional peptide map with any one of the H3 viruses we assayed might yield a radically different epitope, it's more likely that the difference between H1 and H3 binding is based in conformational dissimilarities that are not apparent in a linear array. Instead there are other some experiments which may be able to discern differences in mechanism of 1G3 inhibition between H1 and H3 viruses. We suspect that 1G3 inhibits membrane fusion as that has been implicated with every HA stem antibody in the literature. However, testing the relative efficacy of 1G3 against H1 and H3 mediated fusion would provide some operational insight.

There are two widely accepted approaches to measuring fusion inhibition by stem antibodies. The first is to transiently express the HA of a virus type of interest, here at least one H1 and one H3 virus, on the surface of HeLa cells or another similarly permissive cell line. At a pH of roughly 5.0 the HA expressed on these cells will allow for the formation of syncytia that are easily seen and scored with a light microscope. We would predict that syncytia formation by H1 or H3 protein would be inhibited by a sufficient concentration of mAb 1G3, although we would likely observe that concentrations would differ between HAs.

However, mAb 1G3 did not bind recombinant HA on Western blot and is acutely sensitive to HA conformation, therefore transient surface expression from a plasmid may not best reflect the activity of 1G3. Another experiment which may be better suited to 1G3's unique character involves directly observing membrane fusion through a single particle fusion assay developed by Crucell, the same group who developed CR9114 and CR8020. The enveloped membrane of virus is first labeled with fluorescent lipophilic dye in a concentration sufficient to result in self-quenching. Following pre-incubation with either a control or the stem antibody of interest, the virus-antibody complexes are bound to sialic acid residue embedded in a target membrane and imaged. When the pH is lowered from 7.4 to 5, fusion is measured as a rapid increase in fluorescence signal due to de-quenching through diffusion. Live imaging of this event would provide direct evidence of inhibition of membrane fusion by 1G3 on intact virions with biologically relevant HA.

Another possible mechanism of action for 1G3 is the prevention of proteolytic cleavage of HA prior to viral internalization. We saw that following overnight trypsin treatment 1G3 could no longer bind purified H3 virus on Western blot, heavily implicating the protease recognition site in antibody binding. We would also like to incubate both H1

and H3 viruses with 1G3 first, then probe with 1G3 by Western blot following overnight treatment with trypsin. We suspect that the 1G3 epitope straddles the trypsin recognition site for both H1 and H3 viruses and therefore only one band would be visible in reducing conditions as the HA0 monomer would remain intact. However, more important than this would be to test the additive effect of inhibition of cleavage *in vitro*. To do this we would need to generate a batch of each virus of interest with uncleaved HA. As MDCK cells do not produce any proteases capable of cleaving HA endogenously, this can be accomplished by harvesting virus after a single round of replication in the absence of exogenous trypsin. These viruses will be incompetent for infection. We would then test the contribution of cleavage inhibition by incubating with 1G3 following trypsin treatment of virus or before. If uncleaved virus is incubated with trypsin and then 1G3, the subsequent infection would assay neutralization only the remaining inhibition points, membrane fusion or egress. However, if uncleaved virus and 1G3 are co-incubated together prior to trypsin treatment, the pursuant infection would reflect neutralization by both blocking HA cleavage and membrane fusion. We would expect that adding 1G3 before trypsin treatment would result in the most significant plaque reduction in a PRNT context, as inhibition of cleavage is a supplemental mechanism of viral inhibition that will have an additive effect on controlling *in vitro* infection. We would also expect this effect to be even more pronounced with H3 viruses as is appears from Western blotting that 1G3 binding is disrupted by cleavage.

Most critically, the efficacy of 1G3 needs to be evaluated *in vivo*. We would first model our experiments based on those completed with CR9114 by Dreyfus *et al.* They evaluated the prophylactic efficacy of their antibody by applying 15, 5, 1.7, 0.6, or 0.2 mg/kg intranasaly 24 hours post challenge with 25 LD_{50} of virus. They measured the

animal's survival and body weight for 15 days and also measured viral titer in the lungs following sacrifice (32). We would ideally test at minimum one H1, one H3 and one influenza B virus from each lineage in a similar infection scheme. It would also be of interest to test 1G3 prophylactically against a HPAI H5 or H7 virus, which would require the use of a dedicated BSL-3 animal facility in addition to a BSL-3 laboratory for viral propagation and preparation.

We would also like to test the impact of 1G3 as a possible therapeutic *in vivo*. Our PRNT protocol does call for the application of antibody following 30 mins of infection and those data strongly suggest that 1G3 can dampen an already in-progress infection. Especially salient would be any effect of 1G3 on highly pathogenic avian viruses post infection, as these carry a high mortality rate but have been successfully treated with convalescent sera (3).

Interestingly, there are no data available about the therapeutic value of CR9114. However, another antibody also developed by Crucell, CR8020, completed Phase 2a human clinical trials less than 5 years ago. They tested a single 15 mg/kg injection given 2 days post challenge with an H1N1 virus. Unfortunately, study data are not available. Yet another Crucell antibody, CR6261, is currently being evaluated with its own Phase 2a trial at a reported concentration of 50 mg/kg. This discrepancy drives home the importance of *in vivo* experimentation and the difficulties of antibody therapies for infectious disease.

While there is a significant amount of work needed to translate monoclonal antibody 1G3 from our data to human relevance, we are optimistic that because of 1G3's broad neutralizing profile it is worth pursuing.

Classification	Neutralizing Profile	mAbs
Type 1	Group 1 HA	CR6261, F10, 3.1, FE43, FE17, PN-SIA49, A06
Type 2	Group 2 HA	CR8020, CR8043
Type 3	Groups 1 and 2 HA	**CR9114**, F16, CO5, C179 39.29, 81.39, CT149, VIS410, 1C4, 3C4, 05-2G02, 045-05310-2B06, S6-B01, PN-SIA28, MED18852, 56.a.09, 31.b.09, 16.a.26, 16.g.07, 31.a.83

Figure 46*: Influenza HA targeted broadly neutralizing monoclonal antibodies. Type 1 antibodies target more than one strain of group 1; type 2 targets more than one strain of group 2. Type 3 can target influenza A strains of both groups. CR9114 (highlighted in red) can also target influenza B (32).*

Antibody	Target	Method	Stage	Manufacturer
VIS410	HA(1&2)	Atomic analysis	Phase II	Vistera
MHAA 4549A	HA(1&2)	Human B cell	Phase II	Genentech
CT P27	HA(1&2)	Human B cell	Phase II	Celltrion
CR6261	HA(1&2)	Phage display	Phase II	Crucell
CR8090	HA(2)	Human B cell	Phase II	Crucell
RG 6024	HA(B)	Human B cell	Phase I	Genentech
MEDI 8852	HA(1&2)	Human B cell	Phase I	MedImmune
TCN 032	M2e	Human B cell	Phase II	Theraclone Sciences

Figure 47*: Influenza targeted monoclonal antibodies currently in development in the United States. Seven of eight target the HA glycoprotein while one, TCN 032, instead targets the extracellular region of the M2 ion channel.*

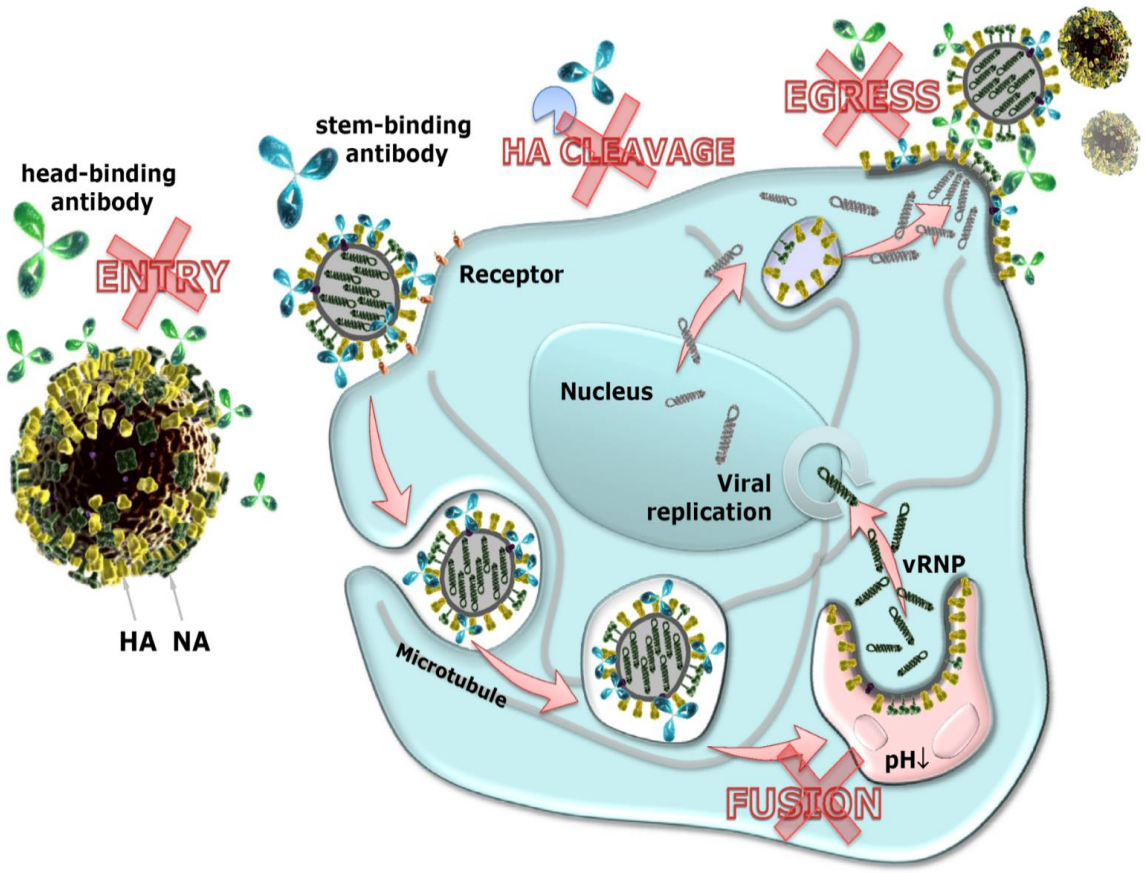

***Figure 48**: Mechanisms of HA antibody inhibition of influenza virus infection. Head targeted antibodies function primarily at the beginning of the virus life cycle, shown on the left, preventing viral attachment. Stem antibodies, right, may prevent HA cleavage before internalization or prevent pH mediated conformational changes in the fusion peptide. Both head and stem antibodies can prevent the egress of progeny virions either by directly crosslinking virus or indirectly inhibited NA via steric hindrance. (11)*

APPENDIX

1. Table of Viruses

Virus	*Abbreviation*	*Subtype*	*Origin*	*Gene Composition*
A/Puerto Rico/8/1934	PR8	IAV, H1N1	Egg adapted	
A/New Caledonia/20/1992		IAV, H1N1	Wildtype	
A/Moscow/10/1999		IAV, H3N2	Wildtype	
A/Wisconsin/67/2005		IAV, H3N2	Wildtype	
A/South Dakota/06/2007		IAV, H1N1	Wildtype	
A/California/07/2009		IAV, H1N1pdm	Wildtype	
A/Hong Kong/50/2014		IAV, H3N2	Wildtype	
B/Brisbane/60/2008		IBV, Victoria	Wildtype	
B/Massachusetts/02/2012		IBV, Yamagata	Wildtype	
NYMC X-162	X-162	IAV, H3N1	High Yield Reassortant	HA: A/Wisconsin/67/2005
NYMC X-179A	X-179A	IAV, H1N1pdm	High Yield Reassortant	HA, PB1: A/California/07/2009
NYMC X-187	X-187	IAV, H3N2	High Yield Reassortant	HA: A/Victoria/2009

2. Peptide Map

		1	2	3
	EQKLISEEDL	G	EQKLISEEDL	G
1	EQKLISEEDL	GSGSGSGMKANLLVL	SGSGSGMKANLLVLL	GSGSGMKANLLVLLC
2	G	GSGSGSGMKANLLVL	SGSGSGMKANLLVLL	GSGSGMKANLLVLLC
3	EQKLISEEDL	LCRLKGIAPLQLGKC	CRLKGIAPLQLGKCN	RLKGIAPLQLGKCNI
4	G	LCRLKGIAPLQLGKC	CRLKGIAPLQLGKCN	RLKGIAPLQLGKCNI
5	EQKLISEEDL	LSSVSSFERFEIFPK	SSVSSFERFEIFPKE	SVSSFERFEIFPKES
6	G	LSSVSSFERFEIFPK	SSVSSFERFEIFPKE	SVSSFERFEIFPKES
7	EQKLISEEDL	GKEVLVLWGIHHPSN	KEVLVLWGIHHPSNS	EVLVLWGIHHPSNSK
8	G	GKEVLVLWGIHHPSN	KEVLVLWGIHHPSNS	EVLVLWGIHHPSNSK
9	EQKLISEEDL	LKPGDTIIFEANGNL	KPGDTIIFEANGNLI	PGDTIIFEANGNLIA
10	G	LKPGDTIIFEANGNL	KPGDTIIFEANGNLI	PGDTIIFEANGNLIA
11	EQKLISEEDL	VTIGECPKYVRSAKL	TIGECPKYVRSAKLR	IGECPKYVRSAKLRM
12	G	VTIGECPKYVRSAKL	TIGECPKYVRSAKLR	IGECPKYVRSAKLRM
13	EQKLISEEDL	AADQKSTQNAINGIT	ADQKSTQNAINGITN	DQKSTQNAINGITNK
14	G	AADQKSTQNAINGIT	ADQKSTQNAINGITN	DQKSTQNAINGITNK
15	EQKLISEEDL	LVLLENERTLDFHDS	VLLENERTLDFHDSN	LLENERTLDFHDSNV
16	G	LVLLENERTLDFHDS	VLLENERTLDFHDSN	LLENERTLDFHDSNV
17	EQKLISEEDL	SEESKLNREKVDGVK	EESKLNREKVDGVKL	ESKLNREKVDGVKLE
18	G	SEESKLNREKVDGVK	EESKLNREKVDGVKL	ESKLNREKVDGVKLE
	EQKLISEEDL	G	EQKLISEEDL	G
	4	5	6	7
	EQKLISEEDL	G	EQKLISEEDL	G
1	SGSGMKANLLVLLCA	GSGMKANLLVLLCAL	SGMKANLLVLLCALA	GMKANLLVLLCALAA
2	SGSGMKANLLVLLCA	GSGMKANLLVLLCAL	SGMKANLLVLLCALA	GMKANLLVLLCALAA
3	LKGIAPLQLGKCNIA	KGIAPLQLGKCNIAG	GIAPLQLGKCNIAGW	IAPLQLGKCNIAGWL

4	LKGIAPLQLGKCNIA	KGIAPLQLGKCNIAG	GIAPLQLGKCNIAGW	IAPLQLGKCNIAGWL
5	VSSFERFEIFPKESS	SSFERFEIFPKESSW	SFERFEIFPKESSWP	FERFEIFPKESSWPN
6	VSSFERFEIFPKESS	SSFERFEIFPKESSW	SFERFEIFPKESSWP	FERFEIFPKESSWPN
7	VLVLWGIHHPSNSKE	LVLWGIHHPSNSKEQ	VLWGIHHPSNSKEQQ	LWGIHHPSNSKEQQN
8	VLVLWGIHHPSNSKE	LVLWGIHHPSNSKEQ	VLWGIHHPSNSKEQQ	LWGIHHPSNSKEQQN
9	GDTIIFEANGNLIAP	DTIIFEANGNLIAPM	TIIFEANGNLIAPMY	IIFEANGNLIAPMYA
10	GDTIIFEANGNLIAP	DTIIFEANGNLIAPM	TIIFEANGNLIAPMY	IIFEANGNLIAPMYA
11	GECPKYVRSAKLRMV	ECPKYVRSAKLRMVT	CPKYVRSAKLRMVTG	PKYVRSAKLRMVTGL
12	GECPKYVRSAKLRMV	ECPKYVRSAKLRMVT	CPKYVRSAKLRMVTG	PKYVRSAKLRMVTGL
13	QKSTQNAINGITNKV	KSTQNAINGITNKVN	STQNAINGITNKVNT	TQNAINGITNKVNTV
14	QKSTQNAINGITNKV	KSTQNAINGITNKVN	STQNAINGITNKVNT	TQNAINGITNKVNTV
15	LENERTLDFHDSNVK	ENERTLDFHDSNVKN	NERTLDFHDSNVKNL	ERTLDFHDSNVKNLY
16	LENERTLDFHDSNVK	ENERTLDFHDSNVKN	NERTLDFHDSNVKNL	ERTLDFHDSNVKNLY
17	SKLNREKVDGVKLES	KLNREKVDGVKLESM	LNREKVDGVKLESMG	NREKVDGVKLESMGI
18	SKLNREKVDGVKLES	KLNREKVDGVKLESM	LNREKVDGVKLESMG	NREKVDGVKLESMGI
	EQKLISEEDL	G	EQKLISEEDL	G
	8	9	10	11
	EQKLISEEDL	G	EQKLISEEDL	G
1	MKANLLVLLCALAAA	KANLLVLLCALAAAD	ANLLVLLCALAAADA	NLLVLLCALAAADAD
2	MKANLLVLLCALAAA	KANLLVLLCALAAAD	ANLLVLLCALAAADA	NLLVLLCALAAADAD
3	APLQLGKCNIAGWLL	PLQLGKCNIAGWLLG	LQLGKCNIAGWLLGN	QLGKCNIAGWLLGNP
4	APLQLGKCNIAGWLL	PLQLGKCNIAGWLLG	LQLGKCNIAGWLLGN	QLGKCNIAGWLLGNP
5	ERFEIFPKESSWPNH	RFEIFPKESSWPNHN	FEIFPKESSWPNHNT	EIFPKESSWPNHNTN
6	ERFEIFPKESSWPNH	RFEIFPKESSWPNHN	FEIFPKESSWPNHNT	EIFPKESSWPNHNTN
7	WGIHHPSNSKEQQNL	GIHHPSNSKEQQNLY	IHHPSNSKEQQNLYQ	HHPSNSKEQQNLYQN
8	WGIHHPSNSKEQQNL	GIHHPSNSKEQQNLY	IHHPSNSKEQQNLYQ	HHPSNSKEQQNLYQN
9	IFEANGNLIAPMYAF	FEANGNLIAPMYAFA	EANGNLIAPMYAFAL	ANGNLIAPMYAFALS
10	IFEANGNLIAPMYAF	FEANGNLIAPMYAFA	EANGNLIAPMYAFAL	ANGNLIAPMYAFALS

11	KYVRSAKLRMVTGLR	YVRSAKLRMVTGLRN	VRSAKLRMVTGLRNI	RSAKLRMVTGLRNIP
12	KYVRSAKLRMVTGLR	YVRSAKLRMVTGLRN	VRSAKLRMVTGLRNI	RSAKLRMVTGLRNIP
13	QNAINGITNKVNTVI	NAINGITNKVNTVIE	AINGITNKVNTVIEK	INGITNKVNTVIEKM
14	QNAINGITNKVNTVI	NAINGITNKVNTVIE	AINGITNKVNTVIEK	INGITNKVNTVIEKM
15	RTLDFHDSNVKNLYE	TLDFHDSNVKNLYEK	LDFHDSNVKNLYEKV	DFHDSNVKNLYEKVK
16	RTLDFHDSNVKNLYE	TLDFHDSNVKNLYEK	LDFHDSNVKNLYEKV	DFHDSNVKNLYEKVK
17	REKVDGVKLESMGIY	EKVDGVKLESMGIYQ	KVDGVKLESMGIYQI	VDGVKLESMGIYQIL
18	REKVDGVKLESMGIY	EKVDGVKLESMGIYQ	KVDGVKLESMGIYQI	VDGVKLESMGIYQIL
	EQKLISEEDL	G	EQKLISEEDL	G
	12	13	14	15
	EQKLISEEDL	G	EQKLISEEDL	G
1	LLVLLCALAAADADT	LVLLCALAAADADTI	VLLCALAAADADTIC	LLCALAAADADTICI
2	LLVLLCALAAADADT	LVLLCALAAADADTI	VLLCALAAADADTIC	LLCALAAADADTICI
3	LGKCNIAGWLLGNPE	GKCNIAGWLLGNPEC	KCNIAGWLLGNPECD	CNIAGWLLGNPECDP
4	LGKCNIAGWLLGNPE	GKCNIAGWLLGNPEC	KCNIAGWLLGNPECD	CNIAGWLLGNPECDP
5	IFPKESSWPNHNTNG	FPKESSWPNHNTNGV	PKESSWPNHNTNGVT	KESSWPNHNTNGVTA
6	IFPKESSWPNHNTNG	FPKESSWPNHNTNGV	PKESSWPNHNTNGVT	KESSWPNHNTNGVTA
7	HPSNSKEQQNLYQNE	PSNSKEQQNLYQNEN	SNSKEQQNLYQNENA	NSKEQQNLYQNENAY
8	HPSNSKEQQNLYQNE	PSNSKEQQNLYQNEN	SNSKEQQNLYQNENA	NSKEQQNLYQNENAY
9	NGNLIAPMYAFALSR	GNLIAPMYAFALSRG	NLIAPMYAFALSRGF	LIAPMYAFALSRGFG
10	NGNLIAPMYAFALSR	GNLIAPMYAFALSRG	NLIAPMYAFALSRGF	LIAPMYAFALSRGFG
11	SAKLRMVTGLRNIPS	AKLRMVTGLRNIPSI	KLRMVTGLRNIPSIQ	LRMVTGLRNIPSIQS
12	SAKLRMVTGLRNIPS	AKLRMVTGLRNIPSI	KLRMVTGLRNIPSIQ	LRMVTGLRNIPSIQS
13	NGITNKVNTVIEKMN	GITNKVNTVIEKMNI	ITNKVNTVIEKMNIQ	TNKVNTVIEKMNIQF
14	NGITNKVNTVIEKMN	GITNKVNTVIEKMNI	ITNKVNTVIEKMNIQ	TNKVNTVIEKMNIQF
15	FHDSNVKNLYEKVKS	HDSNVKNLYEKVKSQ	DSNVKNLYEKVKSQL	SNVKNLYEKVKSQLK
16	FHDSNVKNLYEKVKS	HDSNVKNLYEKVKSQ	DSNVKNLYEKVKSQL	SNVKNLYEKVKSQLK
17	DGVKLESMGIYQILA	GVKLESMGIYQILAI	VKLESMGIYQILAIY	KLESMGIYQILAIYS

18	DGVKLESMGIYQILA	GVKLESMGIYQILAI	VKLESMGIYQILAIY	KLESMGIYQILAIYS
	EQKLISEEDL	G	EQKLISEEDL	G
	16	17	18	19
	EQKLISEEDL	G	EQKLISEEDL	G
1	LCALAAADADTICIG	CALAAADADTICIGY	ALAAADADTICIGYH	LAAADADTICIGYHA
2	LCALAAADADTICIG	CALAAADADTICIGY	ALAAADADTICIGYH	LAAADADTICIGYHA
3	NIAGWLLGNPECDPL	IAGWLLGNPECDPLL	AGWLLGNPECDPLLP	GWLLGNPECDPLLPV
4	NIAGWLLGNPECDPL	IAGWLLGNPECDPLL	AGWLLGNPECDPLLP	GWLLGNPECDPLLPV
5	ESSWPNHNTNGVTAA	SSWPNHNTNGVTAAC	SWPNHNTNGVTAACS	WPNHNTNGVTAACSH
6	ESSWPNHNTNGVTAA	SSWPNHNTNGVTAAC	SWPNHNTNGVTAACS	WPNHNTNGVTAACSH
7	SKEQQNLYQNENAYV	KEQQNLYQNENAYVS	EQQNLYQNENAYVSV	QQNLYQNENAYVSVV
8	SKEQQNLYQNENAYV	KEQQNLYQNENAYVS	EQQNLYQNENAYVSV	QQNLYQNENAYVSVV
9	IAPMYAFALSRGFGS	APMYAFALSRGFGSG	PMYAFALSRGFGSGI	MYAFALSRGFGSGII
10	IAPMYAFALSRGFGS	APMYAFALSRGFGSG	PMYAFALSRGFGSGI	MYAFALSRGFGSGII
11	RMVTGLRNIPSIQSR	MVTGLRNIPSIQSRG	VTGLRNIPSIQSRGL	TGLRNIPSIQSRGLF
12	RMVTGLRNIPSIQSR	MVTGLRNIPSIQSRG	VTGLRNIPSIQSRGL	TGLRNIPSIQSRGLF
13	NKVNTVIEKMNIQFT	KVNTVIEKMNIQFTA	VNTVIEKMNIQFTAV	NTVIEKMNIQFTAVG
14	NKVNTVIEKMNIQFT	KVNTVIEKMNIQFTA	VNTVIEKMNIQFTAV	NTVIEKMNIQFTAVG
15	NVKNLYEKVKSQLKN	VKNLYEKVKSQLKNN	KNLYEKVKSQLKNNA	NLYEKVKSQLKNNAK
16	NVKNLYEKVKSQLKN	VKNLYEKVKSQLKNN	KNLYEKVKSQLKNNA	NLYEKVKSQLKNNAK
17	LESMGIYQILAIYST	ESMGIYQILAIYSTV	SMGIYQILAIYSTVA	MGIYQILAIYSTVAS
18	LESMGIYQILAIYST	ESMGIYQILAIYSTV	SMGIYQILAIYSTVA	MGIYQILAIYSTVAS
	EQKLISEEDL	G	EQKLISEEDL	G
	20	21	22	23
	EQKLISEEDL	G	EQKLISEEDL	G
1	AAADADTICIGYHAN	AADADTICIGYHANN	ADADTICIGYHANNS	DADTICIGYHANNST
2	AAADADTICIGYHAN	AADADTICIGYHANN	ADADTICIGYHANNS	DADTICIGYHANNST
3	WLLGNPECDPLLPVR	LLGNPECDPLLPVRS	LGNPECDPLLPVRSW	GNPECDPLLPVRSWS
4	WLLGNPECDPL	LLGNPECDPLLP	LGNPECDPLLP	GNPECDPLLPV

	LPVR	VRS	VRSW	RSWS
5	PNHNTNGVTAACSHE	NHNTNGVTAACSHEG	HNTNGVTAACSHEGK	NTNGVTAACSHEGKS
6	PNHNTNGVTAACSHE	NHNTNGVTAACSHEG	HNTNGVTAACSHEGK	NTNGVTAACSHEGKS
7	QNLYQNENAYVSVVT	NLYQNENAYVSVVTS	LYQNENAYVSVVTSN	YQNENAYVSVVTSNY
8	QNLYQNENAYVSVVT	NLYQNENAYVSVVTS	LYQNENAYVSVVTSN	YQNENAYVSVVTSNY
9	YAFALSRGFGSGIIT	AFALSRGFGSGIITS	FALSRGFGSGIITSN	ALSRGFGSGIITSNA
10	YAFALSRGFGSGIIT	AFALSRGFGSGIITS	FALSRGFGSGIITSN	ALSRGFGSGIITSNA
11	GLRNIPSIQSRGLFG	LRNIPSIQSRGLFGA	RNIPSIQSRGLFGAI	NIPSIQSRGLFGAIA
12	GLRNIPSIQSRGLFG	LRNIPSIQSRGLFGA	RNIPSIQSRGLFGAI	NIPSIQSRGLFGAIA
13	TVIEKMNIQFTAVGK	VIEKMNIQFTAVGKE	IEKMNIQFTAVGKEF	EKMNIQFTAVGKEFN
14	TVIEKMNIQFTAVGK	VIEKMNIQFTAVGKE	IEKMNIQFTAVGKEF	EKMNIQFTAVGKEFN
15	LYEKVKSQLKNNAKE	YEKVKSQLKNNAKEI	EKVKSQLKNNAKEIG	KVKSQLKNNAKEIGN
16	LYEKVKSQLKNNAKE	YEKVKSQLKNNAKEI	EKVKSQLKNNAKEIG	KVKSQLKNNAKEIGN
17	GIYQILAIYSTVASS	IYQILAIYSTVASSL	YQILAIYSTVASSLV	QILAIYSTVASSLVL
18	GIYQILAIYSTVASS	IYQILAIYSTVASSL	YQILAIYSTVASSLV	QILAIYSTVASSLVL
	EQKLISEEDL	G	EQKLISEEDL	G
	24	25	26	27
	EQKLISEEDL	G	EQKLISEEDL	G
1	ADTICIGYHANNSTD	DTICIGYHANNSTDT	TICIGYHANNSTDTV	ICIGYHANNSTDTVD
2	ADTICIGYHANNSTD	DTICIGYHANNSTDT	TICIGYHANNSTDTV	ICIGYHANNSTDTVD
3	NPECDPLLPVRSWSY	PECDPLLPVRSWSYI	ECDPLLPVRSWSYIV	CDPLLPVRSWSYIVE
4	NPECDPLLPVRSWSY	PECDPLLPVRSWSYI	ECDPLLPVRSWSYIV	CDPLLPVRSWSYIVE
5	TNGVTAACSHEGKSS	NGVTAACSHEGKSSF	GVTAACSHEGKSSFY	VTAACSHEGKSSFYR
6	TNGVTAACSHEGKSS	NGVTAACSHEGKSSF	GVTAACSHEGKSSFY	VTAACSHEGKSSFYR
7	QNENAYVSVVTSNYN	NENAYVSVVTSNYNR	ENAYVSVVTSNYNRR	NAYVSVVTSNYNRRF
8	QNENAYVSVVTSNYN	NENAYVSVVTSNYNR	ENAYVSVVTSNYNRR	NAYVSVVTSNYNRRF
9	LSRGFGSGIITSNAS	SRGFGSGIITSNASM	RGFGSGIITSNASMH	GFGSGIITSNASMHE
10	LSRGFGSGIITSNAS	SRGFGSGIITSNASM	RGFGSGIITSNASMH	GFGSGIITSNASMHE

11	IPSIQSRGLFGAIAG	PSIQSRGLFGAIAGF	SIQSRGLFGAIAGFI	IQSRGLFGAIAGFIE
12	IPSIQSRGLFGAIAG	PSIQSRGLFGAIAGF	SIQSRGLFGAIAGFI	IQSRGLFGAIAGFIE
13	KMNIQFTAVGKEFNK	MNIQFTAVGKEFNKL	NIQFTAVGKEFNKLE	IQFTAVGKEFNKLEK
14	KMNIQFTAVGKEFNK	MNIQFTAVGKEFNKL	NIQFTAVGKEFNKLE	IQFTAVGKEFNKLEK
15	VKSQLKNNAKEIGNG	KSQLKNNAKEIGNGC	SQLKNNAKEIGNGCF	QLKNNAKEIGNGCFE
16	VKSQLKNNAKEIGNG	KSQLKNNAKEIGNGC	SQLKNNAKEIGNGCF	QLKNNAKEIGNGCFE
17	ILAIYSTVASSLVLL	LAIYSTVASSLVLLV	AIYSTVASSLVLLVS	IYSTVASSLVLLVSL
18	ILAIYSTVASSLVLL	LAIYSTVASSLVLLV	AIYSTVASSLVLLVS	IYSTVASSLVLLVSL
	EQKLISEEDL	G	EQKLISEEDL	G
	28	29	30	31
	EQKLISEEDL	G	EQKLISEEDL	G
1	CIGYHANNSTDTVDT	IGYHANNSTDTVDTV	GYHANNSTDTVDTVL	YHANNSTDTVDTVLE
2	CIGYHANNSTDTVDT	IGYHANNSTDTVDTV	GYHANNSTDTVDTVL	YHANNSTDTVDTVLE
3	DPLLPVRSWSYIVET	PLLPVRSWSYIVETP	LLPVRSWSYIVETPN	LPVRSWSYIVETPNS
4	DPLLPVRSWSYIVET	PLLPVRSWSYIVETP	LLPVRSWSYIVETPN	LPVRSWSYIVETPNS
5	TAACSHEGKSSFYRN	AACSHEGKSSFYRNL	ACSHEGKSSFYRNLL	CSHEGKSSFYRNLLW
6	TAACSHEGKSSFYRN	AACSHEGKSSFYRNL	ACSHEGKSSFYRNLL	CSHEGKSSFYRNLLW
7	AYVSVVTSNYNRRFT	YVSVVTSNYNRRFTP	VSVVTSNYNRRFTPE	SVVTSNYNRRFTPEI
8	AYVSVVTSNYNRRFT	YVSVVTSNYNRRFTP	VSVVTSNYNRRFTPE	SVVTSNYNRRFTPEI
9	FGSGIITSNASMHEC	GSGIITSNASMHECN	SGIITSNASMHECNT	GIITSNASMHECNTK
10	FGSGIITSNASMHEC	GSGIITSNASMHECN	SGIITSNASMHECNT	GIITSNASMHECNTK
11	QSRGLFGAIAGFIEG	SRGLFGAIAGFIEGG	RGLFGAIAGFIEGGW	GLFGAIAGFIEGGWT
12	QSRGLFGAIAGFIEG	SRGLFGAIAGFIEGG	RGLFGAIAGFIEGGW	GLFGAIAGFIEGGWT
13	QFTAVGKEFNKLEKR	FTAVGKEFNKLEKRM	TAVGKEFNKLEKRME	AVGKEFNKLEKRMEN
14	QFTAVGKEFNKLEKR	FTAVGKEFNKLEKRM	TAVGKEFNKLEKRME	AVGKEFNKLEKRMEN
15	LKNNAKEIGNGCFEF	KNNAKEIGNGCFEFY	NNAKEIGNGCFEFYH	NAKEIGNGCFEFYHK
16	LKNNAKEIGNGCFEF	KNNAKEIGNGCFEFY	NNAKEIGNGCFEFYH	NAKEIGNGCFEFYHK
17	YSTVASSLVLLVSLG	STVASSLVLLVSLGA	TVASSLVLLVSLGAI	VASSLVLLVSLGAIS

18	YSTVASSLVLLVSLG	STVASSLVLLVSLGA	TVASSLVLLVSLGAI	VASSLVLLVSLGAIS
	EQKLISEEDL	G	EQKLISEEDL	G
	32	33	34	35
	EQKLISEEDL	G	EQKLISEEDL	G
1	HANNSTDTVDTVLEK	ANNSTDTVDTVLEKN	NNSTDTVDTVLEKNV	NSTDTVDTVLEKNVT
2	HANNSTDTVDTVLEK	ANNSTDTVDTVLEKN	NNSTDTVDTVLEKNV	NSTDTVDTVLEKNVT
3	PVRSWSYIVETPNSE	VRSWSYIVETPNSEN	RSWSYIVETPNSENG	SWSYIVETPNSENGI
4	PVRSWSYIVETPNSE	VRSWSYIVETPNSEN	RSWSYIVETPNSENG	SWSYIVETPNSENGI
5	SHEGKSSFYRNLLWL	HEGKSSFYRNLLWLT	EGKSSFYRNLLWLTE	GKSSFYRNLLWLTEK
6	SHEGKSSFYRNLLWL	HEGKSSFYRNLLWLT	EGKSSFYRNLLWLTE	GKSSFYRNLLWLTEK
7	VVTSNYNRRFTPEIA	VTSNYNRRFTPEIAE	TSNYNRRFTPEIAER	SNYNRRFTPEIAERP
8	VVTSNYNRRFTPEIA	VTSNYNRRFTPEIAE	TSNYNRRFTPEIAER	SNYNRRFTPEIAERP
9	IITSNASMHECNTKC	ITSNASMHECNTKCQ	TSNASMHECNTKCQT	SNASMHECNTKCQTP
10	IITSNASMHECNTKC	ITSNASMHECNTKCQ	TSNASMHECNTKCQT	SNASMHECNTKCQTP
11	LFGAIAGFIEGGWTG	FGAIAGFIEGGWTGM	GAIAGFIEGGWTGMI	AIAGFIEGGWTGMID
12	LFGAIAGFIEGGWTG	FGAIAGFIEGGWTGM	GAIAGFIEGGWTGMI	AIAGFIEGGWTGMID
13	VGKEFNKLEKRMENL	GKEFNKLEKRMENLN	KEFNKLEKRMENLNK	EFNKLEKRMENLNKK
14	VGKEFNKLEKRMENL	GKEFNKLEKRMENLN	KEFNKLEKRMENLNK	EFNKLEKRMENLNKK
15	AKEIGNGCFEFYHKC	KEIGNGCFEFYHKCD	EIGNGCFEFYHKCDN	IGNGCFEFYHKCDNE
16	AKEIGNGCFEFYHKC	KEIGNGCFEFYHKCD	EIGNGCFEFYHKCDN	IGNGCFEFYHKCDNE
17	ASSLVLLVSLGAISF	SSLVLLVSLGAISFW	SLVLLVSLGAISFWM	LVLLVSLGAISFWMC
18	ASSLVLLVSLGAISF	SSLVLLVSLGAISFW	SLVLLVSLGAISFWM	LVLLVSLGAISFWMC
	EQKLISEEDL	G	EQKLISEEDL	G
	36	37	38	39
	EQKLISEEDL	G	EQKLISEEDL	G
1	STDTVDTVLEKNVTV	TDTVDTVLEKNVTVT	DTVDTVLEKNVTVTH	TVDTVLEKNVTVTHS
2	STDTVDTVLEKNVTV	TDTVDTVLEKNVTVT	DTVDTVLEKNVTVTH	TVDTVLEKNVTVTHS
3	WSYIVETPNSENGIC	SYIVETPNSENGICY	YIVETPNSENGICYP	IVETPNSENGICYPG
4	WSYIVETPNSE	SYIVETPNSENG	YIVETPNSENGI	IVETPNSENGIC

	NGIC	ICY	CYP	YPG
5	KSSFYRNLLWLTEKE	SSFYRNLLWLTEKEG	SFYRNLLWLTEKEGS	FYRNLLWLTEKEGSY
6	KSSFYRNLLWLTEKE	SSFYRNLLWLTEKEG	SFYRNLLWLTEKEGS	FYRNLLWLTEKEGSY
7	NYNRRFTPEIAERPK	YNRRFTPEIAERPKV	NRRFTPEIAERPKVR	RRFTPEIAERPKVRD
8	NYNRRFTPEIAERPK	YNRRFTPEIAERPKV	NRRFTPEIAERPKVR	RRFTPEIAERPKVRD
9	NASMHECNTKCQTPL	ASMHECNTKCQTPLG	SMHECNTKCQTPLGA	MHECNTKCQTPLGAI
10	NASMHECNTKCQTPL	ASMHECNTKCQTPLG	SMHECNTKCQTPLGA	MHECNTKCQTPLGAI
11	IAGFIEGGWTGMIDG	AGFIEGGWTGMIDGW	GFIEGGWTGMIDGWY	FIEGGWTGMIDGWYG
12	IAGFIEGGWTGMIDG	AGFIEGGWTGMIDGW	GFIEGGWTGMIDGWY	FIEGGWTGMIDGWYG
13	FNKLEKRMENLNKKV	NKLEKRMENLNKKVD	KLEKRMENLNKKVDD	LEKRMENLNKKVDDG
14	FNKLEKRMENLNKKV	NKLEKRMENLNKKVD	KLEKRMENLNKKVDD	LEKRMENLNKKVDDG
15	GNGCFEFYHKCDNEC	NGCFEFYHKCDNECM	GCFEFYHKCDNECME	CFEFYHKCDNECMES
16	GNGCFEFYHKCDNEC	NGCFEFYHKCDNECM	GCFEFYHKCDNECME	CFEFYHKCDNECMES
17	VLLVSLGAISFWMCS	LLVSLGAISFWMCSN	LVSLGAISFWMCSNG	VSLGAISFWMCSNGS
18	VLLVSLGAISFWMCS	LLVSLGAISFWMCSN	LVSLGAISFWMCSNG	VSLGAISFWMCSNGS
	EQKLISEEDL	G	EQKLISEEDL	G
	40	41	42	43
	EQKLISEEDL	G	EQKLISEEDL	G
1	VDTVLEKNVTVTHSV	DTVLEKNVTVTHSVN	TVLEKNVTVTHSVNL	VLEKNVTVTHSVNLL
2	VDTVLEKNVTVTHSV	DTVLEKNVTVTHSVN	TVLEKNVTVTHSVNL	VLEKNVTVTHSVNLL
3	VETPNSENGICYPGD	ETPNSENGICYPGDF	TPNSENGICYPGDFI	PNSENGICYPGDFID
4	VETPNSENGICYPGD	ETPNSENGICYPGDF	TPNSENGICYPGDFI	PNSENGICYPGDFID
5	YRNLLWLTEKEGSYP	RNLLWLTEKEGSYPN	NLLWLTEKEGSYPNL	LLWLTEKEGSYPNLK
6	YRNLLWLTEKEGSYP	RNLLWLTEKEGSYPN	NLLWLTEKEGSYPNL	LLWLTEKEGSYPNLK
7	RFTPEIAERPKVRDQ	FTPEIAERPKVRDQA	TPEIAERPKVRDQAG	PEIAERPKVRDQAGR
8	RFTPEIAERPKVRDQ	FTPEIAERPKVRDQA	TPEIAERPKVRDQAG	PEIAERPKVRDQAGR
9	HECNTKCQTPLGAIN	ECNTKCQTPLGAINS	CNTKCQTPLGAINSS	NTKCQTPLGAINSSL
10	HECNTKCQTPLGAIN	ECNTKCQTPLGAINS	CNTKCQTPLGAINSS	NTKCQTPLGAINSSL

11	IEGGWTGMIDGWYGY	EGGWTGMIDGWYGYH	GGWTGMIDGWYGYHH	GWTGMIDGWYGYHHQ
12	IEGGWTGMIDGWYGY	EGGWTGMIDGWYGYH	GGWTGMIDGWYGYHH	GWTGMIDGWYGYHHQ
13	EKRMENLNKKVDDGF	KRMENLNKKVDDGFL	RMENLNKKVDDGFLD	MENLNKKVDDGFLDI
14	EKRMENLNKKVDDGF	KRMENLNKKVDDGFL	RMENLNKKVDDGFLD	MENLNKKVDDGFLDI
15	FEFYHKCDNECMESV	EFYHKCDNECMESVR	FYHKCDNECMESVRN	YHKCDNECMESVRNG
16	FEFYHKCDNECMESV	EFYHKCDNECMESVR	FYHKCDNECMESVRN	YHKCDNECMESVRNG
17	SLGAISFWMCSNGSL	LGAISFWMCSNGSLQ	GAISFWMCSNGSLQC	AISFWMCSNGSLQCR
18	SLGAISFWMCSNGSL	LGAISFWMCSNGSLQ	GAISFWMCSNGSLQC	AISFWMCSNGSLQCR
	EQKLISEEDL	G	EQKLISEEDL	G
	44	45	46	47
	EQKLISEEDL	G	EQKLISEEDL	G
1	LEKNVTVTHSVNLLE	EKNVTVTHSVNLLED	KNVTVTHSVNLLEDS	NVTVTHSVNLLEDSH
2	LEKNVTVTHSVNLLE	EKNVTVTHSVNLLED	KNVTVTHSVNLLEDS	NVTVTHSVNLLEDSH
3	NSENGICYPGDFIDY	SENGICYPGDFIDYE	ENGICYPGDFIDYEE	NGICYPGDFIDYEEL
4	NSENGICYPGDFIDY	SENGICYPGDFIDYE	ENGICYPGDFIDYEE	NGICYPGDFIDYEEL
5	LWLTEKEGSYPNLKN	WLTEKEGSYPNLKNS	LTEKEGSYPNLKNSY	TEKEGSYPNLKNSYV
6	LWLTEKEGSYPNLKN	WLTEKEGSYPNLKNS	LTEKEGSYPNLKNSY	TEKEGSYPNLKNSYV
7	EIAERPKVRDQAGRM	IAERPKVRDQAGRMN	AERPKVRDQAGRMNY	ERPKVRDQAGRMNYY
8	EIAERPKVRDQAGRM	IAERPKVRDQAGRMN	AERPKVRDQAGRMNY	ERPKVRDQAGRMNYY
9	TKCQTPLGAINSSLP	KCQTPLGAINSSLPY	CQTPLGAINSSLPYQ	QTPLGAINSSLPYQN
10	TKCQTPLGAINSSLP	KCQTPLGAINSSLPY	CQTPLGAINSSLPYQ	QTPLGAINSSLPYQN
11	WTGMIDGWYGYHHQN	TGMIDGWYGYHHQNE	GMIDGWYGYHHQNEQ	MIDGWYGYHHQNEQG
12	WTGMIDGWYGYHHQN	TGMIDGWYGYHHQNE	GMIDGWYGYHHQNEQ	MIDGWYGYHHQNEQG
13	ENLNKKVDDGFLDIW	NLNKKVDDGFLDIWT	LNKKVDDGFLDIWTY	NKKVDDGFLDIWTYN
14	ENLNKKVDDGFLDIW	NLNKKVDDGFLDIWT	LNKKVDDGFLDIWTY	NKKVDDGFLDIWTYN
15	HKCDNECMESVRNGT	KCDNECMESVRNGTY	CDNECMESVRNGTYD	DNECMESVRNGTYDY
16	HKCDNECMESVRNGT	KCDNECMESVRNGTY	CDNECMESVRNGTYD	DNECMESVRNGTYDY
17	ISFWMCSNGSLQCRI	SFWMCSNGSLQCRIC	FWMCSNGSLQCRICI	WMCSNGSLQCRICIG

18	ISFWMCSNGSLQCRI	SFWMCSNGSLQCRIC	FWMCSNGSLQCRICI	WMCSNGSLQCRICIG
	EQKLISEEDL	G	EQKLISEEDL	G
	48	49	50	51
	EQKLISEEDL	G	EQKLISEEDL	G
1	VTVTHSVNLLEDSHN	TVTHSVNLLEDSHNG	VTHSVNLLEDSHNGK	THSVNLLEDSHNGKL
2	VTVTHSVNLLEDSHN	TVTHSVNLLEDSHNG	VTHSVNLLEDSHNGK	THSVNLLEDSHNGKL
3	GICYPGDFIDYEELR	ICYPGDFIDYEELRE	CYPGDFIDYEELREQ	YPGDFIDYEELREQL
4	GICYPGDFIDYEELR	ICYPGDFIDYEELRE	CYPGDFIDYEELREQ	YPGDFIDYEELREQL
5	EKEGSYPNLKNSYVN	KEGSYPNLKNSYVNK	EGSYPNLKNSYVNKK	GSYPNLKNSYVNKKG
6	EKEGSYPNLKNSYVN	KEGSYPNLKNSYVNK	EGSYPNLKNSYVNKK	GSYPNLKNSYVNKKG
7	RPKVRDQAGRMNYYW	PKVRDQAGRMNYYWT	KVRDQAGRMNYYWTL	VRDQAGRMNYYWTLL
8	RPKVRDQAGRMNYYW	PKVRDQAGRMNYYWT	KVRDQAGRMNYYWTL	VRDQAGRMNYYWTLL
9	TPLGAINSSLPYQNI	PLGAINSSLPYQNIH	LGAINSSLPYQNIHP	GAINSSLPYQNIHPV
10	TPLGAINSSLPYQNI	PLGAINSSLPYQNIH	LGAINSSLPYQNIHP	GAINSSLPYQNIHPV
11	IDGWYGYHHQNEQGS	DGWYGYHHQNEQGSG	GWYGYHHQNEQGSGY	WYGYHHQNEQGSGYA
12	IDGWYGYHHQNEQGS	DGWYGYHHQNEQGSG	GWYGYHHQNEQGSGY	WYGYHHQNEQGSGYA
13	KKVDDGFLDIWTYNA	KVDDGFLDIWTYNAE	VDDGFLDIWTYNAEL	DDGFLDIWTYNAELL
14	KKVDDGFLDIWTYNA	KVDDGFLDIWTYNAE	VDDGFLDIWTYNAEL	DDGFLDIWTYNAELL
15	NECMESVRNGTYDYP	ECMESVRNGTYDYPK	CMESVRNGTYDYPKY	MESVRNGTYDYPKYS
16	NECMESVRNGTYDYP	ECMESVRNGTYDYPK	CMESVRNGTYDYPKY	MESVRNGTYDYPKYS
17	MCSNGSLQCRICIGS	CSNGSLQCRICIGSG	SNGSLQCRICIGSGS	NGSLQCRICIGSGSG
18	MCSNGSLQCRICIGS	CSNGSLQCRICIGSG	SNGSLQCRICIGSGS	NGSLQCRICIGSGSG
	EQKLISEEDL	G	EQKLISEEDL	G
	52	53	54	55
	EQKLISEEDL	G	EQKLISEEDL	G
1	HSVNLLEDSHNGKLC	SVNLLEDSHNGKLCR	VNLLEDSHNGKLCRL	NLLEDSHNGKLCRLK
2	HSVNLLEDSHNGKLC	SVNLLEDSHNGKLCR	VNLLEDSHNGKLCRL	NLLEDSHNGKLCRLK
3	PGDFIDYEELREQLS	GDFIDYEELREQLSS	DFIDYEELREQLSSV	FIDYEELREQLSSVS
4	PGDFIDYEELRE	GDFIDYEELRE	DFIDYEELREQL	FIDYEELREQLS

	QLS	QLSS	SSV	SVS
5	SYPNLKNSYVNKKGK	YPNLKNSYVNKKGKE	PNLKNSYVNKKGKEV	NLKNSYVNKKGKEVL
6	SYPNLKNSYVNKKGK	YPNLKNSYVNKKGKE	PNLKNSYVNKKGKEV	NLKNSYVNKKGKEVL
7	RDQAGRMNYYWTLLK	DQAGRMNYYWTLLKP	QAGRMNYYWTLLKPG	AGRMNYYWTLLKPGD
8	RDQAGRMNYYWTLLK	DQAGRMNYYWTLLKP	QAGRMNYYWTLLKPG	AGRMNYYWTLLKPGD
9	AINSSLPYQNIHPVT	INSSLPYQNIHPVTI	NSSLPYQNIHPVTIG	SSLPYQNIHPVTIGE
10	AINSSLPYQNIHPVT	INSSLPYQNIHPVTI	NSSLPYQNIHPVTIG	SSLPYQNIHPVTIGE
11	YGYHHQNEQGSGYAA	GYHHQNEQGSGYAAD	YHHQNEQGSGYAADQ	HHQNEQGSGYAADQK
12	YGYHHQNEQGSGYAA	GYHHQNEQGSGYAAD	YHHQNEQGSGYAADQ	HHQNEQGSGYAADQK
13	DGFLDIWTYNAELLV	GFLDIWTYNAELLVL	FLDIWTYNAELLVLL	LDIWTYNAELLVLLE
14	DGFLDIWTYNAELLV	GFLDIWTYNAELLVL	FLDIWTYNAELLVLL	LDIWTYNAELLVLLE
15	ESVRNGTYDYPKYSE	SVRNGTYDYPKYSEE	VRNGTYDYPKYSEES	RNGTYDYPKYSEESK
16	ESVRNGTYDYPKYSE	SVRNGTYDYPKYSEE	VRNGTYDYPKYSEES	RNGTYDYPKYSEESK
17	GSLQCRICIGSGSGS	SLQCRICIGSGSGSG		
18	GSLQCRICIGSGSGS	SLQCRICIGSGSGSG		
	EQKLISEEDL	G	EQKLISEEDL	G
	56	57	58	59
1	EQKLISEEDL	G	EQKLISEEDL	G
2	LLEDSHNGKLCRLKG	LEDSHNGKLCRLKGI	EDSHNGKLCRLKGIA	DSHNGKLCRLKGIAP
3	LLEDSHNGKLCRLKG	LEDSHNGKLCRLKGI	EDSHNGKLCRLKGIA	DSHNGKLCRLKGIAP
4	IDYEELREQLSSVSS	DYEELREQLSSVSSF	YEELREQLSSVSSFE	EELREQLSSVSSFER
5	IDYEELREQLSSVSS	DYEELREQLSSVSSF	YEELREQLSSVSSFE	EELREQLSSVSSFER
6	LKNSYVNKKGKEVLV	KNSYVNKKGKEVLVL	NSYVNKKGKEVLVLW	SYVNKKGKEVLVLWG
7	LKNSYVNKKGKEVLV	KNSYVNKKGKEVLVL	NSYVNKKGKEVLVLW	SYVNKKGKEVLVLWG
8	GRMNYYWTLLKPGDT	RMNYYWTLLKPGDTI	MNYYWTLLKPGDTII	NYYWTLLKPGDTIIF
9	GRMNYYWTLLKPGDT	RMNYYWTLLKPGDTI	MNYYWTLLKPGDTII	NYYWTLLKPGDTIIF
10	SLPYQNIHPVTIGEC	LPYQNIHPVTIGECP	PYQNIHPVTIGECPK	YQNIHPVTIGECPKY
11	SLPYQNIHPVTIGEC	LPYQNIHPVTIGECP	PYQNIHPVTIGECPK	YQNIHPVTIGECPKY

12	HQNEQGSGYAADQKS	QNEQGSGYAADQKST	NEQGSGYAADQKSTQ	EQGSGYAADQKSTQN
13	HQNEQGSGYAADQKS	QNEQGSGYAADQKST	NEQGSGYAADQKSTQ	EQGSGYAADQKSTQN
14	DIWTYNAELLVLLEN	IWTYNAELLVLLENE	WTYNAELLVLLENER	TYNAELLVLLENERT
15	DIWTYNAELLVLLEN	IWTYNAELLVLLENE	WTYNAELLVLLENER	TYNAELLVLLENERT
16	NGTYDYPKYSEESKL	GTYDYPKYSEESKLN	TYDYPKYSEESKLNR	YDYPKYSEESKLNRE
17	NGTYDYPKYSEESKL	GTYDYPKYSEESKLN	TYDYPKYSEESKLNR	YDYPKYSEESKLNRE
18				
	EQKLISEEDL	G	EQKLISEEDL	G
	60	61	62	63
	EQKLISEEDL	G	EQKLISEEDL	G
1	SHNGKLCRLKGIAPL	HNGKLCRLKGIAPLQ	NGKLCRLKGIAPLQL	GKLCRLKGIAPLQLG
2	SHNGKLCRLKGIAPL	HNGKLCRLKGIAPLQ	NGKLCRLKGIAPLQL	GKLCRLKGIAPLQLG
3	ELREQLSSVSSFERF	LREQLSSVSSFERFE	REQLSSVSSFERFEI	EQLSSVSSFERFEIF
4	ELREQLSSVSSFERF	LREQLSSVSSFERFE	REQLSSVSSFERFEI	EQLSSVSSFERFEIF
5	YVNKKGKEVLVLWGI	VNKKGKEVLVLWGIH	NKKGKEVLVLWGIHH	KKGKEVLVLWGIHHP
6	YVNKKGKEVLVLWGI	VNKKGKEVLVLWGIH	NKKGKEVLVLWGIHH	KKGKEVLVLWGIHHP
7	YYWTLLKPGDTIIFE	YWTLLKPGDTIIFEA	WTLLKPGDTIIFEAN	TLLKPGDTIIFEANG
8	YYWTLLKPGDTIIFE	YWTLLKPGDTIIFEA	WTLLKPGDTIIFEAN	TLLKPGDTIIFEANG
9	QNIHPVTIGECPKYV	NIHPVTIGECPKYVR	IHPVTIGECPKYVRS	HPVTIGECPKYVRSA
10	QNIHPVTIGECPKYV	NIHPVTIGECPKYVR	IHPVTIGECPKYVRS	HPVTIGECPKYVRSA
11	QGSGYAADQKSTQNA	GSGYAADQKSTQNAI	SGYAADQKSTQNAIN	GYAADQKSTQNAING
12	QGSGYAADQKSTQNA	GSGYAADQKSTQNAI	SGYAADQKSTQNAIN	GYAADQKSTQNAING
13	YNAELLVLLENERTL	NAELLVLLENERTLD	AELLVLLENERTLDF	ELLVLLENERTLDFH
14	YNAELLVLLENERTL	NAELLVLLENERTLD	AELLVLLENERTLDF	ELLVLLENERTLDFH
15	DYPKYSEESKLNREK	YPKYSEESKLNREKV	PKYSEESKLNREKVD	KYSEESKLNREKVDG
16	DYPKYSEESKLNREK	YPKYSEESKLNREKV	PKYSEESKLNREKVD	KYSEESKLNREKVDG
17				
18				
	EQKLISEEDL	G	EQKLISEEDL	G

	64			
	EQKLISEEDL	G		
1	KLCRLKGIAPLQLGK	EQKLISEEDL		
2	KLCRLKGIAPLQLGK	G		
3	QLSSVSSFERFEIFP	EQKLISEEDL		
4	QLSSVSSFERFEIFP	G		
5	KGKEVLVLWGIHHPS	EQKLISEEDL		
6	KGKEVLVLWGIHHPS	G		
7	LLKPGDTIIFEANGN	EQKLISEEDL		
8	LLKPGDTIIFEANGN	G		
9	PVTIGECPKYVRSAK	EQKLISEEDL		
10	PVTIGECPKYVRSAK	G		
11	YAADQKSTQNAINGI	EQKLISEEDL		
12	YAADQKSTQNAINGI	G		
13	LLVLLENERTLDFHD	EQKLISEEDL		
14	LLVLLENERTLDFHD	G		
15	YSEESKLNREKVDGV	EQKLISEEDL		
16	YSEESKLNREKVDGV	G		
17		EQKLISEEDL		
18		G		
	EQKLISEEDL	G		

CITATIONS

1. **Acharya KR**, **Lloyd MD**. The advantages and limitations of protein crystal structures. *Trends Pharmacol Sci* 26: 10–14, 2005.

2. **Air GM**. Influenza neuraminidase. *Influenza Other Respi Viruses* 6: 245–256, 2012.

3. **Akanbi OB**, **Taiwo VO**. Mortality and Pathology Associated with Highly Pathogenic Avian Influenza H5N1 Outbreaks in Commercial Poultry Production Systems in Nigeria. *Int Sch Res Not* 2014: 1–7, 2014.

4. **Appleyard G**, **Maber HB**. Plaque Formation by Influenza Viruses in the Presence of Trypsin. *J Gen Virol* 25: 351–357, 1974.

5. **Balannik V**, **Wang J**, **Ohigashi Y**, **Jing X**, **Magavern E**, **Lamb RA**, **DeGrado WF**, **Pinto LH**. Design and Pharmacological Characterization of Inhibitors of Amantadine-Resistant Mutants of the M2 Ion Channel of Influenza A Virus. *Biochemistry* 48: 11872–11882, 2009.

6. **Bancroft CT**, **Parslow TG**. Evidence for segment-nonspecific packaging of the influenza a virus genome. *J Virol* 76: 7133–9, 2002.

7. **Beyer WEP**, **Palache AM**, **de Jong JC**, **Osterhaus ADME**. Cold-adapted live influenza vaccine versus inactivated vaccine: systemic vaccine reactions, local and systemic antibody response, and vaccine efficacy. A meta-analysis. *Vaccine* 20: 1340–53, 2002.

8. **Biogen**. Prescribing Information – Tysabri. Food and Drug Administration, 2019.

9. **Both GW**, **Sleigh MJ**, **Cox NJ**, **Kendal AP**. Antigenic Drift in Influenza Virus H3 Hemagglutinin from 1968 to 1980: Multiple Evolutionary Pathways and Sequential Amino Acid Changes at Key Antigenic Sites. *J Virol* 48: 52–60, 1983.

10. **Böttcher E**, **Freuer C**, **Steinmetzer T**, **Klenk HD**, **Garten W**. MDCK cells that express proteases TMPRSS2 and HAT provide a cell system to propagate influenza viruses in the absence of trypsin and to study cleavage of HA and its inhibition. *Vaccine* 27: 6324–6329, 2009.

11. **Brandenburg B**, **Koudstaal W**, **Goudsmit J**, **Klaren V**, **Tang C**, **Bujny M V.**, **Korse HJWM**, **Kwaks T**, **Otterstrom JJ**, **Juraszek J**, **van Oijen AM**, **Vogels R**, **Friesen RHE**. Mechanisms of Hemagglutinin Targeted Influenza Virus Neutralization. *PLoS One* 8: e80034, 2013.

12. **Browning M**. Why Recombinant Proteins Make Poor Antibody Validation Tools . *PhosphoSolutions*: 2015.

13. **Bucher DJ**. Purification of neuraminidase from influenza viruses by affinity chromatography. *Biochim Biophys Acta - Enzymol* 482: 393–399, 1977.

14. **Bui M**, **Wills EG**, **Helenius A**, **Whittaker GR**. Role of the influenza virus M1 protein in nuclear export of viral ribonucleoproteins. *J Virol* 74: 1781–6, 2000.

15. **Carr CM**, **Kim PS**. A Spring-Loaded Mechanism for the Conformational Change of Influenza Hemagglutinin. *Cell* 73: 823–832, 1993.

16. **Carrat F**, **Flahault A**. Influenza vaccine: The challenge of antigenic drift. *Vaccine* 25: 6852–6862, 2007.

17. **Centers for Disease Control**. Influenza (Flu): Seasonal Influenza. 2018.

18. **Chaimayo C**, **Hayashi T**, **Underwood A**, **Hodges E**, **Takimoto T**. Selective incorporation of vRNP into influenza A virions determined by its specific interaction with M1 protein. *Virology* 505: 23–32, 2017.

19. **Chames P**, **Van Regenmortel M**, **Weiss E**, **Baty D**. Therapeutic antibodies: successes, limitations and hopes for the future. *Br J Pharmacol* 157: 220–33, 2009.

20. **Cobbin JCA**, **Verity EE**, **Gilbertson BP**, **Rockman SP**, **Brown LE**. The source of the PB1 gene in influenza vaccine reassortants selectively alters the hemagglutinin content of the resulting seed virus. *J Virol* 87: 5577–85, 2013.

21. **Collins PL**, **Graham BS**. Viral and host factors in human respiratory syncytial virus pathogenesis. *J Virol* 82: 2040–55, 2008.

22. **Corti D**, **Cameroni E**, **Guarino B**, **Kallewaard NL**, **Zhu Q**, **Lanzavecchia A**. Tackling influenza with broadly neutralizing antibodies. *Curr Opin Virol* 24: 60–69, 2017.

23. **Corti D**, **Voss J**, **Gamblin SJ**, **Codoni G**, **Macagno A**, **Jarrossay D**, **Vachieri SG**, **Pinna D**, **Minola A**, **Vanzetta F**, **Silacci C**, **Fernandez-Rodriguez BM**, **Agatic G**, **Bianchi S**, **Giacchetto-Sasselli I**, **Calder L**, **Sallusto F**, **Collins P**, **Haire LF**, **Temperton N**, **Langedijk JPM**, **Skehel JJ**, **Lanzavecchia A**. A Neutralizing Antibody Selected from Plasma Cells That Binds to Group 1 and Group 2 Influenza A Hemagglutinins. *Science (80)* 333: 850–856, 2011.

24. **Cox RJ**, **Brokstad KA**, **Ogra P**. Influenza Virus: Immunity and Vaccination Strategies. Comparison of the Immune Response to Inactivated and Live, Attenuated Influenza Vaccines. *Scand J Immunol* 59: 1–15, 2004.

25. **Cross KJ**, **Langley WA**, **Russell RJ**, **Skehel JJ**, **Steinhauer DA**. Composition and functions of the influenza fusion peptide. *Protein Pept Lett* 16: 766–78, 2009.

26. **Dapat C**, **Kondo H**, **Dapat IC**, **Baranovich T**, **Suzuki Y**, **Shobugawa Y**, **Saito K**, **Saito R**, **Suzuki H**. Neuraminidase inhibitor susceptibility profile of pandemic and seasonal influenza viruses during the 2009–2010 and 2010–2011 influenza seasons in Japan. *Antiviral Res* 99: 261–269, 2013.

27. **Dias A**, **Bouvier D**, **Crépin T**, **McCarthy AA**, **Hart DJ**, **Baudin F**, **Cusack S**, **Ruigrok RWH**. The cap-snatching endonuclease of influenza virus polymerase resides in the PA subunit. *Nature* 458: 914–918, 2009.

28. **DiLillo DJ**, **Palese P**, **Wilson PC**, **Ravetch J V.** Broadly neutralizing anti-influenza antibodies require Fc receptor engagement for in vivo protection. *J Clin Invest* 126: 605–610, 2016.

29. **DiLillo DJ**, **Tan GS**, **Palese P**, **Ravetch J V**. Broadly neutralizing hemagglutinin stalk–specific antibodies require FcγR interactions for protection against influenza virus in vivo. *Nat Med* 20: 143–151, 2014.

30. **Drake LY**, **Iijima K**, **Bartemes K**, **Kita H**. Group 2 Innate Lymphoid Cells Promote an Early Antibody Response to a Respiratory Antigen in Mice. *J Immunol* 197: 1335–42, 2016.

31. **Dreyfus C**, **Ekiert DC**, **Wilson IA**. Structure of a classical broadly neutralizing stem antibody in complex with a pandemic H2 influenza virus hemagglutinin. *J Virol* 87: 7149–54, 2013.

32. **Dreyfus C**, **Laursen NS**, **Kwaks T**, **Zuijdgeest D**, **Khayat R**, **Ekiert DC**, **Lee JH**, **Metlagel Z**, **Bujny M V.**, **Jongeneelen M**, **van der Vlugt R**, **Lamrani M**, **Korse HJWM**, **Geelen E**, **Sahin O**, **Sieuwerts M**, **Brakenhoff JPJ**, **Vogels R**, **Li OTW**, **Poon LLM**, **Peiris M**, **Koudstaal W**, **Ward AB**, **Wilson IA**, **Goudsmit J**, **Friesen RHE**. Highly Conserved Protective Epitopes on Influenza B Viruses. *Science (80)* 337: 1343–1348, 2012.

33. **Ducatez MF**, **Pelletier C**, **Meyer G**. Influenza D virus in cattle, France, 2011-2014. *Emerg Infect Dis* 21: 368–71, 2015.

34. **Ecker DM**, **Jones SD**, **Levine HL**. The therapeutic monoclonal antibody market. *MAbs* 7: 9–14, 2015.

35. **Ekiert DC**, **Bhabha G**, **Elsliger M-A**, **Friesen RHE**, **Jongeneelen M**, **Throsby M**, **Goudsmit J**, **Wilson IA**. Antibody Recognition of a Highly Conserved Influenza Virus Epitope. *Science (80)* 324: 246–251, 2009.

36. **Ekiert DC**, **Kashyap AK**, **Steel J**, **Rubrum A**, **Bhabha G**, **Khayat R**, **Lee JH**, **Dillon MA**, **O'Neil RE**, **Faynboym AM**, **Horowitz M**, **Horowitz L**, **Ward AB**, **Palese P**, **Webby R**, **Lerner RA**, **Bhatt RR**, **Wilson IA**. Cross-neutralization of influenza A viruses mediated by a single antibody loop. *Nature* 489: 526–32, 2012.

37. **Enders G**. Paramyxoviruses. University of Texas Medical at Galveston. 2011.

38. **Ennifar E**. X-ray crystallography as a tool for mechanism-of-action studies and drug discovery. *Curr Pharm Biotechnol* 14: 537–50, 2013.

39. **Fry AM**, **Goswami D**, **Nahar K**, **Sharmin AT**, **Rahman M**, **Gubareva L**, **Azim T**, **Bresee J**, **Luby SP**, **Brooks WA**. Efficacy of oseltamivir treatment started within 5 days of symptom onset to reduce influenza illness duration and virus shedding in an urban setting in Bangladesh: a randomised placebo-controlled trial. *Lancet Infect Dis* 14: 109–18, 2014.

40. **Fu Y**, **Zhang Z**, **Sheehan J**, **Avnir Y**, **Ridenour C**, **Sachnik T**, **Sun J**, **Hossain MJ**, **Chen L-M**, **Zhu Q**, **Donis RO**, **Marasco WA**. A broadly neutralizing anti-influenza antibody reveals ongoing capacity of haemagglutinin-specific memory B cells to evolve. *Nat Commun* 7: 12780, 2016.

41. **Fulvini AA**, **Ramanunninair M**, **Le J**, **Pokorny BA**, **Arroyo JM**, **Silverman J**, **Devis R**, **Bucher D**. Gene Constellation of Influenza A Virus Reassortants with High Growth Phenotype Prepared as Seed Candidates for Vaccine Production. *PLoS One* 6: e20823, 2011.

42. **Galloway SE**, **Reed ML**, **Russell CJ**, **Steinhauer DA**. Influenza HA Subtypes Demonstrate Divergent Phenotypes for Cleavage Activation and pH of Fusion: Implications for Host Range and Adaptation. *PLoS Pathog* 9: e1003151, 2013.

43. **Gamblin SJ**, **Skehel JJ**. Influenza hemagglutinin and neuraminidase membrane glycoproteins. *J Biol Chem* 285: 28403–9, 2010.

44. **Gaush CR**, **Smith TF**. Replication and plaque assay of influenza virus in an established line of canine kidney cells. *Appl Microbiol* 16: 588–94, 1968.

45. **Gershoni JM**, **Roitburd-Berman A**, **Siman-Tov DD**, **Tarnovitski Freund N**, **Weiss Y**. Epitope Mapping. *BioDrugs* 21: 145–156, 2007.

46. **Ghebrehewet S**, **MacPherson P**, **Ho A**. Influenza. *BMJ* 355: i6258, 2016.

47. **Gong J**, **Xu W**, **Zhang J**. Structure and functions of influenza virus neuraminidase. *Curr Med Chem* 14: 113–22, 2007.

48. **Goodwin K**, **Viboud C**, **Simonsen L**. Antibody response to influenza vaccination in the elderly: A quantitative review. *Vaccine* 24: 1159–1169, 2006.

49. **Greenbaum BD**, **Ghedin E**. Viral evolution: beyond drift and shift. *Curr Opin Microbiol* 26: 109–115, 2015.

50. **Hayashi T**, **MacDonald LA**, **Takimoto T**. Influenza A Virus Protein PA-X Contributes to Viral Growth and Suppression of the Host Antiviral and Immune Responses. *J Virol* 89: 6442–6452, 2015.

51. **Heo YA**. Baloxavir: First Global Approval. *Drugs* 78: 693–697, 2018.

52. **Herlocher ML**, **Truscon R**, **Elias S**, **Yen H**, **Roberts NA**, **Ohmit SE**, **Monto AS**. Influenza Viruses Resistant to the Antiviral Drug Oseltamivir: Transmission Studies in Ferrets. *J Infect Dis* 190: 1627–1630, 2004.

53. **Herold S**, **Becker C**, **Ridge KM**, **Budinger GRS**. Influenza virus-induced lung injury: pathogenesis and implications for treatment. *Eur Respir J* 45: 1463–1478, 2015.

54. **Hirst GK**. Adsorption of Influenza Hemagglutinins and Virus by Red Blood Cells. *J Exp Med* 76: 195–209, 1942.

55. **Huber VC**, **Lynch JM**, **Bucher DJ**, **Le J**, **Metzger DW**. Fc receptor-mediated phagocytosis makes a significant contribution to clearance of influenza virus infections. *J Immunol* 166: 7381–8, 2001.

56. **Hurrell J**. Monoclonal Hybridoma Antibodies: Techniques and Applications. CRC Press.

57. **Jacobsen H**, **Rajendran M**, **Choi A**, **Sjursen H**, **Brokstad KA**, **Cox RJ**, **Palese P**, **Krammer F**, **Nachbagauer R**. Influenza Virus Hemagglutinin Stalk-Specific Antibodies in Human Serum are a Surrogate Marker for In Vivo Protection in a Serum Transfer Mouse Challenge Model. *MBio* 8: e01463-17, 2017.

58. **Jansen CA**, **van de Haar PM**, **van Haarlem D**, **van Kooten P**, **de Wit S**, **van Eden W**, **Viertlböck BC**, **Göbel TW**, **Vervelde L**. Identification of new populations of chicken natural killer (NK) cells. *Dev Comp Immunol* 34: 759–767, 2010.

59. **Jefferson T**, **Jones M**, **Doshi P**, **Spencer EA**, **Onakpoya I**, **Heneghan CJ**. Oseltamivir for influenza in adults and children: systematic review of clinical study reports and summary of regulatory comments. *BMJ* 348: g2545, 2014.

60. **JORDAN WS**, **OSEASOHN RO**. The use of RDE to improve the sensitivity of the hemagglutination-inhibition test for the serologic diagnosis of influenza. *J Immunol* 72: 229–35, 1954.

61. **Kaur J**, **Bachhawat AK**. A modified Western blot protocol for enhanced sensitivity in the detection of a membrane protein. *Anal Biochem* 384: 348–349, 2009.

62. **Kilbourne ED**. Future influenza vaccines and the use of genetic recombinants. *Bull World Health Organ* 41: 643–5, 1969.

63. **Kilbourne ED**, **Taylor AH**, **Whitaker CW**, **Sahai R**, **Caton AJ**. Hemagglutinin polymorphism as the basis for low- and high-yield phenotypes of swine influenza virus. *Proc Natl Acad Sci U S A* 85: 7782–5, 1988.

64. **Killian ML**. Hemagglutination Assay for Influenza Virus. *Methods in molecular biology (Clifton, N.J.)*, p. 3–9.

65. **Kim H-R**, **Lee K-K**, **Kwon Y-K**, **Kang M-S**, **Moon O-K**, **Park C-K**. Comparison of serum treatments to remove nonspecific inhibitors from chicken sera for the hemagglutination inhibition test with inactivated H5N1 and H9N2 avian *Influenza A virus* subtypes. *J Vet Diagnostic Investig* 24: 954–958, 2012.

66. **Klenk H-D**, **Rott R**, **Orlich M**, **Blödorn J**. Activation of influenza A viruses by trypsin treatment. *Virology* 68: 426–439, 1975.

67. **Knight DM**, **Trinh H**, **Le J**, **Siegel S**, **Shealy D**, **McDonough M**, **Scallon B**, **Moore MA**, **Vilcek J**, **Daddona P**, **Ghrayeb J**. Construction and initial characterization of a mouse-human chimeric anti-TNF antibody. *Mol Immunol* 30: 1443–1453, 1993.

68. **Kosik I**, **Yewdell JW**. Influenza A virus hemagglutinin specific antibodies interfere with virion neuraminidase activity via two distinct mechanisms. *Virology* 500: 178–183, 2017.

69. **Krammer F**, **Palese P**. Influenza virus hemagglutinin stalk-based antibodies and vaccines. *Curr Opin Virol* 3: 521–30, 2013.

70. **Lee J**, **Yu H**, **Li Y**, **Ma J**, **Lang Y**, **Duff M**, **Henningson J**, **Liu Q**, **Li Y**, **Nagy A**, **Bawa B**, **Li Z**, **Tong G**, **Richt JA**, **Ma W**. Impacts of different expressions of PA-X protein on 2009 pandemic H1N1 virus replication, pathogenicity and host immune responses. *Virology* 504: 25–35, 2017.

71. **Little M**, **Kipriyanov S.**, **Le Gall F**, **Moldenhauer G**. Of mice and men: hybridoma and recombinant antibodies. *Immunol Today* 21: 364–370, 2000.

72. **McCardell BA**, **Sathyamoorthy V**, **Michalski J**, **Lavu S**, **Kothary M**, **Livezey J**, **Kaper JB**, **Hall R**. Cloning, expression and characterization of the CHO cell elongating factor (Cef) from Vibrio cholerae O1. *Microb Pathog* 32: 165–172, 2002.

73. **McKimm-Breschkin JL**. Influenza neuraminidase inhibitors: antiviral action and mechanisms of resistance. *Influenza Other Respi Viruses* 7: 25–36, 2013.

74. **Moldt B**, **Rakasz EG**, **Schultz N**, **Chan-Hui P-Y**, **Swiderek K**, **Weisgrau KL**, **Piaskowski SM**, **Bergman Z**, **Watkins DI**, **Poignard P**, **Burton DR**. Highly potent HIV-specific antibody neutralization in vitro translates into effective protection against mucosal SHIV challenge in vivo. *Proc Natl Acad Sci* 109: 18921–18925, 2012

75. **Moon H-J**, **Nikapitiya C**, **Lee H-C**, **Park M-E**, **Kim J-H**, **Kim T-H**, **Yoon J-E**, **Cho W-K**, **Ma JY**, **Kim C-J**, **Jung JU**, **Lee J-S**. Inhibition of highly pathogenic avian influenza (HPAI) virus by a peptide derived from vFLIP through its direct destabilization of viruses. *Sci Rep* 7: 4875, 2017.

76. **Moretta A**, **Bottino C**, **Vitale M**, **Pende D**, **Cantoni C**, **Mingari MC**, **Biassoni R**, **Moretta L**. Activating Receptors and Coreceptors Involved in Human Natural Killer Cell-Mediated Cytolysis. *Annu Rev Immunol* 19: 197–223, 2001.

77. **Moscona A**. Neuraminidase Inhibitors for Influenza. *N Engl J Med* 353: 1363–1373, 2005.

78. **Mostafa HH**, **Vogel P**, **Srinivasan A**, **Russell CJ**. Non-invasive Imaging of Sendai Virus Infection in Pharmacologically Immunocompromised Mice: NK and T Cells, but not Neutrophils, Promote Viral Clearance after Therapy with Cyclophosphamide and Dexamethasone. *PLOS Pathog* 12: e1005875, 2016.

79. **Muramoto Y**, **Noda T**, **Kawakami E**, **Akkina R**, **Kawaoka Y**. Identification of Novel Influenza A Virus Proteins Translated from PA mRNA. *J Virol* 87: 2455–2462, 2013.

80. **Nachbagauer R**, **Wohlbold TJ**, **Hirsh A**, **Hai R**, **Sjursen H**, **Palese P**, **Cox RJ**, **Krammer F**. Induction of broadly reactive anti-hemagglutinin stalk antibodies by an H5N1 vaccine in humans. *J Virol* 88: 13260–8, 2014.

81. **Negri E**, **Colombo C**, **Giordano L**, **Groth N**, **Apolone G**, **La Vecchia C**. Influenza vaccine in healthy children: a meta-analysis. *Vaccine* 23: 2851–2861, 2005.

82. **Neu KE**, **Henry Dunand CJ**, **Wilson PC**. Heads, stalks and everything else: how can antibodies eradicate influenza as a human disease? *Curr Opin Immunol* 42: 48–55, 2016.

83. **Neulen M-L**, **Göbel TW**. Chicken CD56 defines NK cell subsets in embryonic spleen and lung. *Dev Comp Immunol* 38: 410–415, 2012.

84. **Nicholls JM**, **Bourne AJ**, **Chen H**, **Guan Y**, **Peiris JM**. Sialic acid receptor detection in the human respiratory tract: evidence for widespread distribution of potential binding sites for human and avian influenza viruses. *Respir Res* 8: 73, 2007.

85. **Okuno Y**, **Isegawa Y**, **Sasao F**, **Ueda S**. A common neutralizing epitope conserved between the hemagglutinins of influenza A virus H1 and H2 strains. *J Virol* 67: 2552–8, 1993.

86. **Osterholm M**, **Osterholm MT**, **Kelley NS**, **Sommer A**, **Belongia EA**. Efficacy and effectiveness of influenza vaccines: a systematic review and meta-analysis. *Lancelet* 12: 36-44, 2011

87. **Palese P**, **Tobita K**, **Ueda M**, **Compans RW**. Characterization of temperature sensitive influenza virus mutants defective in neuraminidase. *Virology* 61: 397–410, 1974.

88. **Pandey Smt B P M SR**. Hybridoma Technology for Production of Monoclonal Antibodies. *Int J Pharm Sci Rev Res* 1, 2010.

89. **Park J-K**, **Han A**, **Czajkowski L**, **Reed S**, **Athota R**, **Bristol T**, **Rosas LA**, **Cervantes-Medina A**, **Taubenberger JK**, **Memoli MJ**. Evaluation of Preexisting Anti-Hemagglutinin Stalk Antibody as a Correlate of Protection in a Healthy Volunteer Challenge with Influenza A/H1N1pdm Virus. *MBio* 9: 2284-17, 2018.

90. **Peltola VT**, **Murti KG**, **McCullers JA**. Influenza Virus Neuraminidase Contributes to Secondary Bacterial Pneumonia. *J Infect Dis* 192: 249–257, 2005.

91. **Pielak RM**, **Schnell JR**, **Chou JJ**. Mechanism of drug inhibition and drug resistance of influenza A M2 channel. *Proc Natl Acad Sci U S A* 106: 7379–84, 2009.

92. **Portsmouth S**, **Kawaguchi K**, **Arai M**, **Tsuchiya K**, **Uehara T**. Cap-dependent Endonuclease Inhibitor S-033188 for the Treatment of Influenza: Results from a Phase 3, Randomized, Double-Blind, Placebo- and Active-Controlled Study in Otherwise Healthy Adolescents and Adults with Seasonal Influenza. *Open Forum Infect Dis* 4: S734–S734, 2017.

93. **Potier M**, **Mameli L**, **Bélisle M**, **Dallaire L**, **Melançon SB**. Fluorometric assay of neuraminidase with a sodium (4-methylumbelliferyl-α-d-N-acetylneuraminate) substrate. *Anal Biochem* 94: 287–296, 1979.

94. **Van Poucke SG**, **Nicholls JM**, **Nauwynck HJ**, **Van Reeth K**. Replication of avian, human and swine influenza viruses in porcine respiratory explants and association with sialic acid distribution. *Virol J* 7: 38, 2010.

95. **Qiu X**, **Wong G**, **Audet J**, **Bello A**, **Fernando L**, **Alimonti JB**, **Fausther-Bovendo H**, **Wei H**, **Aviles J**, **Hiatt E**, **Johnson A**, **Morton J**, **Swope K**, **Bohorov O**, **Bohorova N**, **Goodman C**, **Kim D**, **Pauly MH**, **Velasco J**, **Pettitt J**, **Olinger GG**, **Whaley K**, **Xu B**, **Strong JE**, **Zeitlin L**, **Kobinger GP**. Reversion of advanced Ebola virus disease in nonhuman primates with ZMapp. *Nature* 514: 47–53, 2014.

96. **Ramanunninair M**, **Le J**, **Onodera S**, **Fulvini AA**, **Pokorny BA**, **Silverman J**, **Devis R**, **Arroyo JM**, **He Y**, **Boyne A**, **Bera J**, **Halpin R**, **Hine E**, **Spiro DJ**, **Bucher D**. Molecular Signature of High Yield (Growth) Influenza A Virus Reassortants Prepared as Candidate Vaccine Seeds. *PLoS One* 8: 65955, 2013.

97. **Raymond DD**, **Bajic G**, **Ferdman J**, **Suphaphiphat P**, **Settembre EC**, **Moody MA**, **Schmidt AG**, **Harrison SC**. Conserved epitope on influenza-virus hemagglutinin head defined by a vaccine-induced antibody. *Proc Natl Acad Sci* 115: 168–173, 2018.

98. **Rossman JS**, **Lamb RA**. Influenza virus assembly and budding. *Virology* 411: 229–236, 2011.

99. **Russell RJ**, **Haire LF**, **Stevens DJ**, **Collins PJ**, **Lin YP**, **Blackburn GM**, **Hay AJ**, **Gamblin SJ**, **Skehel JJ**. The structure of H5N1 avian influenza neuraminidase suggests new opportunities for drug design. *Nature* 443: 45–49, 2006.

100. **Samji T**. Influenza A: understanding the viral life cycle. *Yale J Biol Med* 82: 153–9, 2009.

101. **Scheiffele P**, **Rietveld A**, **Wilk T**, **Simons K**. Influenza viruses select ordered lipid domains during budding from the plasma membrane. *J Biol Chem* 274: 2038–44, 1999.

102. **Schmidt AG**, **Therkelsen MD**, **Stewart S**, **Kepler TB**, **Liao H-X**, **Moody MA**, **Haynes BF**, **Harrison SC**. Viral Receptor-Binding Site Antibodies with Diverse Germline Origins. *Cell* 161: 1026–1034, 2015.

103. **Sheu TG**, **Deyde VM**, **Okomo-Adhiambo M**, **Garten RJ**, **Xu X**, **Bright RA**, **Butler EN**, **Wallis TR**, **Klimov AI**, **Gubareva L V**. Surveillance for neuraminidase inhibitor resistance among human influenza A and B viruses circulating worldwide from 2004 to 2008. *Antimicrob Agents Chemother* 52: 3284–92, 2008.

104. **Shtyrya YA**, **Mochalova L V**, **Bovin N V**. Influenza virus neuraminidase: structure and function. *Acta Naturae* 1: 26–32, 2009.

105. **da Silva D V**, **Nordholm J**, **Dou D**, **Wang H**, **Rossman JS**, **Daniels R**. The influenza virus neuraminidase protein transmembrane and head domains have coevolved. *J Virol* 89: 1094–104, 2015.

106. **Singh S**, **Kumar N**, **Dwiwedi P**, **Charan J**, **Kaur R**, **Sidhu P**, **Chugh VK**. Monoclonal Antibodies: A Review. *Curr Clin Pharmacol* 12, 2017.

107. **Skehel JJ**, **Bayley PM**, **Brown EB**, **-r Martin S**, **WATERFIELDt MD**, **Whites JM**, **Wilson IA**, **Wiley DC**. Changes in the conformation of influenza virus hemagglutinin at the pH optimum of virus-mediated membrane fusion. *Biochemistry* 79: 968–972, 1982.

108. **Smyth MS**, **Martin JH**. x ray crystallography. *Mol Pathol* 53: 8–14, 2000.

109. **Sriwilaijaroen N**, **Suzuki Y**. Molecular basis of the structure and function of H1 hemagglutinin of influenza virus. *Proc Jpn Acad Ser B Phys Biol Sci* 88: 226–49, 2012.

110. **Stewart DL**, **Ryan KJ**, **Seare JG**, **Pinsky B**, **Becker L**, **Frogel M**. Association of RSV-related hospitalization and non-compliance with Palivizumab among commercially insured infants: a retrospective claims analysis. *BMC Infect Dis* 13: 334, 2013.

111. **Sui J**, **Hwang WC**, **Perez S**, **Wei G**, **Aird D**, **Chen L**, **Santelli E**, **Stec B**, **Cadwell G**, **Ali M**, **Wan H**, **Murakami A**, **Yammanuru A**, **Han T**, **Cox NJ**, **Bankston LA**, **Donis RO**, **Liddington RC**, **Marasco WA**. Structural and functional bases for broad-spectrum neutralization of avian and human influenza A viruses. *Nat Struct Mol Biol* 16: 265–273, 2009.

112. **Sun X**, **Tse L V**, **Ferguson AD**, **Whittaker GR**. Modifications to the hemagglutinin cleavage site control the virulence of a neurotropic H1N1 influenza virus. *J Virol* 84: 8683–90, 2010.

113. **Sutton TC**, **Lamirande EW**, **Bock KW**, **Moore IN**, **Koudstaal W**, **Rehman M**, **Weverling GJ**, **Goudsmit J**, **Subbarao K**. *In Vitro* Neutralization Is Not Predictive of Prophylactic Efficacy of Broadly Neutralizing Monoclonal Antibodies CR6261 and CR9114 against Lethal H2 Influenza Virus Challenge in Mice. *J Virol* 91, 2017.

114. **Takeda M**, **Pekosz A**, **Shuck K**, **Pinto LH**, **Lamb RA**. Influenza a virus M2 ion channel activity is essential for efficient replication in tissue culture. *J Virol* 76: 1391–9, 2002.

115. **Tan GS**, **Lee PS**, **Hoffman RMB**, **Mazel-Sanchez B**, **Krammer F**, **Leon PE**, **Ward AB**, **Wilson IA**, **Palese P**. Characterization of a broadly neutralizing monoclonal antibody that targets the fusion domain of group 2 influenza A virus hemagglutinin. *J Virol* 88: 13580–92, 2014.

116. **Tarentino AL**, **Gomez CM**, **Plummer TH**. Deglycosylation of asparagine-linked glycans by peptide:N-glycosidase F. *Biochemistry* 24: 4665–4671, 1985.

117. **Taubenberger JK**, **Fanning TG**, **Hultin J V.**, **Taubenberger JK**. Influenza virus hemagglutinin cleavage into HA1, HA2: no laughing matter. *Proc Natl Acad Sci U S A* 95: 9713–5, 1998.

118. **Treanor J**. Influenza Vaccine — Outmaneuvering Antigenic Shift and Drift. *N Engl J Med* 350: 218–220, 2004.

119. **Tricco AC**, **Chit A**, **Soobiah C**, **Hallett D**, **Meier G**, **Chen MH**, **Tashkandi M**, **Bauch CT**, **Loeb M**. Comparing influenza vaccine efficacy against mismatched and matched strains: a systematic review and meta-analysis. *BMC Med* 11: 153, 2013.

120. **Trifonov V**, **Khiabanian H**, **Rabadan R**. Geographic Dependence, Surveillance, and Origins of the 2009 Influenza A (H1N1) Virus. *N Engl J Med* 361: 115–119, 2009.

121. **Valkenburg SA**, **Mallajosyula VVA**, **Li OTW**, **Chin AWH**, **Carnell G**, **Temperton N**, **Varadarajan R**, **Poon LLM**. Stalking influenza by vaccination with pre-fusion headless HA mini-stem. *Sci Rep* 6: 22666, 2016.

122. **de Vries RD**, **Nieuwkoop NJ**, **Pronk M**, **de Bruin E**, **Leroux-Roels G**, **Huijskens EGW**, **van Binnendijk RS**, **Krammer F**, **Koopmans MPG**, **Rimmelzwaan GF**. Influenza virus-specific antibody dependent cellular cytoxicity induced by vaccination or natural infection. *Vaccine* 35: 238–247, 2017.

123. **Walker LM**, **Burton DR**. Passive immunotherapy of viral infections: “super-antibodies” enter the fray. *Nat. Rev. Immunol* 18:297-308, 2018.

124. **Wang J**, **Wu Y**, **Ma C**, **Fiorin G**, **Wang J**, **Pinto LH**, **Lamb RA**, **Klein ML**, **Degrado WF**. Structure and inhibition of the drug-resistant S31N mutant of the M2 ion channel of influenza A virus. *Proc Natl Acad Sci U S A* 110: 1315–20, 2013.

125. **Wang TT**, **Tan GS**, **Hai R**, **Pica N**, **Petersen E**, **Moran TM**, **Palese P**. Broadly Protective Monoclonal Antibodies against H3 Influenza Viruses following Sequential Immunization with Different Hemagglutinins. *PLoS Pathog* 6: e1000796, 2010.

126. **Watanabe T**, **Watanabe S**, **Noda T**, **Fujii Y**, **Kawaoka Y**. Exploitation of nucleic acid packaging signals to generate a novel influenza virus-based vector stably expressing two foreign genes. *J Virol* 77: 10575–83, 2003.

127. **Weng W-K**, **Levy R**. Two Immunoglobulin G Fragment C Receptor Polymorphisms Independently Predict Response to Rituximab in Patients With Follicular Lymphoma. *J Clin Oncol* 21: 3940–3947, 2003.

128. **Wingfield PT**. Overview of the Purification of Recombinant Proteins. In: *Current Protocols in Protein Science*. John Wiley & Sons, Inc., p. 6.1.1-6.1.35.

129. **Wohlbold T**, **Krammer F**. In the Shadow of Hemagglutinin: A Growing Interest in Influenza Viral Neuraminidase and Its Role as a Vaccine Antigen. *Viruses* 6: 2465–2494, 2014.

130. **Wohlbold TJ**, **Chromikova V**, **Tan GS**, **Meade P**, **Amanat F**, **Comella P**, **Hirsh A**, **Krammer F**. Hemagglutinin Stalk- and Neuraminidase-Specific Monoclonal Antibodies Protect against Lethal H10N8 Influenza Virus Infection in Mice. *J Virol* 90: 851–61, 2016.

131. **World Health Organization**. WHO | Influenza (Seasonal) [Online]. *WHO*.

132. **Wu C-Y**, **Lin C-W**, **Tsai T-I**, **Lee C-CD**, **Chuang H-Y**, **Chen J-B**, **Tsai M-H**, **Chen B-R**, **Lo P-W**, **Liu C-P**, **Shivatare VS**, **Wong C-H**. Influenza A surface glycosylation and vaccine design. *Proc Natl Acad Sci U S A* 114: 280–285, 2017.

133. **Wu NC**, **Wilson IA**. A Perspective on the Structural and Functional Constraints for Immune Evasion: Insights from Influenza Virus. *J Mol Biol* 429: 2694–2709, 2017.

134. **Wu X**, **Kasper LH**, **Mantcheva RT**, **Mantchev GT**, **Springett MJ**, **van Deursen JMA**, **Levay A**, **Levy DE**, **Fontoura BMA**. Disruption of the FG nucleoporin NUP98 causes selective changes in nuclear pore complex stoichiometry and function. *Proc Natl Acad Sci* 98: 3191–3196, 2001.

135. **Xu X**, **Lindstrom SE**, **Shaw MW**, **Smith CB**, **Hall HE**, **Mungall BA**, **Subbarao K**, **Cox NJ**, **Klimov A**. Reassortment and evolution of current human influenza A and B viruses. *Virus Res* 103: 55–60, 2004.

136. **Yamada T**. Therapeutic Monoclonal Antibodies. *Keio J Med* 60: 37–46, 2011.

137. **Yamayoshi S**, **Uraki R**, **Ito M**, **Kiso M**, **Nakatsu S**, **Yasuhara A**, **Oishi K**, **Sasaki T**, **Ikuta K**, **Kawaoka Y**. A Broadly Reactive Human Anti-hemagglutinin Stem Monoclonal Antibody That Inhibits Influenza A Virus Particle Release. *EBioMedicine* 17: 182–191, 2017.

138. **Yen H-L**, **Herlocher LM**, **Hoffmann E**, **Matrosovich MN**, **Monto AS**, **Webster RG**, **Govorkova EA**. Neuraminidase inhibitor-resistant influenza viruses may differ substantially in fitness and transmissibility. *Antimicrob Agents Chemother* 49: 4075–84, 2005.

139. **Yuan S**, **Chu H**, **Singh K**, **Zhao H**, **Zhang K**, **Kao RYT**, **Chow BKC**, **Zhou J**, **Zheng B-J**. A novel small-molecule inhibitor of influenza A virus acts by suppressing PA endonuclease activity of the viral polymerase. *Sci Rep* 6: 22880, 2016.

140. **Zhao, Xiaopeng. Qin, Kun. Guo, Jinlei. Wang, Donghong. Li, Zi. Zhu, Wenfei. Liu, Liqi. Wang, Dayan. Shu, Yeulong. Zhou J**. Hemagglutinin stem reactive antibody response in individuals immunized with a seasonal influenza trivalent vaccine. *Protein Cell* 6: 453–457, 2015.

141. **Zhao C**, **Xu J**. Toward universal influenza virus vaccines: from natural infection to vaccination strategy. *Curr Opin Immunol* 53: 1–6, 2018.

142. **Zheng J**, **Perlman S**. Immune responses in influenza A virus and human coronavirus infections: an ongoing battle between the virus and host. *Curr Opin Virol* 28: 43–52, 2018.

143. **Zhou Y-H**, **Chen Z**, **Purcell RH**, **Emerson SU**. Positive reactions on Western blots do not necessarily indicate the epitopes on antigens are continuous. *Immunol Cell Biol* 85: 73–78, 2007.